2020-03

ATRX as a Regulator of Telomerase Activity in Cancer Cells

Briggs, Sophie

UNIVERSITY OF CALGARY

ATRX as a Regulator of Telomerase Activity in Cancer Cells

by

Sophie Elizabeth Jay Briggs

A THESIS

SUBMITTED TO THE FACULTY OF GRADUATE STUDIES

IN PARTIAL FULFILMENT OF THE REQUIREMENTS FOR THE

DEGREE OF DOCTOR OF PHILOSOPHY

GRADUATE PROGRAM IN BIOCHEMISTRY AND MOLECULAR BIOLOGY

CALGARY, ALBERTA

MARCH, 2020

Abstract

Telomere maintenance is the central process governing cellular immortality. The two distinct pathways – 1) telomerase activity and 2) the alternative lengthening of telomeres (ALT) – result in telomere elongation and allow cells to evade normal cellular ageing mechanisms. Both telomere maintenance pathways can become activated through gene mutations, leading to genetically unstable cells capable of unlimited proliferation.

Expression of the chromatin remodeling protein ATRX is lost in almost all ALT+ cancers, suggesting a role for ATRX in ALT repression, however its exact role in telomere maintenance remains unclear. This thesis provides novel evidence suggesting ATRX acts to resolve telomeric G-quadruplexes (G4), thereby facilitating telomerase activity and indirectly repressing ALT. Using RNA interference in human cancer cell lines and a novel DNA ELISA-based technique, the data presented here establish that loss of ATRX expression results in increased G4 at the telomere. This G4 enrichment correlates with a reduction in telomerase activity *in vitro* which is exacerbated following treatment with the G4 stabilizing agent, Pyridostatin. Further, loss of the full-length ATRX isoform alone does not directly correlate with the ALT phenotype in the selected cell panel. However, a truncated ATRX isoform, ATRXt, was found to be expressed in all selected telomerase+ cells and shown to maintain key functions of the full-length protein. Therefore, alternative ATRX isoforms may act to facilitate telomerase activity through G4 resolution, even in the absence of full-length protein. Taken together, these data provide novel evidence identifying ATRX as an important factor facilitating telomerase-mediated telomere elongation through G4 resolution at the telomere.

Keywords: G-quadruplex; G4; ATRX; Cancer; Telomerase; Telomere; ELISA; ALT.

Preface

The data presented in this thesis are in partial fulfillment of my PhD in Biochemistry and Molecular Biology and the University of Calgary, Canada. I certify that I conducted all experiments myself (unless otherwise specified) and am proud and confident in the results I have generated.

This thesis aims to shed light on how cancer cells maintain cellular immortality; a key hallmark of cancer. As telomere maintenance represents a defining feature of malignancy, expanding our knowledge of this field will provide new cancer-specific targets for therapy. By expanding our knowledge of pathways and mechanisms common among all cancers, we can identify druggable targets which may apply on a far broader scale than many existing therapies.

The results in this thesis provide novel evidence for the roles of ATRX and the G-quadruplex in regulating telomerase activity in cancer, in addition to a novel method of G-quadruplex detection in genomic DNA samples. I believe this data can be used to inform future research into cancer cell immortality and solidify the roles of ATRX and G-quadruplexes in telomere maintenance.

Acknowledgements

I would like to thank all members of the Beattie lab and Cairncross lab, including both my supervisors, for their constant help and support throughout my project. Thank you to Nancy Adam, Nick Ting and Erin Degelmen for their endless guidance, humour and motivation that got me through the best and worst of times - I could not have done this without them. Additionally, I would like to acknowledge Dr Eric Campos and his lab at SickKids, Toronto for kindly providing plasmids and bacteria for ATRX cloning and overexpression studies. This work was also in collaboration with my wonderful undergraduate student, Vanessa Huynh, and Bo Young Ahn (Senger lab) who worked to develop and optimise our cloning and shRNA protocols. Thank you to the Goodarzi lab members (past and present) for listening to my lunchtime rants and for always being there to help with any and all queries (and reagents when we ran out!). I would like to specifically acknowledge Fang (of the Goodarzi lab) for all her amazing work on ATRXt cloning that was essential in generating the results I present in this thesis. I would like to thank my committee members – Drs Savraj Grewal and Karl Riabowol – for their inspiration and guidance throughout my PhD, ensuring I remained on track and performed to the best of my abilities. Finally, I would like to acknowledge all members of the Robson DNA Science Center and Arnie Charbonneau Cancer Institute for being on hand to help whenever I needed it, always maintaining a kind and caring work environment.

Dedication

Firstly, this thesis is dedicated to my parents, Lynn and David Briggs, who have supported me and my insatiable desire to learn since I came into this world. They have helped guide me through life and educated me along the way, always encouraging me to persevere, be strong and above all, believe in myself. Their love and support throughout my studies helped me navigate the intimidating world of academic science, despite them having absolutely no idea what I was talking about half the time. Fortunately for them, throughout my time at the University of Calgary I had Shaun Moore by my side – and he was familiar with both the complexities and frustrations of academic science. My PhD experience would likely have been very different without the constant encouragement both Shaun and my parents provided. Therefore, I would also like to dedicate this thesis to Shaun as a thank you for his unwavering belief in me (and the continuous supply of wonderful food which kept me going). Thank you all for being such wonderful people, I am very lucky to be able to share my life with you.

Table of Contents

List of tables

List of figures and illustrations

Figure 28: Working model of ATRX and G4 in telomerase-mediated telomere elongation.132

Abbreviations

DNA	Deoxyribonucleic acid
RNA	Ribonucleic acid
DDR	DNA damage response
t-loop	Telomeric loop
p53	Tumour protein 53
Rb	Retinoblastoma protein
TMM	Telomere maintenance mechanism
ALT	Alternative lengthening of telomeres
TERT/hTERT	(human) Telomerase Reverse Transcriptase
TERC	Telomerase RNA component
pTERT	TERT promoter
Ets	E twenty six
IDH	Isocitrate dehydrogenase
ATRX	Alpha thalassemia mental retardation x-linked
ATRXt	truncated isoform of ATRX
RCA	Rolling circle amplification
PML	Promyelocytic leukamia protein
APB	ALT-associated PML bodies
KD	knockdown

ASF1	Anti-silencing factor 1
SWI/SNF	SWItch/Sucrose non-fermentable
ADD	ATRX-DNMT3-DNMT3L
NSCLC	non-small cell lung cancer
H3F3A	Gene encoding histone variant 3.3
DAXX	Death associated protein six
H3.3	Histone variant 3.3
G4	G-quadruplex
MRN	Mre11/Rad50/Nbs1 complex
ATR-X	ATRX syndrome
GB	Glioblastoma
H2A	Histone 2A
H2AX	Histone 2A variant X
PHD	Plant homeodomain
TIF	Telomere dysfunction induced foci
GMP	Guanine monophosphate
BLM	Bloom syndrome protein
WRN	Werner syndrome protein
HERC2	HECT And RLD domain containing E3 ubiquitin protein ligase 2
PIF1	PIF1 5’ – 3’ DNA helicase
HEK293	Human Embryonic Kidney cell line 293
U2OS	Human bone Osteosarcoma epithelial cells
HeLa	Henrietta Lack cervical cancer cells

DMEM	Dulbeccos modified eagle medium
FBS	Fetal bovine serum
BTIC	Brain tumour initiating cells
EGF	Endothelial growth factor
FGF	Fibroblast growth factor
HEK293T	HEK293 containing SV40T antigen
RNAi	RNA interference
shRNA	short hairpin RNA
dsDNA	double-stranded DNA
FACS	fluorescence associated cell sorting
GFP	Green fluorescent protein
cDNA	Complementary DNA
PCR	Polymerase chain reaction
RT-PCR	Reverse-transcription PCR
DTT	1, 4 Dithiothreitol
ddH_20	Double distilled water
qPCR	quantitative PCR
BSA	Bovine serum albumin
TRF	Telomere restriction fragment
HCl	Hydrochloric acid
UV	Ultraviolet
SSC	Saline sodium citrate
TAE	Tris-acetate-EDTA

NP-40	non-idet P40
SDS	Sodium dodecyl sulphate
HRP	Horseradish peroxidase
TBST	Tris-buffered saline with Tween
ECL	Enhanced chemiliminescence
PFA	Paraformaldehyde
PBS	Phosphate buffered saline
IF	Immunofluorescence
DAPI	4′,6-diamidino-2-phenylindole
FISH	Fluorescence in-situ hybridisation
PNA	Peptide nucleic acid
TRAP	Telomere repeat amplification protocol
Ts	Telomere substrate
TBE	Tris-buffered EDTA
CTA	Conventional telomerase assay
RRL	Rabbit reticulocyte lysate
IHC	Immunohistochemistry
DAB	3,3′-Diaminobenzidine

Chapter 1: Introduction

Epigraph

‘I am very poorly today and very stupid and hate everybody and everything’

- Charles Darwin in a letter to Charles Lyell, October 1, 1861.

The knowledge that even the late, great, Charles Darwin had some rough days makes my scientific failings feel far less dramatic.

Introduction

Telomere Maintenance and Cancer

Through decades of cancer research, one central goal has been to identify properties that differentiate malignant from normal cells. If we can define these differences, it may be possible to use the distinguishing properties to target cancer cells without causing harm to healthy tissue. A number of cancer-specific properties were proposed in a 2000 Cell paper by Hanahan and Weinberg - entitled 'The Hallmarks of Cancer'- that discussed some of the characteristic features of cancer cells, thereby enabling and maintaining their malignancy (1). In 2011, an update of these hallmarks was published by the same authors, with a focus on 'enabling and emerging' hallmarks. One of the persisting hallmarks present in both the original and updated articles, describes the ability of cancer cells to evade normal cellular ageing processes and divide without limit. This hallmark is termed 'enabling replicative immortality' and is an essential property of cancer cells because without it, they would be incapable of sustained proliferation (2). The inevitable outcome of this unchecked proliferation is an increasingly unstable genome due to the accumulation of mutations throughout each cell division, which itself is defined as a hallmark of cancer (3). In order for a cell to attain replicative immortality, it must successfully evade cellular ageing in the form of progressive telomere shortening, otherwise known and the 'end replication problem'(4).

The end replication problem is a phenomenon that occurs due to the strict directionality of DNA polymerase. During replication, this enzyme requires a 3'-OH group to initiate synthesis of a new DNA strand. The leading DNA strand is replicated from a single RNA primer without issue because its orientation allows the polymerase to move along in a 3'-5' direction, synthesizing a new DNA strand in a 5'-3' direction. However, as the lagging strand of DNA has the reverse

orientation, the DNA polymerase requires multiple RNA primers to initiate synthesis. These RNA primers bind at intervals along the lagging strand of DNA, providing the 3'-OH required for synthesis initiation (5). This process generates many short fragments of newly synthesized DNA called Okazaki fragments. The RNA primers are then removed from the original DNA strand, allowing DNA polymerase fill in the 'gaps' using the 3'-OH from each Okazaki fragment to initiate synthesis. These fragments are then ligated together to form a continuous strand of DNA. However, at the end of the lagging strand, the terminal RNA primer, once detached, leaves a short section of un-replicated DNA (6)(7). With each round of replication this loss of DNA leads to progressive shortening of the telomeres, eventually resulting in a dysfunctional telomeric state triggering a telomere-specific DNA damage response (8)(9).

The telomeric state – referring to the compaction and organisation of the telomere - is primarily determined by the formation of a loop structure at the terminal telomere end (t-loop). This structure caps the telomere and prevents it from being recognised as a double-strand break by DNA damage response (DDR) factors (10)(11). The t-loop is formed when the 3' G-overhang of telomeric DNA loops back on itself and invades a double stranded section of telomeric DNA. However, the 3' overhang generated through the end replication problem is insufficient to create the t-loop and so further resection takes place to extend the 3' overhang on the lagging strand and to generate a 3' overhang on the leading strand (12). Once formed, the t-loop is predominantly stabilized by a group of 6 proteins collectively referred to as the shelterin complex (13)(10). Telomeric state can therefore be disrupted by short telomere length as well as a lack of functional shelterin proteins, leading to loss of the telomeric 'cap' (8). In both of these scenarios, the terminal ends of the telomeres become exposed, triggering the telomeric DDR and leading to cellular senescence or apoptosis (11)(14).

The progressive attrition of telomeric DNA caused by the end replication problem can be described as an ageing clock, counting down until the cell is no longer able to safely replicate. In cancer, cells can evade this 'clock', and continue to divide beyond what is safe and healthy for the cell. Under most circumstances, dysfunctional telomeric state, loss of the t-loop and induction of DDR caused by the end replication problem will trigger a cascade of signalling events leading to senescence. This process is designed to stop unstable cells from continued proliferation, in turn preventing malignant transformation. However, if a cell has acquired mutations in essential cell cycle or senescence-associated proteins, it may be able to evade senescence and continue dividing. Two key factors known to be involved in cellular ageing and senescence are p53 and Rb (15)(16). These two tumour-suppressor proteins are essential to healthy cellular ageing and loss of either can result in catastrophic changes in the cell that can lead to malignant transformation.

Loss of functional p53 or Rb may be just the first step to cellular immortality. For the cell to continue to divide, a telomere maintenance mechanism (TMM) must be activated to counter the end replication problem. Under normal circumstances, if a cell continues to divide even with dysfunctional telomeres, it will be forced into apoptosis as the telomeric attrition extends into sub-telomeric and coding regions of DNA (17)(18). However, if a TMM is activated, the telomeres can be elongated just enough to allow continued replication. Telomere maintenance is something shared between cancer cells and stem cells, however TMMs remain active throughout the lifespan of a stem cell and are tightly regulated through histone methylation/acetylation to prevent cellular immortality, whilst extending the number of healthy cell divisions (19)(20). This process is essential to stem cells as it allows them to repopulate regions of high cell death and to maintain healthy tissue function. However, unregulated TMM activity in already unstable cells can promote continued proliferation of mutant genomes, triggering the start of malignancy (21).

Two TMMs have been identified in cancer cells; Telomerase-mediated telomere maintenance and the Alternative Lengthening of Telomeres (ALT) (22)(23)(24). Both mechanisms facilitate cellular immortality utilizing two very distinct mechanisms and both are considered potential targets for anti-cancer therapy.

Telomerase-mediated telomere maintenance

In stem cells and ~85-90% of cancers, telomeric attrition is resolved through the action of the ribonucleoprotein complex enzyme, telomerase (25)(26). The core complex of telomerase is composed of the essential Telomerase RNA component (TERC or TR) and telomerase reverse transcriptase (TERT) (27). TERC has an intrinsic RNA template sequence complementary to the telomeric sequence, allowing it to bind to the leading strand of telomeric DNA, providing a template for the addition of telomeric repeats via TERT. This elongates the leading strand of DNA enough for DNA polymerase to fully replicate the original length of the lagging strand, thereby preventing telomeric attrition and allowing the cell to evade the cellular senescence (28).

Similarly, stem cells evade senescence through telomerase activity, although the manner in which they do this is quite different from that of a cancer cell. Firstly, the activity of telomerase in a stem cell is limited by tight regulation of the TERT protein as this directly correlates with abundance and activity of the enzyme (29)(30). In cancer cells however, the production of TERT is dysregulated and far higher than in stem cells, meaning more telomerase is produced (31). Secondly, stem cells have active telomerase throughout their lifespan and therefore, their telomeres are generally maintained at a longer length than those of cancer cells, which may only acquire telomere maintenance following failure to undergo cellular senescence, despite an unstable telomere state (19). There is much discussion in the field regarding the transformation of stem cells

a)

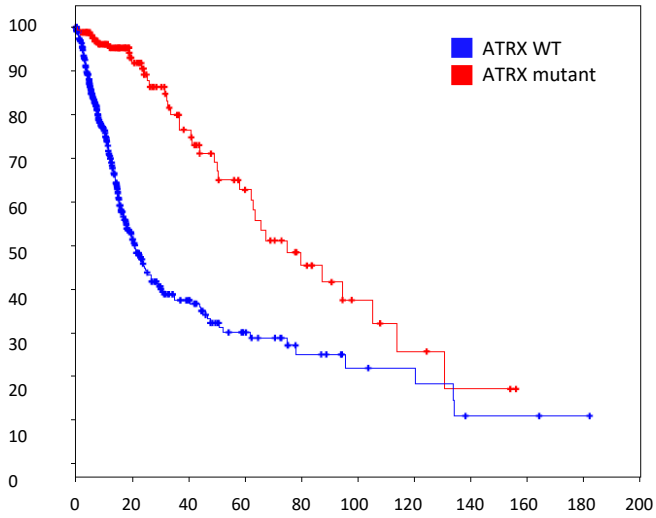

b)

-/-	ALT	Telomerase	
0	115	0	ATRX mutant
47	0	155	ATRX WT

Figure 1: Clinical analysis of ATRX in Glioma using TCGA datasets. **a)** Kaplan-meier survival graph for Glioma cases with mutations in the ATRX gene (red) versus ATRX WT (blue) shows a significant survival benefit of ATRX mutations. **b)** Tabular results of telomere maintenance analysis versus ATRX gene status in Glioma. All 115 ALT+ cases have mutations in ATRX while all 155 telomerase+ cases have ATRX WT gene, suggesting mutual exclusivity between ATRX expression and ALT activity. Additionally, 47 ATRX WT Gliomas did not have classifiable telomere maintenance mechanism. All analysis was performed on TCGA datasets using cBIOPortal.

in cancer. It seems plausible that increasing the activity of a pre-existing TMM might be simpler than activating the entire process in a TMM deficient cell. As stem cells are the only cells in the human body with naturally active telomerase activity, it stands to reason that mutations to these cells may result in increased telomerase activity and increased proliferative capacity. However, stem cells, like other healthy cells, express Rb and p53 which can trigger cellular senescence if the cell becomes unstable, meaning mutations to these proteins must also be acquired for transformation (11). In either circumstance, the development of cancer appears to be a multi-stage process.

Mutations in cell cycle proteins allow replication past the senescence 'checkpoint', a stage sometimes termed 'pre-cancerous', as cells that pass this point tend to have a high mutational burden and genomic instability. These cells eventually reach a point at which almost all will undergo apoptosis due to irreparable damage and high levels of stress (32). However, some cells may progress to the second stage of transformation through activation of a TMM (33). Both telomerase and ALT pathways allow the cell to elongate and maintain its telomeres enough to continue proliferating, creating a highly unstable cell with unlimited replicative capacity (34). In some cases, spontaneous activation of telomerase occurs through mutations in hotspot regions of the TERT promoter (pTERT) (24)(35). These mutations are invariably C>T single nucleotide polymorphisms at -124 and -146bp upstream of the transcription start site and result in increased transcription of the TERT gene (36). It has subsequently been established that mutations at both these sites generate consensus motifs for E twenty six (Ets) transcription factors to bind, thus increasing transcription of the TERT gene, and subsequently telomerase activity, 2- to 4-fold (24).

While the activation of telomerase in specific cancers can be attributed to pTERT mutations, the processes governing ALT activation and/or the choice of TMM remain largely

undefined. One finding that has become clear through studying TMM in cancer is that the distribution of TMM activity between cancers appears to be quite distinct. Whilst most cancers adopt telomerase-mediated telomere maintenance, certain cancers, often of mesenchymal origin, have a much higher prevalence of the ALT phenotype (37). This includes cancers such as leiomyosarcoma, chondrosarcoma and pleiomorphic sarcoma, all of which predominantly possess the ALT phenotype. Similarly, Glioma, a type of brain tumour arising from glial cells, also has an unusually high prevalence of ALT and certain subtypes of this cancer have been suggested to have mesenchymal features (38)(39)(40).

Glioma is divided into sub-classifications based upon histological grade and molecular characteristics. Of the subtypes of Glioma, Astrocytoma and Glioblastoma by far have the highest incidence of the ALT phenotype, which are closely linked to other genetic features, including mutations in the Isocitrate Dehydrogenase 1 and 2 genes (IDH1/2). Astrocytoma is a grade II/III Glioma defined by mutations in IDH1, Tumour Protein 53 (TP53) and Alpha Thalassemia Mental Retardation X-linked (ATRX) genes. Similarly, a subtype of grade IV Glioblastoma defined by mutations in these same genes has an unusually high prevalence of ALT; in these subtypes, ATRX loss and IDH mutations correlate with improved survival rates (Figure 1a). Strikingly, another subtype of Glioblastoma, defined by TP53 and telomerase reverse transcriptase (TERT) promoter mutations, almost exclusively lacks ATRX and IDH mutations and are invariably telomerase positive. Oligodendrogliomas, another grade II/III subtype of Glioma, are defined by loss of chromosome 1p19q in addition to IDH gene mutations. However, this classification very rarely has ATRX or TP53 mutations and is again exclusively telomerase positive (40)(41). The genetic backgrounds of these cancers highlight a commonality in ALT positive tumours; mutations in the

ATRX gene (Figure 1b). These findings have prompted research into this gene in the context of ALT, which has continued to provide tantalizing evidence of its role in telomere maintenance.

Alternative Lengthening of Telomeres

Telomerase-mediated telomere maintenance is the predominant pathway choice in most cancer cells, however, in ~10-15% cancers the ALT pathway is utilized instead (26). Although much is now known about the mechanisms of ALT, questions about its initial activation and the key proteins involved remain. ALT is thought to utilize homologous recombination (HR) machinery to elongate telomeres using the telomeric sequences of other chromosomes as a template, and is entirely independent of telomerase activity (42)(43). As the telomeric sequence is the same for all chromosomes in human cells, the ALT mechanism can use the telomere of any chromosome as a template for elongation. Additionally, due to the repetitive nature of the telomeric sequence, HR-mediated strand invasion can occur at any point in the template telomere. This mechanism is thought to account for the telomere sister chromatid exchange (T-SCE) and copy number alterations seen in ALT cells as a result of chromosomal fusions (44). The variability in strand invasion and elongation also means ALT telomeres are heterogenous in length and, on average, up to 2x longer than telomerase elongated telomeres, providing an ALT-specific feature for detection of this pathway.

ALT and telomerase-mediated pathways of telomere elongation contain a number of specific differences that can be used to distinguish the active pathway in any given cancer. Primarily, the absence of telomerase activity is the central defining feature of ALT, but other key differences have also been noted. As mentioned, ALT positive cancer cells have been shown to possess longer and more heterogenous telomeres than telomerase positive cells (45). This feature is useful for defining human ALT cells but is less effective when analyzing mouse telomeres. This

is because mouse telomeres are in general more heterogeneous and longer than those of humans, meaning all mouse telomeres, regardless of TMM, have ALT-like telomere lengths (20). The presence of circular DNA structures termed C-circles, is perhaps the most intriguing feature of ALT cells. C-circles were characterized by Henson et al in 2009 and are thought to occur through rolling circle amplification (RCA) of telomeric DNA, generating small circular segments of DNA that accumulate in the nucleus of ALT positive cells (46). Recent evidence suggests c-circles develop following failure to rescue collapsed replication forks at the telomere, leading to c-circle and c-overhang generation on leading and lagging strands respectively (47). This data supports other research hinting at a link between c-circle formation and telomeric DDR (48). It appears that the abundance of c-circles is highest during the S phase of the cell cycle and they are predominantly formed from the lagging strand of DNA. This suggests c-circles are formed during telomeric replication and may be associated with the end-replication problem, however further research is needed to clarify the origin of this ALT feature (47).

Early research into ALT in cancer cells uncovered other features specific to ALT cells - including the presence of Promyelocytic Leukaemia bodies (PML bodies) at the telomere - which are currently used as a marker for ALT (49). The localization of PML to the telomeres is something largely absent in somatic and telomerase+ cells, making it a useful identifying feature of ALT activity (50). Formation of these ALT-associated PML bodies (APBs) was shown to be highly specific and inducible in models of ALT, such as with the knockdown (KD) of the histone chaperone protein ASF1. In one report, siRNA induced KD of Anti-silencing factor 1α and β (ASF1α/β) lead to activation of the ALT pathway in previously telomerase positive cell lines (51). The induction of ALT was accompanied by the repression of hTERT expression and telomerase activity, showing for the first time that ALT can be induced by knockdown of a single gene. One

caveat to this study however, is that mutations in ASF1 have not been reported in any ALT cancers to date, suggesting that although ASF1 itself may not be responsible for the induction of ALT *in vivo*, changes to histone deposition and chromatin state may be central to the activation of ALT (52).

Fitting with this concept, mutations in the chromatin remodeling protein, ATRX are heavily associated with ALT. ATRX is a member of the SWI/SNF family of chromatin remodelers with roles in histone deposition and chromatin assembly at repeat regions of DNA. Its association with cancer has become apparent more recently following evidence that loss of ATRX expression occurs in ~80% ALT+ cancers, although the exact reason for this link remains unclear. It is thought that under normal circumstances, ATRX represses the ALT mechanism so normal somatic cells do not become immortalized via ALT (53). It is postulated that repression is then relieved upon loss of ATRX, leading to activation of ALT during malignant transformation. However, a number of studies show that loss of ATRX is insufficient to fully induce ALT in telomerase positive cells. Despite this, ATRX loss is considered a predisposing factor, upon which mutations in other proteins may be necessary to fully activate the ALT pathway (53) (54). These proteins and pathways have remained elusive until now, but by focusing on the defining features of ALT positive cells - such as changes to chromatin, protein expression and telomeric state - it may be possible to elucidate to the protein(s) responsible.

Alpha Thalassemia Mental Retardation X-linked (ATRX)

Alpha Thalassemia Mental Retardation X-linked (ATRX) is a protein encoded by a gene located on the X chromosome. It primarily functions to deposit histone variant 3.3 (H3.3) to repeat regions of DNA, including telomeric and pericentromeric regions amongst other chromatin remodeling roles. The ATRX protein is named as such after the syndrome it was initially

discovered in. Alpha Thalassemia mental retardation X-linked (ATR-X) syndrome is an intellectual disability syndrome with associated symptoms including craniofacial abnormalities, genital anomalies and the characteristic alpha thalassemia (55). Interestingly, this syndrome almost exclusively affects males due to skewing of X-inactivation in females to silence the mutated gene (55)(56). The ATRX gene was found to be directly associated with the syndrome primarily through mutations in the protein's ATRX-DNMT3-DNMT3L (ADD) and helicase domains. The ADD domain is essential to ATRX function as it facilitates binding to specific histone 3 (H3) markers including; H3 lysine 4 and methylation of H3 lysine 9 (57). The regulation of chromatin structure is dependent on the ability of ATRX to detect and interact with specific epigenetic histone markers such as these. ATR-X syndrome mutations appeared to inhibit the ability of ATRX to promote transcription of the α-globin gene which is essential in maintenance of haemoglobin levels in blood cells (58)(59). Although it has been shown that mutations in the ATRX ADD and helicase domains result in conformational changes to the protein, it remains unclear how these conformational changes directly affect ATRX function (60). However, it is apparent that transcriptional regulation of ATRX target genes is heavily affected by mutations in these domains, suggesting either DNA binding or helicase functions are directly affected (59)(61).

Despite the fact that ATRX in relation to ATR-X syndrome was discovered in the mid 1990's, it was not linked to cancer until 2011when Heaphy *et al* published an article in Science showing loss of ATRX protein in multiple cancers was correlated with ALT activity (60)(62). Further, mutations in ATRX have been observed in a number of cancers at varying degrees, with malignant glioma, sarcoma and non-small cell lung cancer (NSCLC) representing those in which ATRX is most frequently mutated (63).

The link between ATRX mutation and glioma was further supported in a 2012 Nature publication by Schwartzentruber *et al*, showing 44% paediatric glioblastoma (GB) cases had mutations in one or more of ATRX, H3F3A or DAXX genes (H3F3A encodes the H3A subunit if histone 3 and DAXX encodes an ATRX-interacting histone chaperone protein) (64)(65). Subsequently, articles reporting a similar link between glioma and ATRX have been published - particularly focusing on how the loss of ATRX in glioma is linked to a favourable prognosis - leading to routine ATRX analysis being performed in the clinic when diagnosing glioma patients. These findings prompted a great degree of interest in ATRX as a potential target for cancer therapy and studies into its role in ALT positive cancers are ongoing.

As more studies have focused on ATRX in the context of cancer, multiple interacting partners have been identified, building a comprehensive ATRX interactome (Figure 2). Initial studies demonstrated that ATRX is part of a replication-independent chromatin remodeling complex with Death associated protein 6 (DAXX). The ATRX/DAXX complex is primarily responsible for deposition of histone variant 3.3 (H3.3) at repetitive regions of DNA, including telomeres and peri-centromeres. The complex binds directly to H3.3 via DAXX and with ATRX acting as a guide to target regions, allowing DAXX to deposit H3.3 at specific chromosomal locations (66).

Initially, the regulation of α-globin gene expression in ATR-X syndrome represented the first evidence that ATRX was directly involved in epigenetic regulation. However, other than H3.3 deposition, its role in gene regulation remains unclear (67). As evidence regarding alternative DNA secondary structures – in addition to the canonical double helix - was established, a potential link between ATRX and resolution of these structures became apparent. Studies demonstrated that both α-globin genes and telomeric DNA were capable of forming a distinct DNA secondary structure

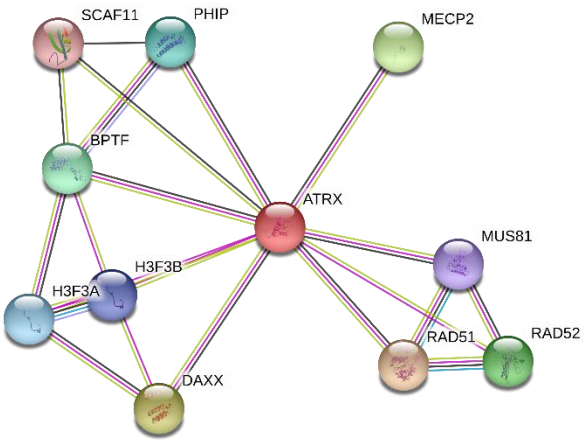

Figure 2: ATRX interactome map. Direct ATRX interactions based upon existing literature. Lines between proteins represent interactions and line colour represents the source of information. Known interactions: Curated databases (teal), experimentally determined (pink); Predicted interactions: gene neighbourhood (green), gene fusions (red), gene co-occurrence (blue); Other: tex-tmining (yellow), co-expression (black), protein homology (light blue). The human ATRX interactome map was generated using STRING software version 11.0 (available online).

known as a G-quadruplex (G4) which was associated with gene regulation (68)(69). Subsequently, it was shown that ATRX localises to chromosomal regions enriched for G4, suggesting it may play a role in resolving these structures (70)(71).

DNA G-quadruplexes form in G-rich genomic regions, including gene promoters and telomeric DNA, and are considered to be important for transcriptional regulation (68). As active genomic regions are often enriched for G4 DNA, it stands to reason that G4 may provide a level of epigenetic regulation in the cell. What has been established is that, if not appropriately resolved, G4 can act as barriers to fork progression in both replication and transcription. This suggests certain factors are required to help break down G4 and promote smooth progression of transcriptional and replication machinery through G4-rich regions (72). ATRX, in addition to other helicases, has been shown to have some G4 resolution ability, suggesting it may be involved in resolving G4 either directly or indirectly - which would explain its localisation to G4 DNA (73).

In addition to ATRX's affinity for repetitive and G4 DNA, it has also been shown to colocalize with PML bodies (74). These 'clusters' of PML protein form in most mammalian cell types but localise specifically to the telomeres of ALT cells (in this context they are termed APBs). The loss of functional ATRX as well as the accumulation of APBs in ALT-positive cancer cells suggests ATRX might play a role in regulating PML cluster formation at ALT telomeres (75). Further, it has been shown that factors involved in homologous recombination (HR) localize to APBs in ALT-positive cells, suggesting these structures may act as hubs for HR-mediated telomere elongation. This is further supported by interactions between ATRX and the MRN (Mre11/Rad50/Nbs1) complex. MRN is an essential complex involved in the early stages of HR and interaction with ATRX represses MRN localization to telomeres, thereby repressing ALT activity (54)(76). Interestingly, ATRX targeting to PML bodies was shown to be reduced by

mutations derived from ATR-X patients, tracing back to the ATRX ADD domain (77). Although in ATR-X syndrome the ATRX ADD and helicase domains appear to be hotspots for mutation, in adult glioma ATRX mutations are distributed throughout the gene and are not confined to any specific domains (41). Despite what is known about ATRX and its links to TMM, the exact role of ATRX in cellular immortalization and the ALT pathway remain unclear. The association between ATRX mutants and paediatric GBM, in addition to the high frequency of ALT in adult glioma, raises the possibility that ATRX may also be fundamentally involved in the development of certain cancer types, including glioma.

Epigenetic gene regulation and chromatin remodeling

Traditionally, DNA is depicted in its primary form as a double-stranded molecule followed by its canonical secondary double-helix structure. The DNA molecule is then wrapped tightly around histone octamers to form the tertiary DNA structure of a nucleosome. This multi-layered organisation has been considered for decades to be the primary mechanism by which genes are regulated. However, developments in the field of epigenetics have introduced a new layer of complexity to the process and identified additional key players in gene regulation.

In most regions, epigenetic regulation of genes is determined by chromatin state. This is a dynamic process and reflects the activity of the genes, with euchromatin being associated with active genes and heterochromatin associated with repressed gene regions. At the telomeres, chromatin exists in a tightly compact, heterochromatin-like state as the telomeric sequence is non-coding (78). The chromatin state itself can be regulated by chromatin remodeling enzymes which can move, insert and eject histones as well as switch canonical histones for variants. This action results in changes to nucleosome density and provides a more open or closed chromatin state, thereby regulating access of transcriptional factors to discrete regions of DNA. Another method of

epigenetic regulation occurs through histone modifications. These alterations bring about a change in chromatin state by providing binding sites for chromatin-associated factors and modifying histone charges to facilitate changes in chromatin organisation (79). Histone variants are another essential factor in chromatin regulation as certain variants can replace canonical histones to alter chromatin state and influence transcription of target genes. Histone 3 variant, H3.3, is mostly associated with active chromatin, however has also been found at some repressed gene regions including the telomere, suggesting it has dual roles (80). Similarly the H2A variant, H2AX, is deposited at damaged DNA regions as the initializing step in many DDR pathways (81).

The substitution of canonical histones with their variant counterparts is dependent on histone chaperones and chromatin remodeling proteins that perform differing roles depending on the family from which they originate. The chromatin remodeler ATRX has key structural features of the SWI/SNF family, including the C-terminal helicase domain and highly conserved PHD domain. The SWI/SNF family of proteins are responsible for sliding and ejecting nucleosomes along DNA to increase or decrease nucleosome density in a particular region (82). Interestingly, ALT cells, which are predominantly ATRX negative, have been shown to display reduced nucleosome density at telomeres compared to telomerase positive cells, suggesting there may be dysregulation of telomeric chromatin in these cells (83). This concept is further supported by increased levels of telomere dysfunction induced foci (TIFs) in ALT cells. These features occur as a result of increased localisation of DDR proteins at telomeres, again providing evidence that the telomeric state in these cells is altered (44).

G-Quadruplexes

The discovery that certain G-rich regions of DNA can form alternative secondary structures has changed the way we view DNA, creating the impression of a more fluid, transient molecule capable of regulating cellular behaviours through altering its own 3-dimensional structure. In the 1960's, Gellert *et al*. reported how a solution with high concentrations of guanine monophosphate (GMP) form a viscous gel when cooled. Using x-ray diffraction, the authors observed helical structures forming within the GMP gel, with 4 units per helical turn (84). This was the first evidence of G4 forming *in vitro*. In the 1980's, a number of articles developed this concept further, providing biochemical evidence of DNA oligonucleotides folding into G4 structures *in vitro*, even demonstrating their formation in the telomeric sequence (85)(86). Subsequent research has led to the development of tools to detect G4 *in vivo*, such as anti-G4 antibodies, allowing more in depth analysis of the role these structures play in the cell (87)(88).

G4 structures form in guanine (G)-rich DNA and RNA sequences - known as G4 motifs - and typically contain 4 GGG repeats broken up by between 1 and 25 nucleotides, forming the 'loops' between guanine repeats (89). These motifs fold into planar assemblies called G-tetrads that 'stack' onto one another, forming the complete G4 structure (90)(91). Further stability comes from intracellular monovalent cations that sit at the centre of the G4 structure and counter the negative charges from the O_6 position in each guanine (Figure 3a) (92).

The variability in loop sequence length and orientation of guanine repeats within each tetrad allows for many diverse organisations (93)(89)(94). For example: G4 can form within a single strand of DNA (intramolecular); between 2 strands of DNA (intermolecular/bimolecular); or between 4 strands of DNA (tetramolecular); and be parallel or anti-parallel in nature (Figure 11b) (90)(95). The latter designations are given when all 4 strands within the G4 face the same

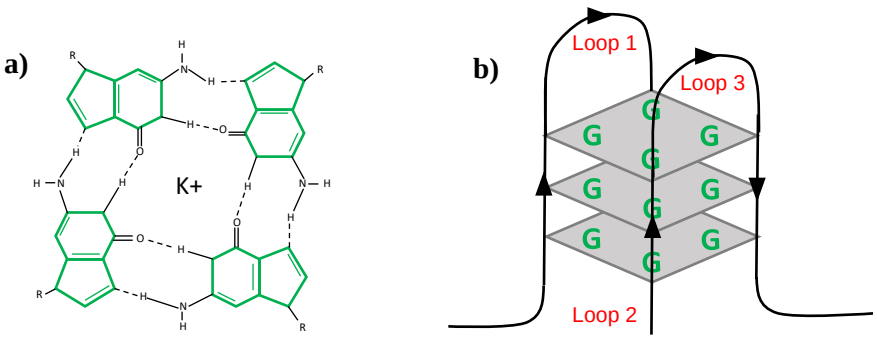

Figure 3: Development of oligonucleotide standards and controls. **a)** G-quadruplex structure depicted from above, stabilized through K+ ions at the centre. Guanine molecules in green are linked through Hoogsteen hydrogen bonding. **b)** Representation of a single G-tetrad within a single DNA strand (intrastrand).

direction or at least one strand is anti-parallel to the others, respectively (96). Even within these subtypes of G4, there are additional orientations which affect their stability in addition to the physiological concentration of monovalent cations (97). Additionally, despite G4 being able to form spontaneously, they are unlikely to breakdown in a passive manner. This is because G4 structures are more stable than even double stranded DNA once formed, suggesting certain protein(s) have an active role in G4 regulation (96). The diverse organisations of G4 as well as their non-random distribution and stable nature, brings forth questions regarding the role of G4, the mechanisms of G4 maintenance and the relevance of these structures in human disease (98).

Certain genomic regions including gene promoters, are hotspots for G4 formation, suggesting a role in transcriptional regulation (68)(99). It has been shown that G4, if unresolved, can act as barriers to transcriptional and replication machinery, triggering DNA damage responses which could be extremely detrimental to the cell (100). Telomeric DNA is also enriched for G4, however unlike gene promoters, these regions are consistently maintained as heterochromatin and transcriptional regulation is minimal (101). Despite the telomere being invariably heterochromatic, some transient changes in telomere structure do occur. During the S phase of the cell cycle, the telomere is de-compacted, allowing replication machinery to access DNA ends (9). In stem cells and most cancers, the telomerase enzyme utilises this opportunity to access the telomere, elongating the sequence and extending the cells lifespan (102). However, evidence has shown that telomerase-mediated telomere elongation can be inhibited by stable G4, suggesting telomeric G4 must be resolved for telomerase to function effectively (103). As telomerase activity is replication-dependent, it could be that unresolved G4 in this region prevents the decompaction of chromatin, thus inhibiting telomerase mediated telomere elongation (104)(105).

In recent years, studies a have shown ATRX deficiency results in increased global G4 expression, replication stress, DDR at G4 regions, TIFs and copy number alterations; all suggesting ATRX promotes genomic stability (106)(101)(100). However, it performed poorly in G4 resolution assays *in vitro*, suggesting ATRX may have an indirect effect on G4 or an affinity for specific G4 structures (107). Other helicases also possess G4 resolution ability. BLM and WRN helicases - with the help of HERC2 – resolve G4 structures with great efficiency, superior to that of ATRX (73). Similarly, the heterogenous nuclear ribonucleoprotein A1 (hnRNPA1) possesses G4 binding and resolving functions, and has been associated with the telomere (108). However, mutations in the genes encoding these proteins have not been associated with ALT, but they may act to resolve G4 in tandem with ATRX or even in its absence.

Regardless of chromosomal location, is it clear that transient resolution of G4 is essential to maintain normal cellular function. Thus, we could take advantage of the characteristic genomic instability in cancer by stabilising G4 to promote DNA damage and cell death.

G-Quadruplex stabilizers as an anti-cancer therapy

The abundance of G4 within the genome has become apparent in recent years, with prediction software highlighting over 700,000 possible G4-forming sequences in the human genome (109). The actual number of experimentally confirmed G4-forming sequences is far fewer, but still represents a surprisingly large portion of the genome (110). However, the distribution of G4 appears non-random; specific G4 enrichment has been identified in telomeres and gene promoters, with some promoters forming G4 more readily than others (95). Interestingly, many well-known oncogenes form G4, creating a potential therapeutic target for cancer (98)(111). As unresolved G4 lead to increased DDR, transcriptional dysfunction and replication fork stalling,

stabilizing G4 may increase genomic instability in the already unstable cancer cells, inducing cell death. Early on, small molecules targeting G4 DNA were developed as a way to both inhibit telomerase activity and stabilize G4. One such agent, telomestatin, is a potent telomerase inhibitor that interacts with telomeric G4 sequences and either assists in the formation of, or stabilizes pre-formed G4 in a 1:2 ratio (G4 to telomestatin) (112). However, as with many of the earlier G4 ligands, selectivity, bioactivity and toxicity were a problem.

As our understanding of G4 progresses, new generations of G4 ligands are being produced without the limitations of the earlier agents. These small molecule stabilizers are increasingly being designed to bind specific G4 structures, providing a more direct approach for G4 targeting (113). Quarfloxin (CX-3453), is a specific rDNA G4 ligand that stabilises ribosomal G4, disrupting nucleolin binding and thus RNA polymerase I transcriptional activity and is currently the only G4 ligand in phase II clinical trials (114). Following successful phase I trials on solid tumours and lymphomas, Quarfloxin is currently it is being assessed for treatment of neuroendocrine carcinoma (115).

The benefit of these more targeted G4 ligands is that off-target effects are reduced due to increased selectivity (which also permits targeting to specific G4 structures, such as the telomeric repeats). For instance, if we can develop a G4 ligand that binds with a high affinity to telomeric G4 structures and possesses the characteristics allowing it to cross the blood brain barrier, we can target telomerase-mediated telomere maintenance in brain tumours through G4 stabilization, telomerase inhibition and telomere dysfunction. Additionally, it has become evident that G4 stabilizers may be effective for inhibiting telomere maintenance in both telomerase and ALT positive cancers, making the treatment more inclusive than many others. Wang et al. recently published evidence supporting this concept, showing glioma cells treated with G4 ligands

(Quarfloxin, Pyridostatin and CX-4561) resulted in increased DNA damage and cell death. These treatments were not only effective alone, but acted synergistically with other DNA damaging agents, providing further support for the use of G4 ligands in Glioma therapy (100). Interestingly, the authors utilised an inducible ATRX knockdown model to demonstrate how loss of ATRX causes increased sensitivity to G4 ligands. This suggests ATRX expression may act to counter some of the effects of G4 stabilization, supporting the idea that ATRX acts to resolve G4, even in the presence of G4 ligands (100).

Rationale summary

G-rich telomeric DNA has been shown to form G4 DNA both *in vitro* and *in vivo*. If unresolved, telomeric G4 structures can prevent successful telomerase-mediated telomere elongation, a finding shown to be exacerbated following stabilization using G4 ligands. Addition of these ligands can result in increased DNA damage and sensitivity to DNA damaging agents, especially in the absence of ATRX. In cancer, telomerase activity has a positive correlation with expression of ATRX, suggesting the two may be linked. Further, upon ATRX loss in telomerase positive cancer cells, global expression of G4 is increased, suggesting ATRX acts either directly or indirectly to resolve G4. In total these findings support investigation into ATRX as a facilitator of telomerase activity in cancer through telomeric G4 resolution.

Hypothesis

ATRX resolves telomeric G4 to facilitate telomerase-mediated telomere elongation in cancer cells, promoting cellular immortality.

Chapter 2: Materials and Methods

Buffers and Reagents

10x TRAP buffer	10x stock; 200 mM Tris-HCL pH8.3, 150 mM $MgCl_2$, 630 mM KCL, 0.5 % Tween-20, 10 mM EGTA pH8.0.
TRAP loading dye	0.25 % bromophenol blue, 0.25 % xylene cyanol and 30 % glycerol.
TBE buffer (10x)	891.5 mM Tris base, 890 mM Boric acid and 0.01 M EDTA; pH8.0.
TAE buffer (50x)	2 M Tris base, 5.7 % Glacial acetic acid, 0.0001 M EDTA; pH8.0.
TBST	89.1 mM Tris base, 5 M NaCl, 0.1 % Tween – pH 7.5.
Tris-EDTA (TE)	100 mM Tris-HCl; pH 7.4, 10 mM EDTA; pH 8.0.
Cell lysis buffer	10mM Tris-HCl; pH 7.5, 1mM EGTA, 1mM $MgCl_2$, 150mM NaCl, 1% NP-40 (v/v), 10% glycerol.
CTA loading dye	0.2 mM EDTA, 9.5ml ddH_20, 0.05 % Xylene cyanol, 0.05 % Bromophenol blue (made up to 10ml ddH_20).
CTA buffer A	1 M NaCl, 0.5 mM EDTA, 10 mM Tris-HCl; pH7.6 (made up to 100ml dH_20).
CTA buffer B	10 mM Tris-HCl; pH 7.5.
CTA stop buffer	0.1mg/ml RNAse A, 10 mM EDTA, 2 M NaCl.
25x TNT buffer	500 mM Tris-HCl; pH 8.0, 1,5 mM $MgCl_2$, 2.5 mM each of ATP, UTP, CTP and GTP, 4 mM MgAc, 250 mM DTT.
Western running buffer	1 M Tris base, 7.6 M glycine, 1 % Sodium Dodecyl Sulfate (SDS) made to pH 8.3.
Western transfer buffer	20 % methanol, 38.6 mM Glycine, 48 mM Tris base.

Western loading dye (4x)	0.2M Tris-HCl; pH 6.8, 0.08 % SDS, 40 % glycerol, 20 % β-mercaptoethanol, 2 % bromophenol blue.
Western blocking buffer	TBST with 10 % milk (w/v).
IF blocking buffer	10 % Goat serum in PBS (v/v).
FISH wash buffer #1	70% (v/v) formamide, 10mM Tris-HCl; pH 7.2.
FISH wash buffer #2	0.1M Tris-HCl; pH 7.2, 0.15M NaCl, 0.05% Tween-20.
FISH Hybridisation buffer	70 % deionized formamide (>99.5%), 0.5% Maleic acid, 10 mM Tris-HCl; pH 7.2, 2 % PNA probe.
ELISA blocking buffer	1x PBS with 3% milk (w/v).
ELISA wash buffer	1x PBS, 0.05% Tween.
Western Blot gel (8%)	2.3ml H20, 8 % bis-acrylamide (29:1), 4 mM Tris-HCl; pH8.8, 0.1 % Sodium Dodecyl Sulfate, 0.1% Ammonium persulfate, 0.0005 % TEMED.
Agarose gel (1%)	1 % Agarose (w/v) in 1x TBE.
TRAP gel	50 % 1x TBE, 10 % bis-acrylamide (29:1), 0.004 % Ammonium Persulfate, 0.0005 % TEMED.
CTA gel (8%)	20g Urea, 1x TBE, 10 % bis-acrylamide, 0.05 % APS, 0.005 % TEMED.
Denaturation solution	0.5 M NaOH, 1.5 M NaCl
Neutralisation buffer	0.5 M Tris-HCl, 3 M NaCl, pH 7.5
20x SSC	3 M NaCl, 0.3 M Sodium citrate, pH 7.0
Hybridisation buffer	5ul Telomeric probe, 5ml DIG Easy Hyb granules (Roche)
Stringent wash buffer I	2× SSC, 0.1% SDS

Stringent wash buffer II 0.2× SSC, 0.1% SDS

AR buffer 3ml 10x Rodent de-cloaker, dH_20 27ml

Antibodies

Target	Name/Catalog #	Dilution
ATRX (C-terminal)	ab97508	1:1000
ATRX (N-terminal)	HPA001906	1:1000
ATRX (C-terminal)	H-300; sc-15408	1:1000
DAXX	H-7; sc-0843	1:1000
PML	PG-M3; sc-966	1:1000
TERT	Y182; ab32020	1:1000
β-Actin	AC15; ab6276	1:3000
G-Quadruplex	Clone BG4; MABE917	1:1000
FLAG (OctA)	H-5; sc-166355	1:200
Goat anti-mouse HRP-labelled	BioRad #1706516	1:3000
Goat anti-rabbit HRP-labelled	BioRad # 1706515	1:3000

Methods

Cell Culture

All cell lines were cultured at 37°C and 5% CO_2. HEK293, U2OS and HeLa cells were cultured in high glucose Dulbeccos Modified eagle Medium (DMEM) with 10% Fetal Bovine Serum (FBS) and 1% *Penicillin and Streptomycin*. All human Brain Tumour Initiating Cells (BTICs) were cultured in Neurocult medium supplemented with NS-A, Endothelial Growth Factor (EGF) and Fibroblast Growth Factor (FGF). BT073 and BT053 were not supplemented with FGF or EGF to regulate growth. All cells were passaged 1:4 every 5-7 days.

Generation of stable hTERT expressing cells

Retroviral plasmids pCL-10A1 (helper) and pBABE-Puro-hTERT were transfected into HEK293T cells using XtremeGene 9 transfection reagent. Plasmid DNA at 1ug was added to OptiMEM medium with 1ug helper plasmid in a 3:1 ratio with XtremeGene transfection reagent. This solution was mixed and incubated at room temperature for 15 minutes. Each well of a 6-well plate containing HEK293T cells at 70% confluence was incubated with this transfection solution for 24 hours at 37°C. At 24 hours, the transfection was repeated and 8 hours after the second transfection, media was replaced with fresh DMEM culture media. 24 hours following the second transfection, media was removed from all wells and added to a 15ml tube. The cell media was replaced, and cells were incubated for a further 24 hours. The stored media was then filtered through a 0.45uM filter by syringe into a fresh tube to remove viral particles. This media was then added to a 6-well plate containing U2OS cells at 70% confluence in the presence of 8ug/ml polybrene. U2OS cells were incubated for 24hours in the virus-containing media. The viral media was again removed, filtered and added to U2OS cells 80 hours after the initial HEK293T

transfection. Infected U2OS cells could recover for 24 hours in DMEM culture media before being put under selection in DMEM containing 0.5ug/ml and cultured as normal.

Generation of transient ATRX and ATRXt expressing cells

An ATRX overexpression plasmid was generated using the Gateway expression system. An entry vector containing full length ATRX was provided as a gift from the Campos Lab at SickKids Hospital, Toronto. Using LR clonase, the ATRX sequence was cloned out of the entry vector and inserted into a MAC-tag-N destination vector. This destination vector was another gift kindly provided by the Schriemer Lab at University of Calgary.

Generation of ATRX knockdown cells using shRNA

shRNA was designed manually based upon the sequences reported in Lovejoy *et al*, 2012 (PLoS Genetics) and generated by the DNA core facility at the University of Calgary. The scramble sequence was designed using Stealth RNAi primer design (ThermoFisher Scientific) and generated by the University of Calgary DNA core facility. All sequences were designed with *Eco*RI and *Bam*HI restriction sites at the terminal ends to allow for ligation into the selected plasmid. shRNA sequences and complimentary DNA sequences were annealed to form dsDNA which was run on a 1% agarose gel to ensure annealing was successful. The ds-shRNA sequences were then cloned into a PB-CMV-GreenPuro-M1-MCS plasmid provided by the Senger Lab at the University of Calgary. Plasmids were linearized prior to addition of shRNA using *Eco*RI and *Bam*HI restriction enzymes at 37°C for 1 hour and run on a 1% agarose gel to confirm linearization. The linearized plasmid was then isolated from the gel using a scalpel and purified using QIAquick PCR and Gel cleanup kit (Qiagen) following manufacturers instructions. Following this, a ligation reaction was performed to ligate the shRNA sequence into the linearized plasmid. The reaction mixture was then run on a 1% agarose gel to confirm success. Following this, the successfully

ligated plasmid was transformed into STABL3 bacteria as described previously. Bacterial colonies were selected and propagated overnight at 37°C on a bacterial shaker. Plasmid DNA was isolated from bacteria using the Geneaid plasmid midi-kit (Geneaid) following manufacturers instructions, and concentration determined by NanoDrop 2000.

HeLa and HEK293 cells were seeded at 500,000 cells per well in 6-well plates and allowed to adhere overnight. Plasmid DNA was transfected into the cells using Lipofectamine 3000 following manufacturers instructions. 24 hours after the first transfection, a second transfection was performed. Cells were then harvested at described timepoints between 24 – 72 hours following final transfection. If cells were put under selection, media containing 0.1ug/ml Puromycin was added to cells 24 hours after the second transfection and allowed to grow for 2 weeks before Fluorescence Associated Cell Sorting (FACS) was performed for GFP expression. All transfected cells were checked for ATRX expression via western blot to confirm knockdown.

Reverse Transcription - Polymerase Chain Reaction (RT-PCR) and Quantitative Polymerase Chain Reaction (qPCR)

RNA was extracted using TRIzol reagent according to manufacturers instructions. Following RNA extraction, concentration was determined via NanoDrop 2000. For cDNA generation, a total of 1ug RNA was then added to a RT-PCR mastermix containing; 200ng/ul random primers and 10mM each of dTTP, dCTP, dGTP and dATP to a final volume of 12ul. Samples were then incubated at 65°C for 5 minutes, then chilled quickly on ice and spun down briefly. Next, 4ul First Strand buffer and 2uL DTT was added to the RT-PCR mix which was incubated at 25°C for 2 minutes. Following this, 1ul SuperScript Reverse Transcriptase II was added to each tube and all samples were incubated at; 25°C for 10 minutes, 42°C for 50 minutes

and finally, 70°C for 15 minutes. All cDNA solutions were diluted to 100ul total with ddH20 and stored at -20°C.

qPCR mastermixes were prepared containing; 2x SYBR green mastermix and 10mM of each forward and reverse primer in a 20ul reaction. The mastermix was added to each well of a 96-well qPCR plate to which 5ul of cDNA from the RT-PCR reaction was added in triplicate wells. Plates were spun down at 2000rpm for 2 minutes before loading onto the Applied Biosciences QuantStudio Flex 6 qPCR machine. All qPCR experiments used the following thermal cycle; 95°C for 2 minutes then 40 cycles of 95°C for 15 seconds, 60°C for 30 seconds and 72°C for 30 seconds followed by a standard melt curve. All experiments were performed in both biological and technical replicates and analysed using ΔΔCt method to provide the fold change in RNA from a control sample. Calculations are as follows:

target mRNA Ct mean-control mRNA Ct mean= ΔCt

sample ΔCt-control sample ΔCt= ΔΔCt

$2^{\Delta\Delta Ct}$=Fold change in mRNA levels

C-Circle Assay (CC-assay)

DNA was extracted from cell pellets using Qiagen QiAmp DNA mini kit following manufacturers instructions. For rolling circle amplification of c-circles, a PCR was performed using 80ng sample DNA. DNA was added to a reaction mix containing; 0.2ug/ml BSA, 4uM DTT, 1mM each of dATP, dTTP, dGTP and dCTP, 0.1% Tween, 3.5U Φ29 DNA polymerase and 1x Φ29 DNA polymerase buffer to a final volume of 10ul. All samples were subjected to amplification in duplicate tubes, one tube containing Φ29 DNA Polymerase and one not containing the polymerase. All samples were run through a PCR thermal cycle of; 30°C for 8 hours

followed by 65°C for 20 minutes. Following amplification, 30ul Tris-EDTA buffer (pH7.6) was added to each tube and samples were either frozen at -20°C or used immediately for qPCR.

qPCR assays were set up using telomeric forward and reverse primers and control primers for the single-copy gene, 36B4. qPCR reactions were set up in the same manner as described in the qPCR method section. The thermal cycle performed during qPCR was as follows; 95°C for 15 minutes followed by 40 cycles of 95°C for 15 seconds and 60°C for 60 seconds. The thermal cycle was followed by a standard melt curve cycle. To calculate the fold change in c-circles in experimental samples compared to control samples, the following calculations were used:

$$\text{experimental telomeric Ct} \div \text{36B4 telomeric Ct} = \Delta Ct$$

$$\text{experimental (pol+) } \Delta Ct - \text{experimental (pol-) } \Delta Ct = \Delta\Delta Ct$$

$$2^{-(\Delta\Delta Ct)} = \text{Fold change}$$

Telomere Length Assay

Telomere length was assayed using a qPCR-based method. DNA from cell pellets was isolated using QiAmp DNA mini kit (Qiagen) following manufacturers instructions. Sample DNA was diluted in ddH20 to a final concentration of 5ng/ul. Next, 20ng of DNA was added to a reaction mix containing SYBR Green Master Mix and 0.1uM of both forward and reverse primers. The primers used for telomere length were designed to target telomeric sequence (telomeric) and a single copy gene control (36B4). The prepared reaction mix was then added onto a 96-well qPCR plate and run through the following thermal cycle; 95°C for 10 minutes, then 40 cycles of 95°C

for 15 seconds and 60°C for 60 seconds followed by a single melt curve. Telomere length was calculated using the following equations:

$$\text{mean telomeric Ct-mean 36B4 Ct= } \Delta Ct$$

$$\text{experimental } \Delta Ct\text{-control } \Delta Ct = \Delta\Delta Ct$$

$$2^{-(\Delta\Delta Ct)} = \text{Fold change}$$

Telomere Restriction Fragment Analysis (TRF)

DNA was extracted using QIAmp DNA mini kit following manufacturers instructions. TRF analysis was performed using the Telo TAGGG telomere length assay (Roche). DNA was digested using Hinf1/Rsa1restriction enzymes in a reaction mix with digestion buffer (Roche) and nuclease-free H_20. Reactions were incubated at 37°C for 2 hours. To stop digestion, 5uL gel electrophoresis buffer (Roche) was added. To separate digested DNA fragments, a 0.8% agarose gel was run in 1x TAE with 1-2ug digested DNA added to each well alongside a DIG-labelled ladder. The gel was run for 1.5-2 hours at 5V/cm. Southern blotting was then performed to transfer the DNA onto a membrane using capillary transfer. The gel was submerged in 0.25M hydrochloric acid (HCl) buffer for 5-10 minutes before washing twice in H_20. The gel was then submerged in denaturation solution for 2 X 15 minutes before rinsing twice in H_20 then re-submerging in neutralisation buffer for 2 X 15 minutes. The gel was then transferred to a nylon membrane overnight by capillary action using 20x SSC buffer. The DNA was then fixed onto the membrane via UV-crosslinking before washing in twice in 2x SSC buffer. Blots were pre-hybridized by incubating with DIG Easy Hyb granules (Roche) for 45 minutes at 42°C with gentle agitation. Hybridisation was then performed by adding Hybridisation buffer containing telomeric probe to

the membrane and incubating for 3 hours at 42°C with gentle agitation. The membrane was then washed 2x 5 minutes with stringent wash buffer 1 followed by 2 X 15 minutes in stringent wash buffer 2. The membrane was then washed twice in wash buffer (Roche) before incubation in blocking solution (Roche) for 30 minutes at room temperature. The anti-DIG-AP working solution (Roche) was then added to the membrane and incubated for 30 minutes at room temperature. The membrane was then washed 2 X 15 minutes in wash buffer followed by incubation in detection buffer for 2-5 minutes at room temperature. Substrate solution (Roche) was added to the membrane which was then placed into a hybridisation bag and incubated at room temperature for 5 minutes. The membrane was finally imaged using BioRad Chemidoc imaging system to detect signal.

Polymerase Chain Reaction (PCR) and DNA gels

For hTR analysis by PCR, cDNA was generated as described in the RT-PCR method section. A PCR mastermix containing; 10x AmpliTaq buffer, 10mM each of dATP, dCTP, dGTP and dTTP, 25mM $MgCl_2$, 10uM 46s primer, 10uM 148A primer and AmpliTaq Polymerase was made up and aliquoted into labelled tubes. cDNA was then added to each corresponding tube and all samples spun down briefly. Samples were then run through the following thermal cycle; 94°C for 2 minutes, then 25 cycles of 94°C for 45 seconds, 68°C for 60 seconds and 72°C for 30 seconds on a MasterCycler Gradient 5331 PCR machine. PCR products were then run on a 1% agarose gel containing SafeView Classic DNA dye in TAE buffer for ~20-30 minutes at 75V. PCR gels were imaged using a BioRad ChemiDoc imaging system.

Western Blotting

Protein was isolated using NP-40 lysis buffer for 30 minutes on ice and spun down to remove cell debris. Protein extracts were then quantified by Bradford assay using the NanoDrop 2000 system. For all experiments 40ug of protein was loaded onto the gel following centrifugation at boiling in SDS loading dye for 5 minutes. Gels were run at 100V through stacking gel, then at 120V through running gel for a total of 1.5-2.5 hours depending on protein target. Transfer onto a nitrocellulose membrane was performed at 100V for 1 hour in transfer buffer. Following transfer, the membrane was incubated at room temperature in blocking buffer for 1 hour. Primary antibodies were then added and incubated with the membrane at 4°C overnight. Following primary incubation, the primary antibody was removed, and membranes washed in 1x TBST for 3 X 10 minutes. Secondary HRP-labelled antibodies were then incubated with the membrane at 1:3000 dilution in 1% blocking buffer for 1 hour at room temperature. Membranes were then washed again in 1x TBST for 3 X 10 minutes before ECL reagents were added. Blots were exposed to ECL reagents for 3 minutes before imaging via BioRad Chemidoc imaging system. All quantification was performed using ImageLab software.

Immunofluorence (IF) and Fluorescence In Situ Hybridisation (FISH)

For IF assays, cells were seeded onto glass coverslips at 200,000 cells per well in a 12-well plate and allowed to adhere for 24 hours. Coverslips were then washed 2x in PBS before fixing in a 3% Paraformaldehyde (PFA), 2% sucrose solution for 20 minutes. Coverslips were then washed 2x in PBS and permeabilized in 0.5% Triton X-100 for 3 minutes followed by two more PBS washes. All coverslips were then incubated at room temperature in blocking buffer (10% goat serum) for 30 minutes. Primary antibodies were then diluted in 2% BSA and added to the coverslips. All coverslips were incubated at room temperature in a dark, humidity chamber for 1

hour. Coverslips were then washed 3x fast in PBS followed by 3 X 5 minutes in PBS. Secondary antibodies wee then added to the coverslips in 2% BSA and incubated in a dark humidity chamber for 30 minutes. Coverslips were then washed 3x fast followed by 3 X 5 minutes in PBS. For IF only, DAPI at 1:10,000 dilution in 2% BSA was added during the second 5-minute wash.

For IF-FISH, coverslips were re-fixed for 20 minutes in 3% PFA, 2% sucrose following the final IF wash step. Coverslips were then washed twice in PBS before undergoing dehydration in increasing concentrations of ethanol (70%, 80%, 90% and 100% Ethanol) for 5 minutes each. Coverslips were then allowed to dry briefly in air before adding hybridisation solution containing the telomeric Peptide Nucleic Acid (PNA) probe. Coverslips with hybridisation buffer were sealed onto glass slides using rubber cement and denatured by heating at 85°C for 7 minutes on a heat block. Coverslips were then incubated in a dark, humidity chamber overnight to allow hybridisation. Rubber cement was removed, and coverslips were washed 2 X 15 minutes in washing solution 1 followed by 3 X 5 minutes in washing solution 2. DAPI was added to washing solution 2 during the second wash at 1:10,000 dilution. All coverslips were air-dried at room temperature for 10 minutes before mounting onto glass slides using Fluoromount-G (Electron Microscopy Sciences) mounting media. Images were acquired with an AxioObserver Inverted microscope (Zeiss) using a 100x oil immersion 1.30 N.A. objective. The system is controlled by ZEN 2 (blue edition) software. Z-stacks were acquired with 0.28 µm step size and 17 steps in total. All images were flatfield and dark noise corrected using ImageJ software. Images were deconvolved with Huygens Essential version 18.10 (Scientific Volume Imaging, The Netherlands, http://svi.nl), using the Classic Maximum Likelihood Estimation (CMLE) algorithm, with SNR:40 and 50 iterations.

Telomere Repeat Amplification Protocol (TRAP)

Protein was extracted using NP-40 lysis buffer as described in Western Blotting. All protein samples were diluted in double distilled water (ddH_20) to a concentration of 1ug/ml. An aliquot of this protein dilution was then added into a separate Eppendorf tube and treated with RNase at a final concentration of 0.2mg/ml to degrade any TERC in the sample. For extension, 1ul of either diluted protein or RNase-treated protein was then added to a mastermix containing 10x TRAP buffer, 2.5mM each of dATP, dTTP, dCTP and dGTP, 0.1ug Ts primer and 2U *Taq* polymerase. This mastermix was incubated with 1ug of protein sample at room temperature for 30 minutes to allow telomerase extension. Following this, 0.1ug Cx primer and 0.5ul of [α-^{32}P]dGTP (3000 Ci/mmol, 10mCi/ml) was added to the mastermix solution and spun down to collect all liquid at the bottom of the tube. Extension reaction samples were then amplified via PCR using a Robocycler Gradient 40 (Stratagene) machine for 25-30 cycles with a thermal cycle of; 95°C for 30 seconds, 50°C for 30 seconds and 72°C for 90 seconds. Following PCR amplification, 6x loading dye was added to each mix to a final concentration of 1x. 9ul of each PCR reaction mix is then loaded onto a non-denaturing, 12% polyacrylamide (29:1, 30% acrylamide-bisacrylamide) gel and run at 1500V for 30 minutes in 0.5x TBE. The gel is then transferred onto Whatman filter paper and dried at 80°C for 1 hour on a Model 583, vacuum-sealed gel dryer. Dried gels were exposed to a phosphor-imager screen (Perkin Elmer, Super Resolution Film) for 1-2 hours at room temperature before imaging on a phosphor-imager (Perkin Elmer, Cyclone Plus) or alternatively exposed to high performance autoradiography film (Amersham Hyperfilm MP) overnight and developed manually. Any quantifications for TRAP were done by densitometry analysis using BioRad ImageLab software.

Conventional Telomerase Assay (CTA)

The CTA was performed using *in vitro* transcribed hTERT generated using the Rabbit Reticulocyte Lysate (RRL) system. For the RRL reaction to reconstitute human telomerase, the RRL TNT T7 coupled Transcription-Translation system (Promega) was used. Reaction mixtures to a total of 10ul were assembled containing; 5ul of RRL, 0.8ul TNT reaction buffer, 0.8ul TNT amino acid mixture (minus leucine), 0.8ul TNT amino acid mixture (minus methionine), 0.2ul T7 RNA polymerase, 250ng FLAG-hTERT plasmid and 250ng hTR. This mixture was incubated at 30°C for 1.5-2 hours and immediately snap frozen in liquid nitrogen and stored at -80°C.

For the CTA reaction, a 40ul reaction mixture was set up containing; 24.5ul RRL reaction product, 1x CTA buffer, 1mM each of dATP and dTTP, 1.25μM dGTP, 1.5mM 5' biotinylated telomeric ssDNA primer and 6ul [α-^{32}P]dGTP (3000 Ci/mmol, 10mCi/ml). This reaction mixture was incubated at 30°C for 3.5 hours before adding 50ul of stop buffer and incubating at 37°C for an additional 15 minutes. Streptavidin Magnasphere Paramagnetic Particles (Promega) were equilibrated by washing three times in CTA buffer A (250ul buffer per 50ul beads) before being added to the CTA reaction. The bead:CTA reaction was incubated at room temperature for 1 hour and mixed by pipetting every 15 minutes to allow the beads to bind the biotinylated primer. The beads were then separated from the reaction mix using a magnetic tube rack, then washed three times in CTA buffer and then twice in CTA buffer B. The remaining beads were then resuspended in 10ul CTA loading dye and boiled for 30 minutes before running on a Urea gel (8M) containing 8% polyacrylamide (19:1) for 1.5 hours at 1500V in 1x TBE. Gels were dried onto Whatman filter paper for 1.5 hours at 80°C and exposed to phosphor-imager screen overnight before imaging on the phosphor-imager (see TRAP method).

G-Quadruplex Enzyme-Linked ImmunoSorbant Assay (G4 ELISA)

DNA was isolated from cell pellets using the Qiagen Qi-AMP DNA mini kit according to manufacturers instructions and quantified using NanoDrop 2000. For plate set-up, a white, clear bottom 96-well plate was coated with 800ug/ml Protamine sulfate and incubated at 37°C overnight. The plate was then washed three times in wash buffer and 1ug DNA was added to each well (unless otherwise stated). The DNA coated plate was then incubated at 37°C overnight with agitation to allow the DNA to dry onto the protamine layer. The DNA was then washed three times in wash buffer followed by blocking buffer for 1 hour at room temperature. Blocking buffer was removed and the plate washed three times in PBS, followed by adding 50ul primary antibody (α-G4) per well which was incubated on the plate for 1 hour at 37°C. Primary antibody was removed and the plate was washed 3x in wash buffer followed by adding 50uL secondary antibody (α-FLAG) per well. The secondary antibody was incubated on the plate for 1 hour at 37°C, followed by washing 3x in wash buffer. Finally, 50ul of the tertiary antibody (HRP-labelled goat anti-mouse) was added to each well and incubated for 1 hour at 37°C. The plate was then thoroughly washed 6x in wash buffer and 40ul ECL solution was added to each well. The plate was incubated for 3 minutes in the dark before imaging using the BioRad Chemidoc imaging system.

Immunohistochemistry (IHC)

To generate tumours in mice for IHC staining, 100,000 cells from described BTIC lines were injected into C57/Bl6 mice subcutaneously by Haley Pederson of the Cairncross lab. These mice were then maintained in the animal facility at the University of Calgary. Mice believed to have developed tumours either due to significant weight loss and/or palpable tumour masses were sacrificed and the brain was surgically removed for analysis. Brains were initially preserved in 3%

PFA for <5 days, then transferred to 70% ethanol until sectioning was performed. Brain sections were obtained by Dr Kimberly-Ann Goring of the Senger Lab using a microtome and adhered to glass slides for staining.

Following this, tissue slices were de-paraffinized in Xylene for 2x 15 minutes followed by rehydration in decreasing concentrations of ethanol; 100%, 100%, 95% and 75% for 2 minutes each followed by distilled H_20. Antigen retrieval was then performed by submerging the slides in AR buffer in a coplin jar which was then placed inside a de-cloaker. The de-cloaker was set to heat samples at 95℃ for 45min then 121℃ for 6 minutes before being cooled gradually at room temperature.

Endogenous peroxidases were inactivated by washing slides in TBS 3 X 2 minutes followed by a 5-minute incubation in peroxidase block. Samples were then washed again in TBS for 3 X 2 minutes. Samples were then blocked in rodent block containing Triton X for 15 minutes at room temperature. Primary antibody was added to slides at a 1:500 dilution in signal stain diluent and incubated for 1 hour at room temperature in a humidity chamber. Samples were then washed 3x 2 minutes in TBS, followed by addition of a secondary polymer-HRP anti-rabbit reagent for 30 minutes at room temperature in a humidity chamber. Slides were then washed 3 X 2 minutes in TBS before DAB reagent was added to each slide and incubated for 5 minutes. Samples were then washed in distilled H_20 for 2 minutes followed by counterstaining with haematoxylin for 5 minutes. Slides were then washed in lukewarm H_20 for 1 minutes followed by 1 minute in TBST and 1 minute in lukewarm H_20 again. All slides were then dehydrated by dipping 15x in increasing concentrations of ethanol; 70%, 95%, 100% and 100% followed by 2x in Xylene. One drop of EcoMount mounting media was then used to mount a coverslip onto the slide for imaging. Imaging was performed using a color microscope.

Chapter 3: Results

In this chapter, TRF analysis was performed to determine telomere length by Nancy Adam of the Beattie and Riabowol labs (University of Calgary).

All shRNA cloning was performed in collaboration between myself , Vanessa Huynh of the Beattie Lab and Bo Young Ahn of the Senger lab (University of Calgary).

Results

Characterisation of Telomere Maintenance Mechanisms (TMMs) in a panel of human cancer cells.

The elongation and maintenance of telomeric DNA is a feature of all cancer cells, making it an effective target for therapeutic intervention (1)(2). However, agents targeting these mechanisms have proven less effective than hoped (116)(117)(118). With the development of each new drug, we discover that much remains unknown about how telomere maintenance pathways function and what key players are involved.

The Alternative Lengthening of Telomeres (ALT) mechanism is the less prevalent and less well-understood pathway compared to that of telomerase (119)(120). Investigation of the ALT pathway is dominated by identifying how the loss of chromatin remodelling protein, ATRX, is involved in both pathway activation and maintenance. It has been shown that ATRX loss alone is not sufficient to induce full activation of ALT in telomerase positive cell lines, yet expression of the protein is lost in >80% ALT cancers (121). This may be due to additional factors involved in ALT repression but one possibility to consider is rather than actively repressing ALT, this protein may be facilitating telomerase activity, thereby indirectly repressing ALT activation.. It has been shown that knocking down ATRX expression leads to a reduction in telomerase activity, coupled with an increase in some ALT features (122). ***Therefore, I hypothesized that ATRX acts to promote telomerase activity in a direct or indirect capacity.*** The mechanism by which this occurs however, remains to be elucidated.

Selecting a panel of immortalized human cell lines

When selecting a panel of cell lines to address the hypothesis, it was important to include cell lines with telomerase activity and others with ALT activity, so comparisons could be made between the two. It was essential to the project that differences in ATRX expression and activity between the two phenotypes could be determined to establish the role of ATRX in telomere maintenance. Following these criteria, human Brain Tumour Initiating cells (BTICs) isolated from Glioblastoma tumours were considered ideal as ~15-20% of these cancers have ALT activity, a higher proportion than many other cancers (37)(123). This is of particular importance as the prognosis and classification of Glioblastomas considers TMM in addition to genetic characteristics including IDH1 mutation, 1p19q loss and more recently, ATRX expression. Additionally, through the Terry Fox Research Institute (TFRI) and Brain Tumour Biobank at the University of Calgary, I had access to over 200 BTIC lines, many of which had been sequenced for mutations in both ATRX and TERT as part of a broader sequencing protocol. (124)(65)(125). Therefore, I determined that human Brain Tumour Initiating Cells derived from patient Glioblastoma samples would be an excellent source of cell lines for the purposes of this study. Additionally, sequencing data was available for a large proportion of BTICs stored at the University of Calgary through the Terry Fox Research Institute (TFRI) database, courtesy of the Cairncross and Chan laboratories. Due to the association between ATRX mutations and ALT, and TERT expression and telomerase activity, sequencing data was used to initially identify cell lines that contained mutations in either the ATRX gene or promoter region of the TERT gene for subsequent analysis. An initial panel of; BT147, BT142, BT119, BT100, BT089, BT073, BT067 and BT053, was selected for analysis to establish and characterise TMM in these cells (Table 1).

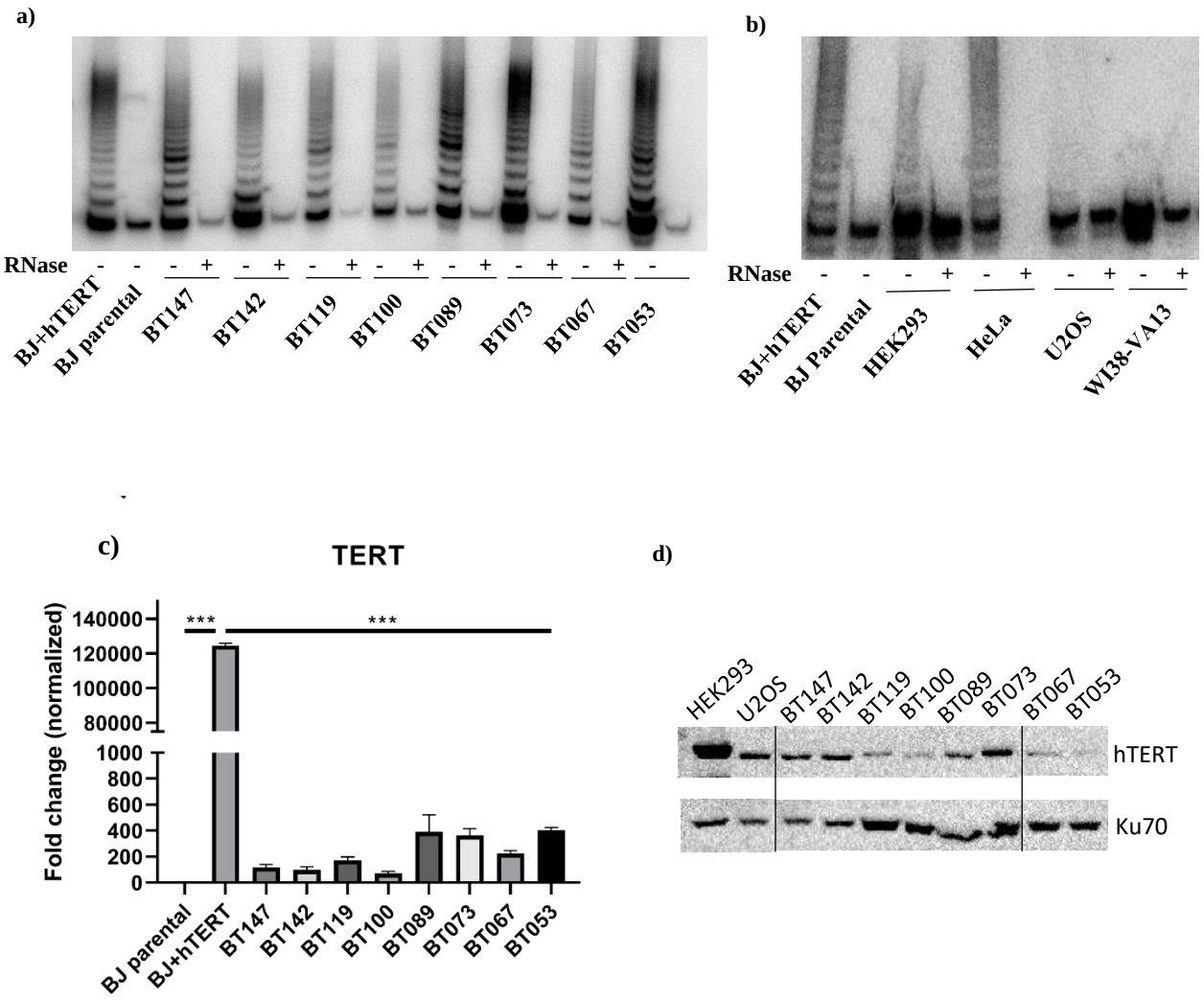

Figure 4: All human BTICs have detectable levels of telomerase activity. a) Telomerase Repeat Amplification protocol (TRAP) was used to determine telomerase activity in a panel of human BTICs or **b)** control cell lines in the presence or absence (+/-) of RNase. **c)** hTERT mRNA expression was determined through qPCR analysis and fold change was calculated relative to BJ Parental. **d)** Representative western blot for hTERT in a panel of human BTICs (n=3 for all; qPCR mean±SEM).

In addition to the panel of human BTICs, Human Embryonic Kidney (HEK293), Osteosarcoma (U2OS), cervical cancer (HeLa) and a mutant strain of lung fibroblasts (WI38-VA13) were also utilised as controls due to well-established telomerase positive (HeLa and HEK293) or ALT positive (U2OS and WI38-VA13) phenotypes (42)(126).

All BTICs in selected panel are telomerase positive and ALT negative

I initially characterised the cells lines by testing for telomerase activity by Telomere Repeat Amplification Protocol (TRAP) assay. The TRAP assay provides information regarding overall activity of the telomerase enzyme, including repeat addition processivity - the ability for telomerase to remain bound to a DNA sequence whilst continually adding repeats - in a protein lysate sample (127). TRAP data shows that all Brain Tumour Initiating Cells (BTICs) have varying levels of telomerase activity, alongside HEK293 and HeLa (Figure 4a and 4b). Conversely, WI38-VA13 and U2OS cell lines did not appear to have any detectable telomerase activity, confirming their telomerase-negative status (Figure 4b). Corresponding with TRAP results, all BTICs express hTERT mRNA and protein, as determined by qPCR and western blot respectively (Figure 4c and 4d).

To establish whether the telomerase positive cell lines were a pure population or mixed with cells utilising the Alternative Lengthening of Telomeres (ALT) pathway, further assays were used to assess ALT activity. WI38-VA13 and U2OS cell lines were used for all these assays as positive controls for ALT, confirming assay efficacy and as a direct comparison for non-characterised cell lines.

The C-Circle (CC) assay is used to determine the presence of extra chromosomal telomeric repeats (ECTR) inside the nucleus, a feature specific to ALT positive cells. Although

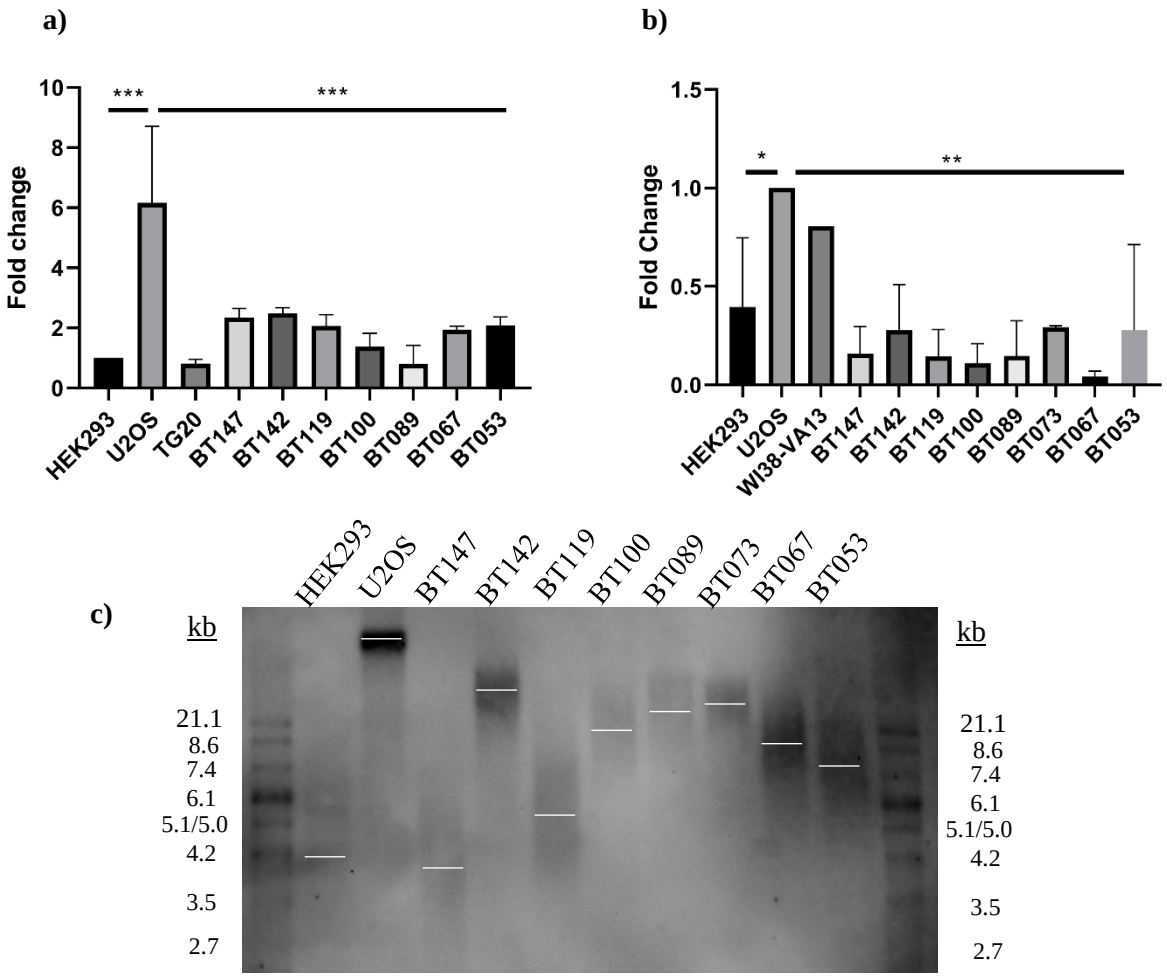

293 – 4.9 kb, **U2OS** >21 kb, **BT147** – 3.9 kb, **BT142** – 14.6 kb, **BT119** – 4.2 kb, **BT100** – 8.6 kb, **BT089** – 10kb, **BT073** – 9.7 kb, **BT067** – 7.5 kb, **BT053 -** 6.9 kb,

Figure 5: Characterisation of Telomere Maintenance Mechanism (TMM). a) A c-circle assay was used to identify any potential ALT+ cell lines through detection of extra chromosomal telomeric repeats (ECTR). Results were normalised to known ALT+ line, U2OS. **b)** Telomere length analysis via qPCR was used to identify heterogenous and long telomere populations specific to ALT+ cells. **c)** Telomere Restriction Fragment analysis (TRF) of telomere lengths in human BTICs (Completed by Nancy Adam). Statistics were performed by one-way ANOVA with Tukeys multiple comparison test (n=3 for all; qPCR mean±SEM). P<0.01**, 0.001***.

Table 1: Sequencing data for all BTICs was obtained through the Terry Fox Research Institute database (TFRI) and was analysed specifically for any alterations in ATRX and TERT genes. Results from preliminary experiments looking at TMM are summarized. Cell lines selected for further analysis are highlighted in red. + represents increasing levels of activity. 'Normal' telomere length refers to those considered ALT-.

Cell line	ATRX gene status	TERT gene status	TRAP activity	Telomere Length	C-circles
BT147	WT	C250T	++	normal	No
BT142	Q1747H	WT	++	normal/long	No
BT119	P1490S	C250T	+	normal	No
BT100	WT	C228T	+	normal	No
BT089	WT	C228T	++	normal	No
BT073	-	-	+++	normal	No
BT067	WT	C250T	+	normal	No
BT053	WT	WT	+++	normal	No

the origin of these structures is unclear, ALT+ cells express significantly more ECTR than telomerase positive or somatic cells. Many different forms of ECTR exist in nature, each with slightly different sequence confirmation. However, C-circles – defined as ECTR with the repeat sequence, AATCCC, are present at ~50-200x more in ALT+ cells making them an excellent feature to identify ALT+ cells. Following discovery of these structures, a qPCR-based technique to detect C-circles was developed and is now widely use to identify ALT activity in large cell populations (46). Results from the C-circle assay confirm the absence of C-circles in all cells with telomerase activity (Figure 5a).

I further confirmed these results by a qPCR-based telomere length assay which demonstrated that all telomerase positive cell lines tested have shorter and more homogenous telomeres when compared to ALT positive cell lines (U2OS and WI38-VA13) which have longer and more heterogenous telomeres (Figure 5b) (128). A Telomere Restriction Fragment (TRF) analysis was also performed as this is a more rigorous and widely accepted method of analysis for telomere length (129)(130). The TRF method utilises a Southern blot-based approach and is extremely well established in the field as a method of telomere length analysis, providing a strong set of results when combined with the more modern, qPCR method (131). The TRF in this thesis was performed by Nancy Adam, another student in the Beattie Lab. TRF results for all cell lines confirmed qPCR results and supported the TMM characterisations (Figure 5c). A summary of the results used for initial TMM characterisation can be seen in Table 1.

Another feature of the ALT phenotype is the localisation of the PML protein to the telomere. In ALT+ cells, PML has been shown to encapsulate telomeric DNA and this is believed to be the 'hub' of ALT mediated telomere extension (50). To detect PML localisation at the telomere, standard immunofluorescence staining was performed in conjunction with Fluorescence

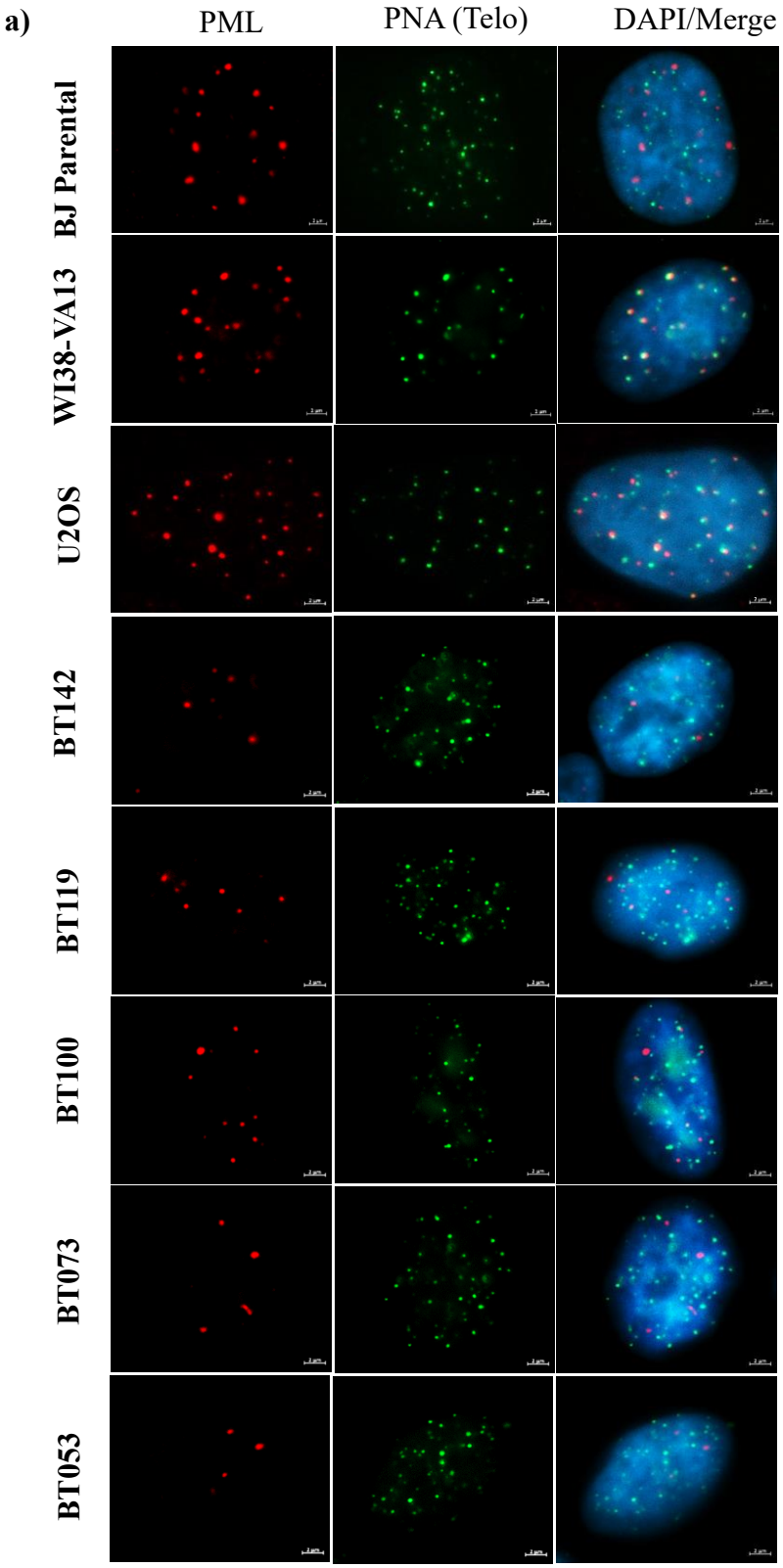
a)
PML
PNA (Telo)
DAPI/Merge
BJ Parental
WI38-VA13
U2OS
BT142
BT119
BT100
BT073
BT053

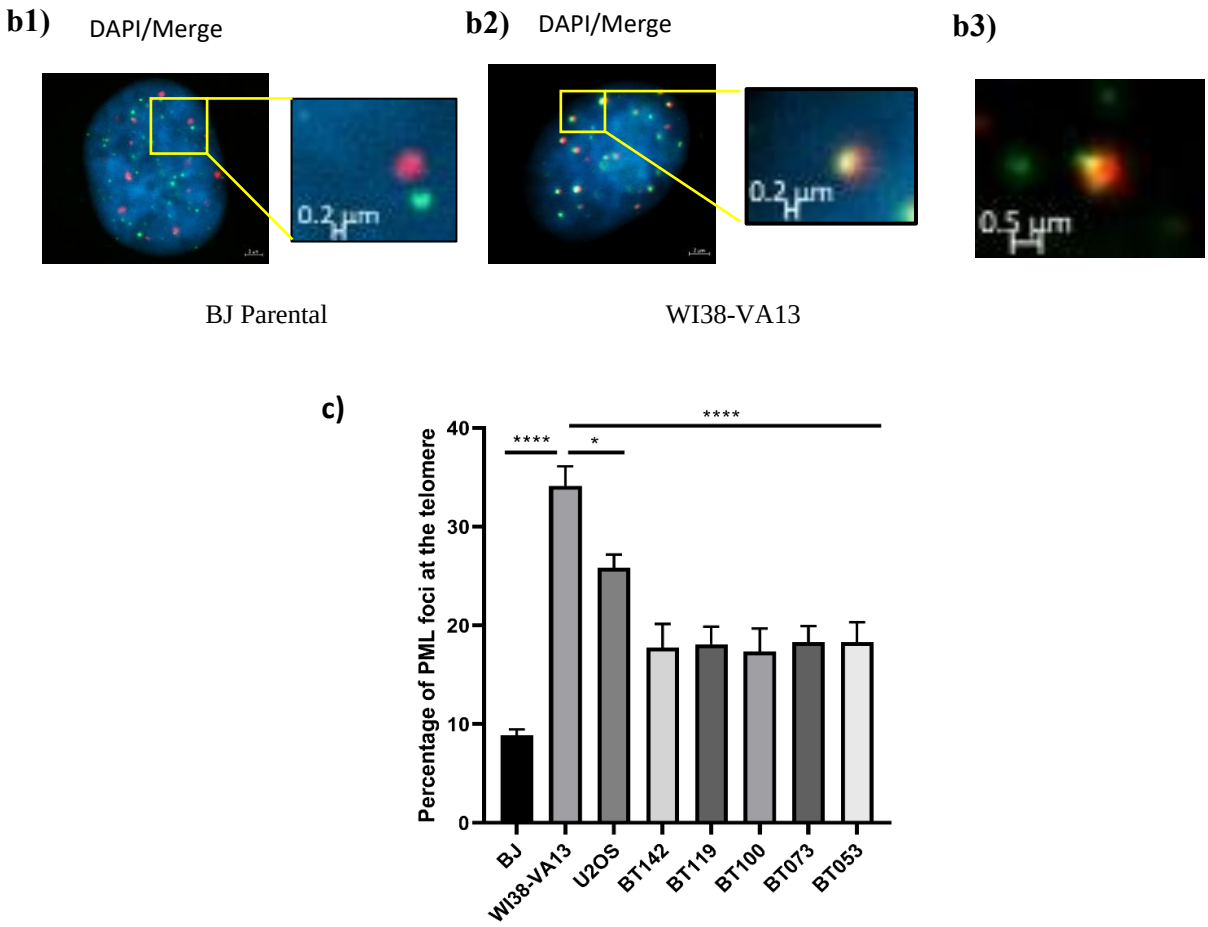

Figure 6: ALT-associated PML bodies are significantly lower in all human BTICs compared to ALT+ controls, confirming the ALT- status of selected BTICs. a) Representative images at 100x magnification show PML (red) co-localisation with telomeres stained using a telomeric PNA probe (green). **b)** Further magnified images demonstrate **(1)** lack of co-localisation versus **(2)** typical co-localisation and **(3)** multiple telomeres encapsulated in a single PML foci. **c)** Quantification of imaging represented as the percentage of PML foci located at the telomere. Statistics were performed by one-way ANOVA with Brown-Forsythe correction and Tukeys multiple comparison test. (n=3±SEM; >30 cells/repeat). P=<0.05*, 0.0001****.

In Situ Hybridisation (FISH) on the selected panel of cells. In ALT+ cell controls, telomeric DNA was encapsulated in a 'layer' of PML protein at ~30-50% telomeres, a site considered the 'hub' of ALT activity (Figure 6b.2 and 6b.3)(51)(126). In our cell panel, ALT associated PML bodies (APBs) were present in between 12-18% of telomeres as compared with between 25-35% in ALT positive cells and <10% in somatic cell controls (BJ Parental) (Figure 6a and 6c). This provides mixed results as the numbers of APBs are higher than predicted for somatic cells but not high enough to be considered ALT positive. This could be a feature of cancerous Glioma cells which has not been described previously or could suggest there is a mixed population of telomerase and ALT positive cells in these samples. The former is more likely due to the additional ALT feature analysis we performed with clear cut results. Therefore, all BTICs are considered telomerase positive and ALT negative for the purposes of this study.

Full-length ATRX protein expression does not correlate with ALT activity

The first step in establishing the role of ATRX in telomere maintenance is to determine the expression of ATRX in telomerase positive versus ALT positive cell lines. This experiment allowed me to determine if ATRX protein is lost in any telomerase positive BTIC lines, including those with genetic ATRX mutations.

To do this, western blot analysis was performed using one N- terminal and two different C-terminal antibodies. It has been reported in the literature that degradation products of ATRX can be detected via western blot and that this can be avoided by using an N-terminal antibody which binds to the first section of the protein sequence, thereby not recognising any C-terminal degradation products (132). The western blot results showed that at the predicted size of 280kDa, bands are present in all cell lines except for U2OS, BT073 and BT053 (Figure 7a and 7b). This

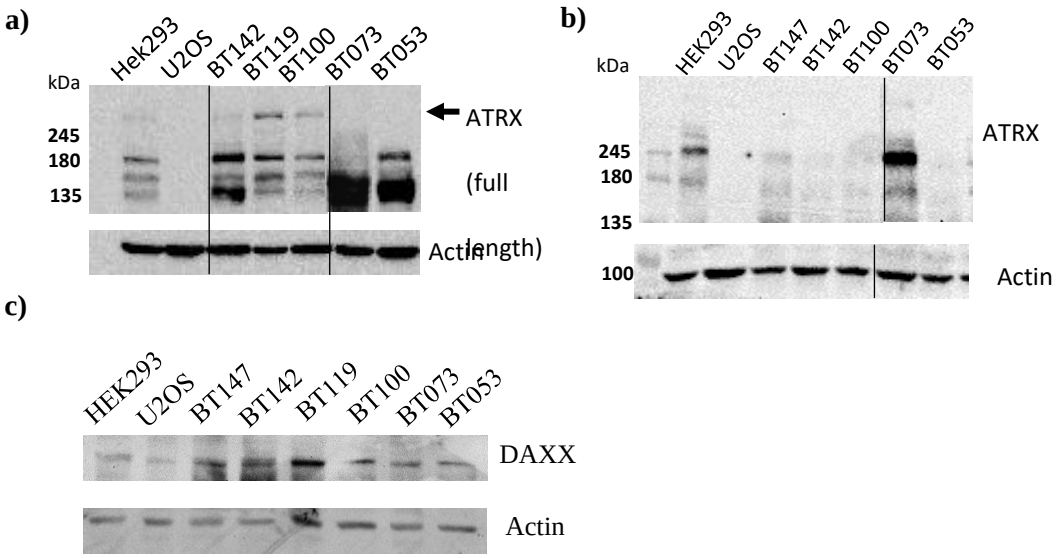
a)
Hek293
U2OS
BT142
BT119
BT100
BT073
BT053
kDa
245
180
135
ATRX
(full
length)
Actin
b)
HEK293
U2OS
BT147
BT142
BT100
BT073
BT053
kDa
245
180
135
100
ATRX
Actin
c)
HEK293
U2OS
BT147
BT142
BT119
BT100
BT073
BT053
DAXX
Actin

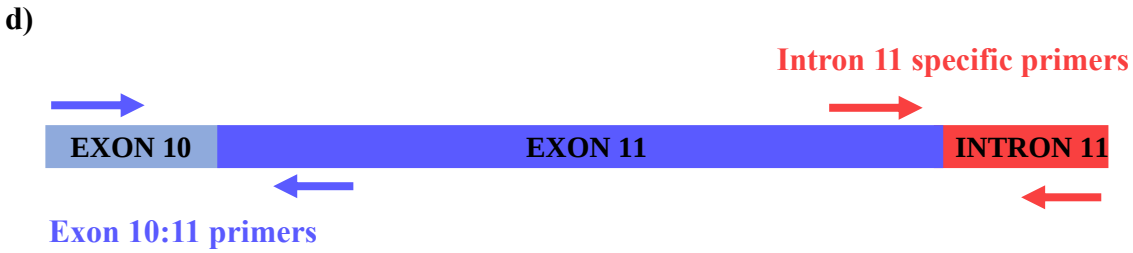
d)
Intron 11 specific primers
EXON 10
EXON 11
INTRON 11
Exon 10:11 primers

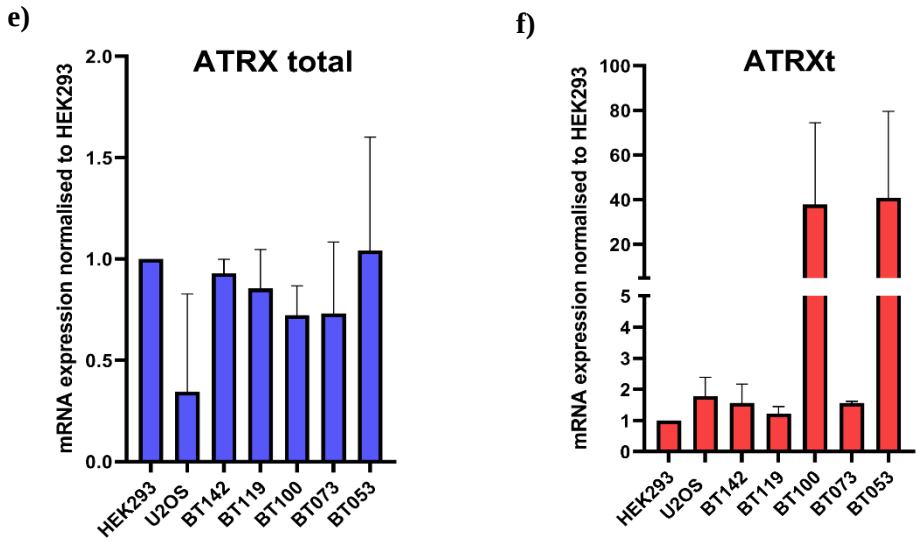
e)
ATRX total
mRNA expression normalised to HEK293
2.0
1.5
1.0
0.5
0.0
HEK293
U2OS
BT142
BT119
BT100
BT073
BT053
f)
ATRXt
mRNA expression normalised to HEK293
100
80
60
40
20
5
4
3
2
1
0
HEK293
U2OS
BT142
BT119
BT100
BT073
BT053

Figure 7: Multiple isoforms of ATRX are expressed in a panel of immortalised human cell lines. **a)** Representative western blot using a C-terminal antibody against ATRX in a panel of human cell lines. **b)** Representative western blot using an N-terminal antibody against ATRX. **c)** Representative western blot of DAXX to confirm protein expression. **d)** Linear representation of primer binding specific for ATRXt at intron 11. **e)** qPCR analysis of total ATRX mRNA using primers targeting a region common to all ATRX isoforms. **f)** qPCR analysis of ATRXt using primers targeting intron 11, specific to ATRXt (n=2; mean±SEM). Statistics performed using one-way ANOVA and Tukeys multiple comparison test. $P<0.05$*, 0.001*** (n=3 for westerns).

presented an interesting finding as both BT073 and BT053 are confirmed to be telomerase positive, with no detectable ALT features. However, lack of ATRX protein is also considered a strong feature of the ALT phenotype, making these cells lines a complex classification (44)(125). Additionally, multiple, lower molecular weight bands were consistently seen when probed with for both N- and C-terminal antibodies (Figure 7a and 7b). In this experiment it was important to use antibodies against different regions of ATRX as some C-terminal antibodies may pick up degradation products, whereas the N-terminal antibody should not. Thus, results from both antibodies suggest the presence of genuine ATRX isoforms as the same bands are detected using both N and C-terminal antibodies (with the exception of a band at ~150kDa detected by only the C-terminal antibody which was excluded as an isoform). One known isoform, ATRXt, is a truncated isoform of ATRX shown to be expressed in many tissues of the body at up to 50% the expression of the full-length protein (133). This truncated version of ATRX has a predicted band size of ~180-200kDa, which we see prominently featured on our gels (Figure 7a and 7b). Is it not clear however, whether the remaining bands seen on the western blot correspond to any know isoforms of ATRX. Additionally, all cell lines were probed for DAXX, a known binding partner of ATRX (Figure 7c). I probed for DAXX in addition to ATRX, as it has been reported that for ATRX to function as a chromatin remodeler in the cell, DAXX must be present and loss of DAXX expression is associated with induction of ALT in some cell types (64)(134)(135). Western blots for DAXX showed expression in all BTIC lines, confirming that any detectable ALT activity likely does not result from DAXX loss. It does not however, rule out the possibility of non-functional proteins. Sequencing data confirmed the WT status of the DAXX gene in the cell panel, so any functional issues with DAXX in these lines would likely be post-translational. Therefore, these *in vitro* findings confirm the ALT+ status of U2OS and WI38-VA13, the telomerase positive status

of HEK293 and HeLa and demonstrate that although some of the BTICs present with mixed expression of ATRX protein, I conclude that they should be considered telomerase positive.

To further confirm that the truncated isoform of ATRX, ATRXt, is present in the selected panel of cell lines, qPCR was performed using primers targeting either the exon:exon junction between exons 10 and 11, common to all isoforms, or primers targeting the first 183bp of intron 11, a region specific to ATRXt (Figure 7d). qPCR analysis was performed for both total ATRX (all isoforms) and ATRXt specifically. ATRXt was present in all samples to varying degrees, with BT100 and BT053 having the highest expression of this isoform, almost 40-fold higher than the HEK293 control (Figure 7e and 7f). This does not correlate directly with the total ATRX bands seen via western blot or total ATRX mRNA levels. It does however, confirm that all BTICs express ATRXt mRNA and that this mRNA largely appears to be translated into protein.

As the expression of proteins has been shown to change when cells are cultured for extended periods of time, I wanted to determine if ATRX protein expression was altered when cell lines were allowed to grow in a physiological setting. As human BTICs are stem-like in nature, they are able to form palpable tumours starting with as little as 100,000 cells. Therefore, I used the selected panel of BTICs to determine if any differences in ATRX expression were seen in cell culture versus *in vivo*. For this experiment, BTICs were injected subcutaneously into C57/Bl6 mice and allowed to form tumours. Tumour bearing mice were then sacrificed and their brain tissue subjected to IHC analysis to detect ATRX expression throughout the tumour. In order for the IHC analysis to be unbiased, both myself and a colleague (Gallo Lab) scored the samples based upon existing guidelines whilst blinded to the cell line information (136). The existing guidelines for ATRX scoring in IHC analysis are somewhat unclear, so for the purpose of this study we identified 3 groups of staining score; positive score means <90% cells stained for ATRX, negative score

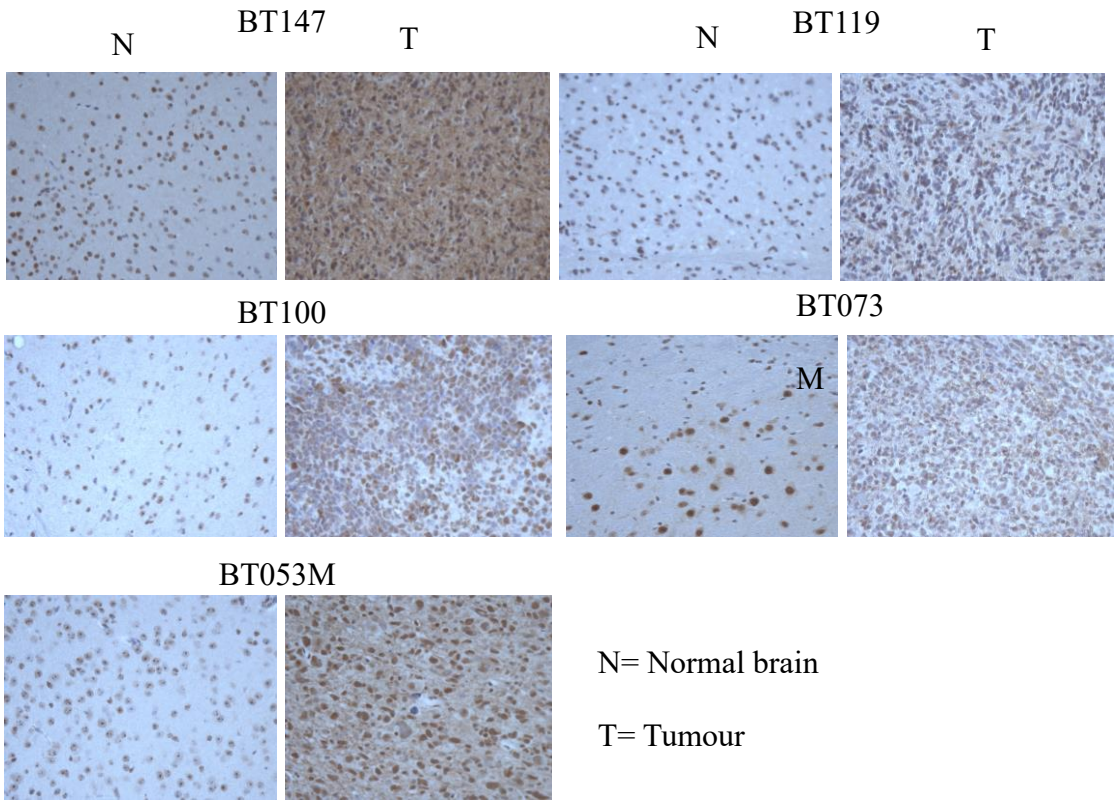

Figure 8: Clinical ATRX determination via IHC is not specific for full-length ATRX and is likely detecting alternative isoforms. Immunohistochemical analysis of ATRX in murine brain tissue sections following subcutaneous injection of BTIC cells. Animals were sacrificed only when they were showing symptoms of tumour burden. Staining was graded as positive or negative based upon existing criteria used clinically for Glioma diagnosis (n=3).

Table 2: Summary of ATRX expression documented through qPCR (qPCR), Western Blot (WB) and Immunohistochemistry (IHC) for the selected panel of BTICs. + represents expression of ATRX and – represents no expression pf ATRX for western blot analysis. For IHC analysis, + represents a positive ATRX profile, Int. represents an intermediate ATRX profile and – represents a negative profile for ATRX staining.

Cell Line	ATRX (qPCR)	ATRX (WB)	ATRXt (WB)	ATRX (IHC)
BT142	0.777	+	Strong +	+
BT119	0.540	Strong +	+	+
BT100	0.837	+	+	Int.
BT073	0.441	-	-	-
BT053	0.007	-	Strong +	+

means <10% cells stained for ATRX and intermediate score means between 10-90% cells stained for ATRX (137). Interestingly, ATRX expression in many of the BTICs correlated best with the ATRXt band seen in the previous western blot analysis (refer to figure 7a). For example, BT053 shows no full-length ATRX expression via western blot but had very strong expression of a band corresponding to the 200kDa ATRXt isoform, which matched IHC results also showing very strong ATRX expression within the tumour mass. Similarly, BT073 showed no expression of ATRX or ATRXt bands via western blot and shows little to no expression of ATRX within the tumour via IHC analysis (Figure 8 and Table 2). These data raise two key questions regarding ATRX expression as a marker for ALT; does ATRX expression differ in cell culture versus *in vivo* and do clinical antibodies detect alternative ATRX isoforms in tumour samples? Answering these questions could be of vital importance to the clinic as expression of ATRX and therefore ALT, in Glioma can significantly alter patient prognosis (Figure 1a and 1b) (125).

ATRX localisation with PML is maintained to some degree by the ATRXt isoform in absence of full length ATRX

One question that remains is although ATRX may be detectable in many of these BTICs, is it functional? To begin to answer this question, IF analysis was performed on the selected BTICs with U2OS and BJ fibroblasts acting as ALT positive and telomerase positive controls respectively. By analysing the co-localization of ATRX with PML, it was possible to determine if this role of ATRX was maintained in all BTICs or perhaps compromised in those lacking the full-length protein (77)(138). Results show that >97% ATRX foci co-localised with PML in BJ fibroblasts whilst in U2OS, absence of ATRX expression was confirmed. Co-localization between ATRX and PML in BTICs was an average of ~70%, over 20% less than the positive control (Figure 9a and 9b).

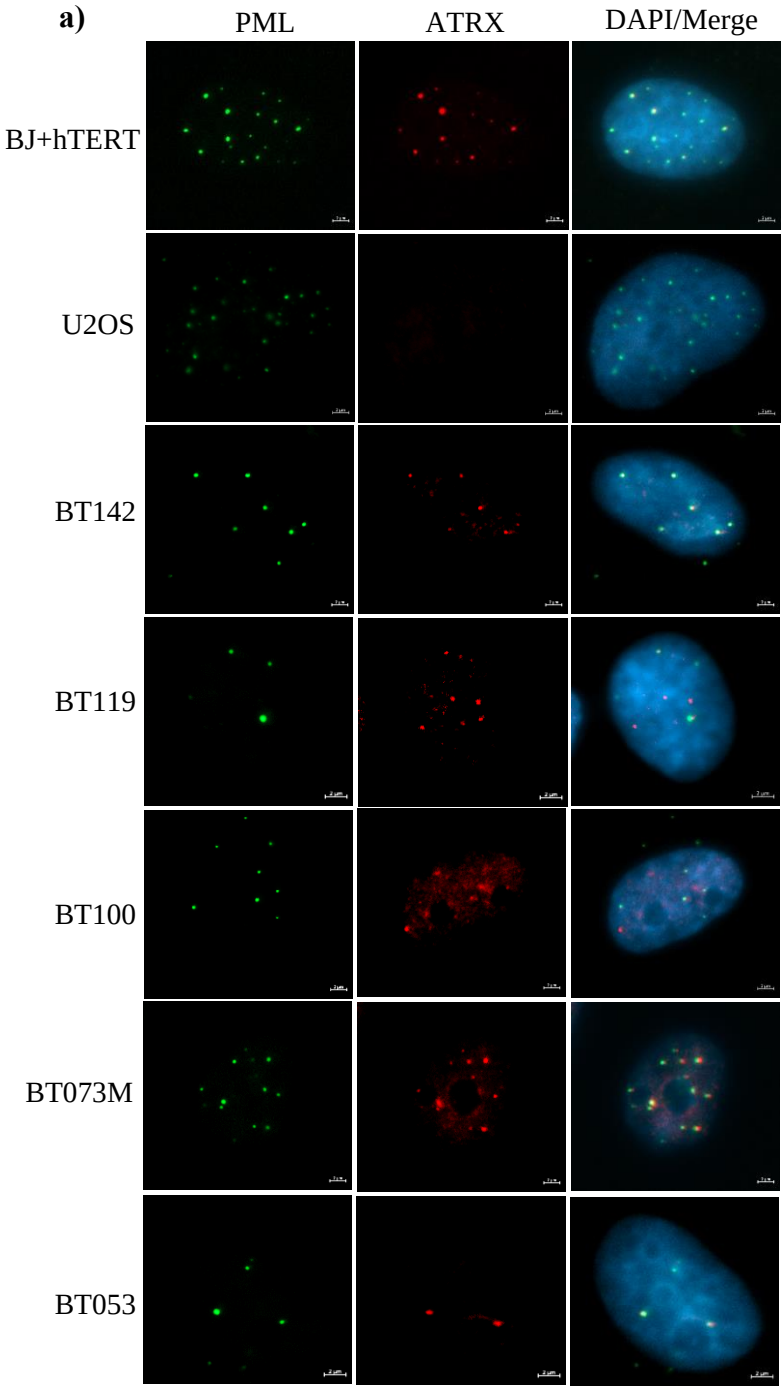
a)
PML
ATRX
DAPI/Merge
BJ+hTERT
U2OS
BT142
BT119
BT100
BT073M
BT053

b)

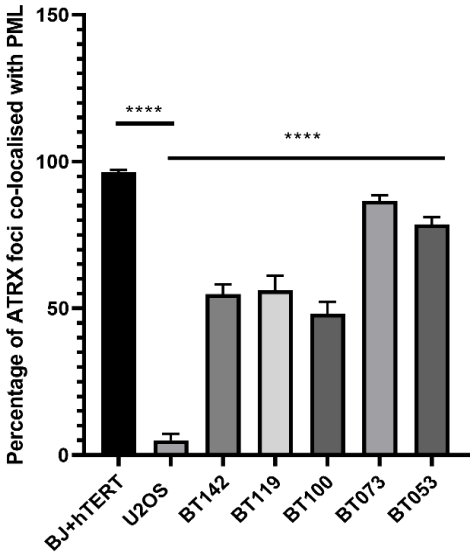

Figure 9: Functional assessment of ATRX through immunofluorescence co-localisation with known interacting partner, PML. **a)** Representative images at 100x magnification show PML (green) and ATRX (red) co-localisation for the selected panel of human cell lines. U2OS represents a negative control due to absence of ATRX expression while BJ+hTERT represents an ATRX and telomerase+ control. **b)** Quantification of ATRX and PML co-localisation shown as the percentage of ATRX foci co-localised with PML foci, per nuclei averaged over 60-90 cells per condition. Statistical analysis by one-way ANOVA with Brown-Forsythe correction. P<0.0001****. (n=3; >30 cells per repeat)

This confirmed their ALT- status, however provided a somewhat intermediate phenotype. Interestingly, the two BTICs lacking full-length ATRX had the highest degree of co-localisation at >80%. This data suggests that additional ATRX isoforms may be able to compensate for lack of the full-length protein in some aspects of ATRX activity. This could explain why the two BTIC lines lacking the full-length ATRX protein are not ALT positive, perhaps truncated isoforms are able to maintain suppression of the ALT pathway and allow telomerase activity to prevail.

To further test the ability of ATRX and ATRXt to localise with PML, I generated U2OS cells expressing either full-length ATRX full length or ATRXt. For the ATRX expression vector, the gateway system was used. An entry vector containing the full-length ATRX sequence was kindly provided as a gift by the Campos Laboratory at SickKids Hospital (Figure 10a). This vector is designed for one-step resection and ligation into a gateway destination vector as all gateway vector contain the same attL and attR cut sites, allowing the ATRX construct to be cut out of the entry vector and ligated into the MAC-N-tag destination vector in a single reaction utilising the LR clonase enzyme (Figure 10b)(139). This generated a successful set of clones which were then grown up and transfected into U2OS cells. U2OS was selected for this purpose as it has no telomerase or ATRX expression, providing a 'blank slate' for expression of either ATRX or ATRXt alone, without interference from endogenous protein. Western blot analysis confirmed expression of ATRX in U2OS following transfection (Figure 10c).

For ATRXt expression in U2OS cells, the ATRX-gateway-entry vector was used to transfer the full-length isoform into an eGFP-C2 plasmid (Figure 10a). PCR primers with restriction cut sites were then designed to target the region of ATRX to be truncated, providing targeted cut sites for restriction enzymes to truncate the sequence at the desired site. This produced the eGFP-C2-ATRXt plasmid which was subsequently transformed into bacteria and transfected into U2OS

a)

ATRX-gateway-entry vector

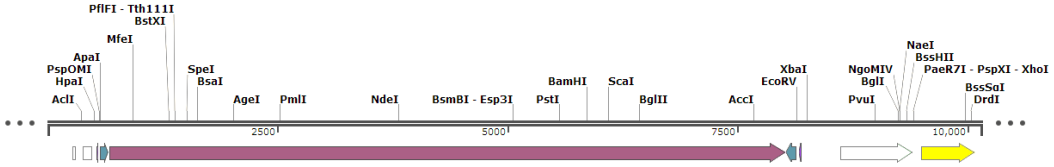

b)

MAC-N-Gateway vector

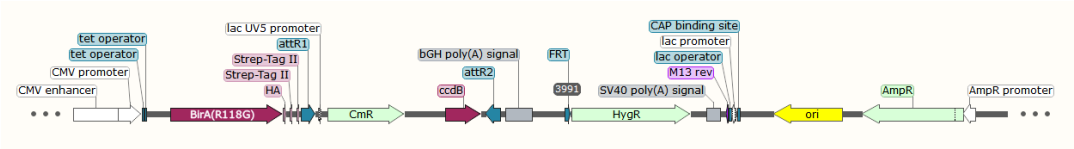

c)

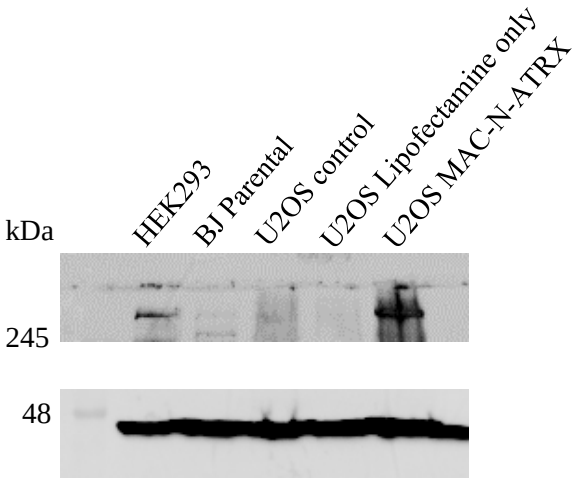

Figure 10: Generation of ATRX expressing U2OS cells using the Gateway expression system. **a)** Linear map of the ATRX-Gateway-Open entry vector and **b)** the MAC-tag-N destination vector used for cloning (plasmid maps generated by Snapgene). The ATRX sequence is cut out of the entry vector and inserted into the destination vector in a single reaction using LR clonase to generate the MAC-N-ATRX plasmid. **c)** A western blot was performed following transfection with the MAC-N-ATRX plasmid. Protein was lysed directly on plate in 20ul NP-40 and 10uL SDS LB (for all conditions other than HEK293 and BJ Parental)(n=2).

a)

eGFP-C2 plasmid

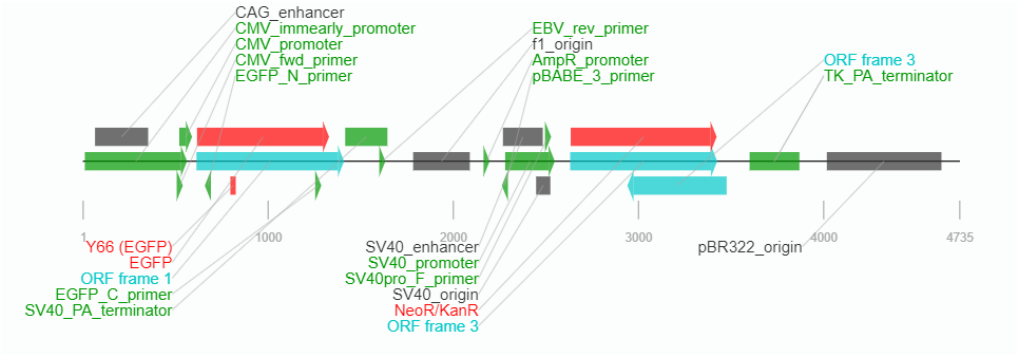

b)

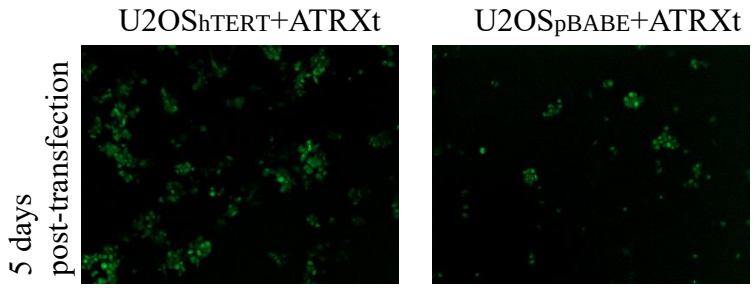

Figure 11: Generation of stable hTERT expressing U2OS cells and transient ATRX and ATRXt expressing U2OS cells. a) Linear plasmid map of eGFP-C2 plasmid used for generation of ATRXt cells. All cloning was performed by Fang (RDSC member). ATRXt was generated in a reaction with primers designed with internal restriction sites to cut at the beginning of the ATRX sequence and 183bp into exon 12 to result in the truncated ATRXt isoform. **b)** Representative images show GFP signal in transfected U2OShTERT and U2OSpBABE cells.

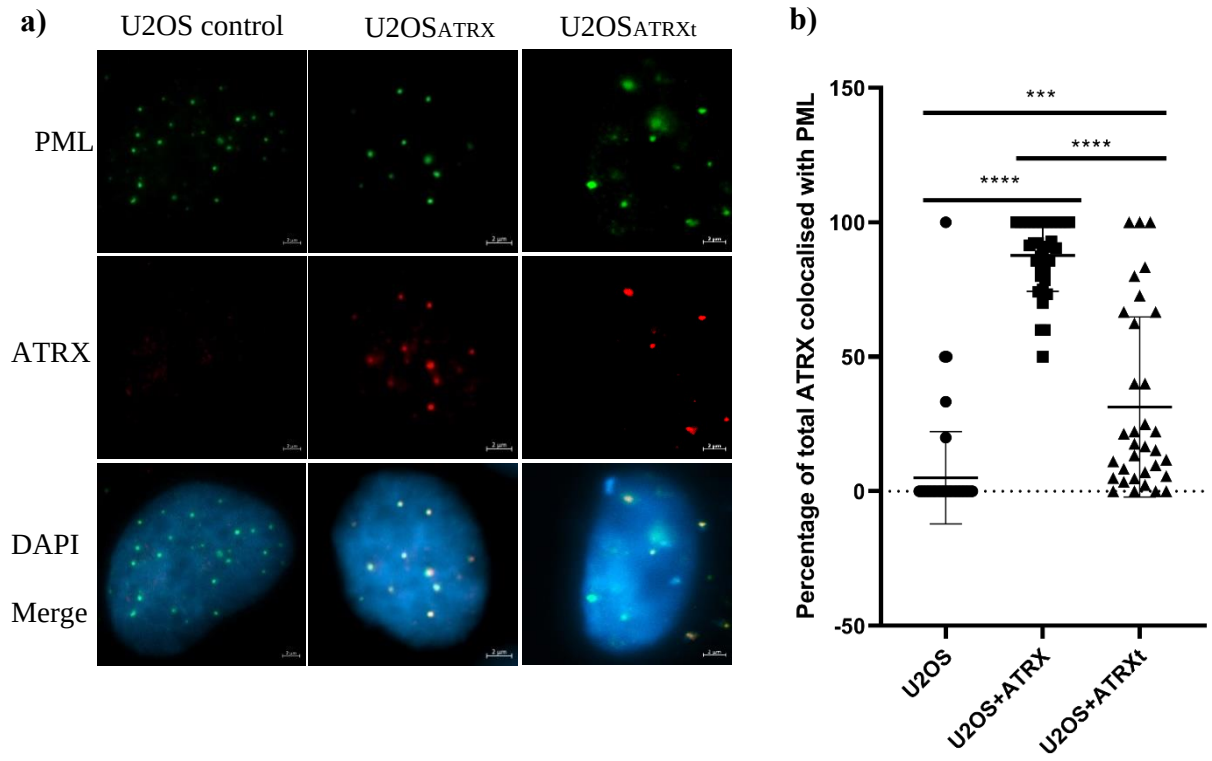

Figure 12: Immunofluorescence analysis of ATRX and PML in U2OSATRX cells. **a)** Representative images at 100x magnification show ATRX (red) and PML (green) co-localisation in U2OSATRX and U2OSATRXt cells. **b)** ATRX co-localization with PML in U2OSATRX and U2OSATRXt cells is significantly higher than control U2OS cells. However, U2OSATRXt cells also show a significant defect in colocalization compared to U2OSATRX cells. Results are shown as the percentage of total ATRX co-localised with PML foci on average per cell. Statistical analysis by Welch's ANOVA with Brown-Forsythe correction. P=<0.001***, 0.0001**** (n=3; >30 cells per repeat).

cells. Western blot analysis was not able to be completed for this transfection as the maximum transfection efficiency only reached 30%. However, as the plasmid expressed both GFP and the ATRXt protein under the same promoter, GFP signal was used to establish expression of ATRXt for IF analysis (Figure 10b).Immunofluorescence analysis of ATRX and PML co-localisation following transfection of U2OS with either ATRX or ATRXt showed full-length ATRX maintained complete co-localisation with PML as expected, however, ATRXt showed a significant defect in ability to co-localise with PML in these cells (Figure 12a and 12b). The co-localisation between ATRXt and PML was on average ~40% of the full-length protein, which could suggest that even functioning at 40% capacity, ATRX is still able to repress ALT and support telomerase-mediated telomere maintenance (Figure 12b). In support of the association between ATRX and telomerase activity, a moderate positive correlation was found between total ATRX protein expression and overall telomerase activity (Figure 13a). This correlation was not seen at mRNA levels however, further supporting that the mRNA expression of ATRX is of less consequence to telomerase activity than protein expression (Figure 13b). However, by simply using IF co-localisation, it is not possible to establish if ATRXt maintains the helicase or DNA binding abilities of the full-length ATRX protein.

ATRX has a number of established roles within the cells, however, in this study we focus on one in particular. ATRX has been shown to breakdown a secondary DNA structure known as a G-quadruplex. These structures form in G-rich DNA and can form a blockade to replication and transcription machinery if unresolved. It is currently thought that G4 exist as a means of epigenetic regulation for genes and research into these structures is becoming increasingly prominent. In addition to genetic regulation, G4 are also found at the telomere, a region abundant in guanine repeats. As it has been established that ATRX localises to telomeric DNA for chromatin

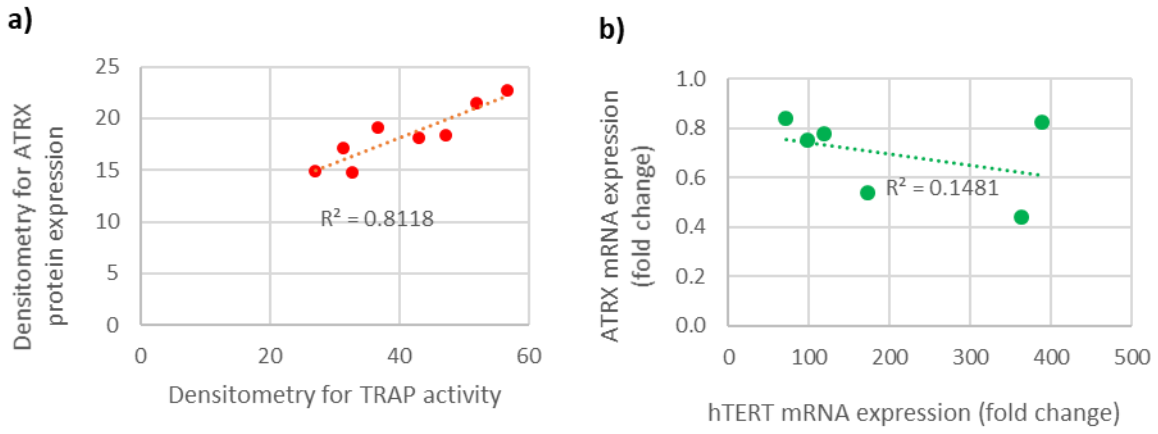

Figure 13: ATRX protein expression correlates with telomerase activity. **a)** The correlation between telomerase activity and ATRX protein expression shows a strong positive relationship. **b)** The correlation between ATRX and TERT mRNA expression shows little to no relationship (n=3).

remodelling purposes and possesses G4 resolution abilities, it follows that ATRX may have a role in telomeric G4 resolution. Therefore, I wanted to determine if ATRX loss could impact global and telomeric G4 DNA. Unfortunately, techniques to measure G4 in genomic DNA are lacking, and those that have been developed do not allow accurate quantification,

Part two of my results describes the development and optimisation of a novel method for G4 detection in genomic DNA samples that can be quantified using oligonucleotide standards. This method allows accurate and quantifiable detection of G4 in genomic DNA samples, thereby providing a method to analyse the effect of ATRX loss on G4 structures in vitro.

Development of a novel G-Quadruplex detection method

To investigate the role of ATRX in G4 resolution, I needed to develop an assay which accurately measures and quantifies G4 in gDNA samples. The breakdown of G4 by ATRX is a key avenue of interest in this study as it will help determine whether this function is related to the role of ATRX in facilitating telomerase mediated telomere maintenance. It has been well-established that telomeres, with their G-rich, repetitive sequences are hotspots for G4 formation (140)(93). Interestingly, it has also been shown that telomerase, although possessing some G4 resolution ability, cannot fully resolve stable G4 structures alone (141)(142). Thus, another G4-resolving protein likely plays a role at the telomere to facilitate telomerase-mediated telomere elongation. ATRX has been shown to localize to G4 enriched DNA and possess some G4 resolution abilities (71)(143)(122). ***Therefore, we hypothesize that ATRX is an essential regulator of telomeric G4 structures and is required to resolve G4 both globally, and at the telomere to facilitate telomerase-mediated telomere elongation.***

To determine if ATRX is involved with G4 resolution, we must be able to investigate G4 levels in cell population both specifically at the telomere and more globally. One current method for global G4 analysis uses IF to detect any G4 DNA present in the nucleus, however this technique comes with significant disadvantages (87)(144). Issues common to IF analysis are even more pronounced when staining for G4; high foci count, background fluorescence and lack of standardized analysis guidelines are all limitations which make optimization extremely important yet time-consuming. Other methods have been established as an alternative to IF, however these are only applicable to a more targeted analysis of specific G4 regions. Techniques such as chromatin-immunoprecipitation coupled with qPCR (ChIP-qPCR) or Chromatin Immunoprecipitation coupled with DNA sequencing (ChIP-Seq), have been successfully used to identify G4-forming sequences and the protein which interact with them (69)(145). More recently, a qPCR-based stop assay has been developed to detect G4 in specific DNA sequences. The results of this assay show reduced Ct values following amplification of known G4-forming sequences in the presence of G4 stabilizing compounds, providing another targeted assay for G4 (89). Each of the described methods has its own advantages and drawbacks, however the inability to utilise these methods to accurately measure global G4 in genomic DNA samples remains consistent. Due to these constraints, we set out to develop a more reproducible and time-efficient assay for global G4 quantification in genomic DNA samples. However, if a new method is to be established for G4 quantification, it is essential to compare findings to the existing method. Therefore, IF for G4 was performed on a refined panel of cell lines with either telomerase or ALT TMMs.

Immunofluorescence analysis of global and telomere-specific DNA G-quadruplexes

Through human genome sequencing, it has become clear certain regions of mammalian chromosomes are more G-rich than others, creating hotspots for G4 formation. These

chromosomal regions include repetitive DNA, such as telomeres and centromeres, as well as regions involved in transcription, such as gene promoters (146)(98)(147). However, detecting these structures *in vivo* has proven somewhat difficult. Recent advances have led to the development of specific G4 antibodies, which can detect both DNA and RNA G4 structures in human cells and are amenable to immunofluorescence-based assays (87)(88). One such antibody, clone BG4, has been used extensively to visualise G4 in IF, providing an excellent starting point for global G4 analysis in our panel of cells. Using this antibody, G4 were detected in a refined panel of human cell lines; HEK293, U2OS, HeLa, WI38-VA13 and BT073M (Figure 13a and 13c).

Unfortunately, this method of G4 detection was insufficient to accurately quantify G4 in some of the cell lines due to high background and indistinguishable foci (Figure 14b). However, IF analysis of G4 and TRF2 in combination did allow for quantification of telomeric G4 in HeLa, U2OS and WI38-VA13, demonstrating that the BG4 antibody appears to be targeting DNA G4 hotspots with an affinity supported by literature (Figure 15a and 15b) (87)(148). To further assess the accuracy of G4-binding by the BG4 antibody, positive and negative controls were used. As it is not possible for a cell line to be G4-deficient or overexpressing, we utilised both G4 stabilizing and destabilizing agents to increase or decrease G4 signal. Using 1mM of the potent G4-stabilizer, Pyridostatin (PDS), G4 signal in HeLa, U2OS and WI38-VA13 was significantly increased, confirming both the ability of PDS to stabilize G4 and BG4 binding affinity (Figure 16a and 16b)(111). Unfortunately, the negative control, 2mM Zinc Chloride ($ZnCl_2$), had a detrimental affect on cellular morphology, making IF imaging extremely difficult and accurate analysis impossible (90).

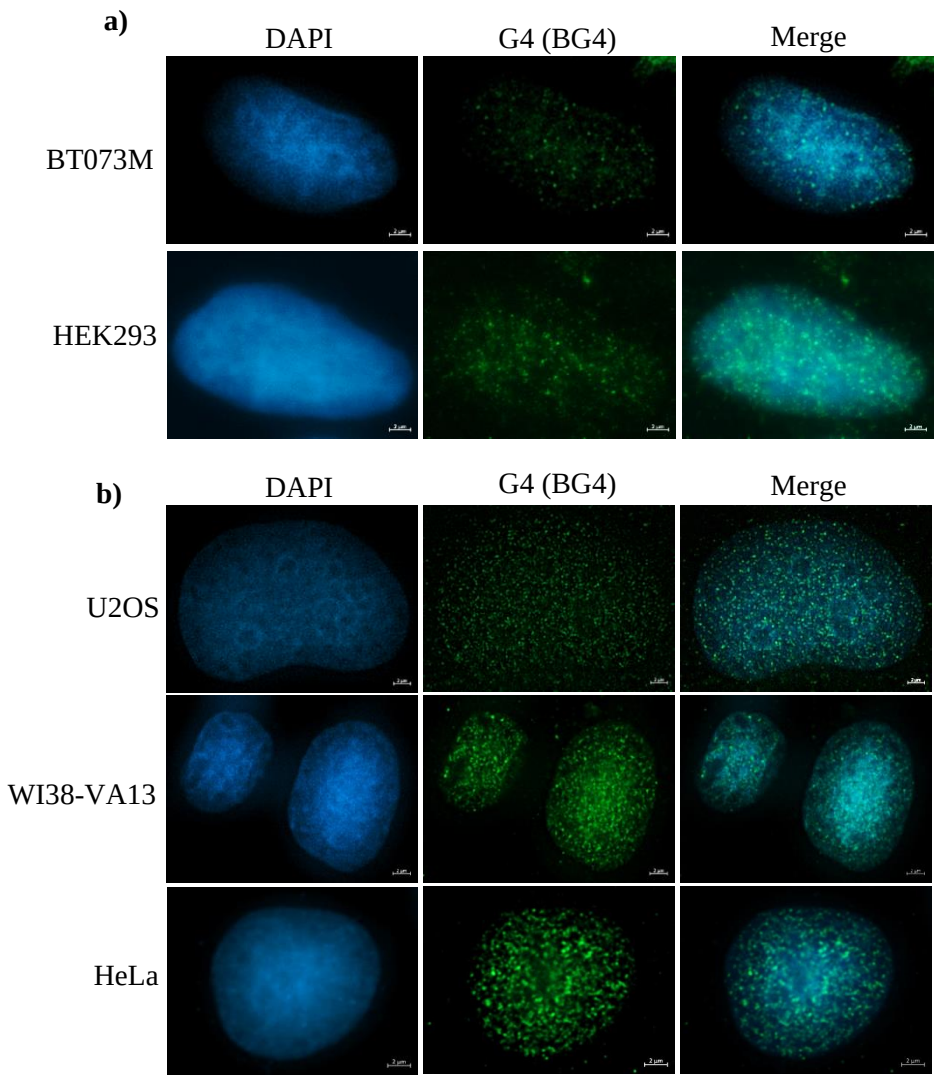
a)
DAPI
G4 (BG4)
Merge
BT073M
HEK293
b)
DAPI
G4 (BG4)
Merge
U2OS
WI38-VA13
HeLa

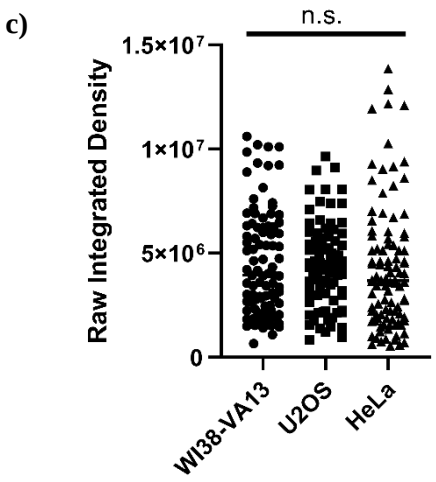

Figure 14: Comparison of G4 quantification using current G4 analysis via immunofluorescence with G4 ELISA. a) Representative images at 100x magnification for BT073M and HEK293 cells stained via IF. However, due to the nature of staining for G4, the image quality was not consistently sufficient for accurate quantification. **b)** Representative immunofluorescence images showing staining for G-quadruplexes using BG4 antibody in U2OS, WI38-VA13 and HeLa cells. **c)** Quantitation of raw integrated density values from each of the cell lines measured. Statistical analysis by Welch ANOVA with Brown-Forsythe correction (n=3; >30 cells per repeat).

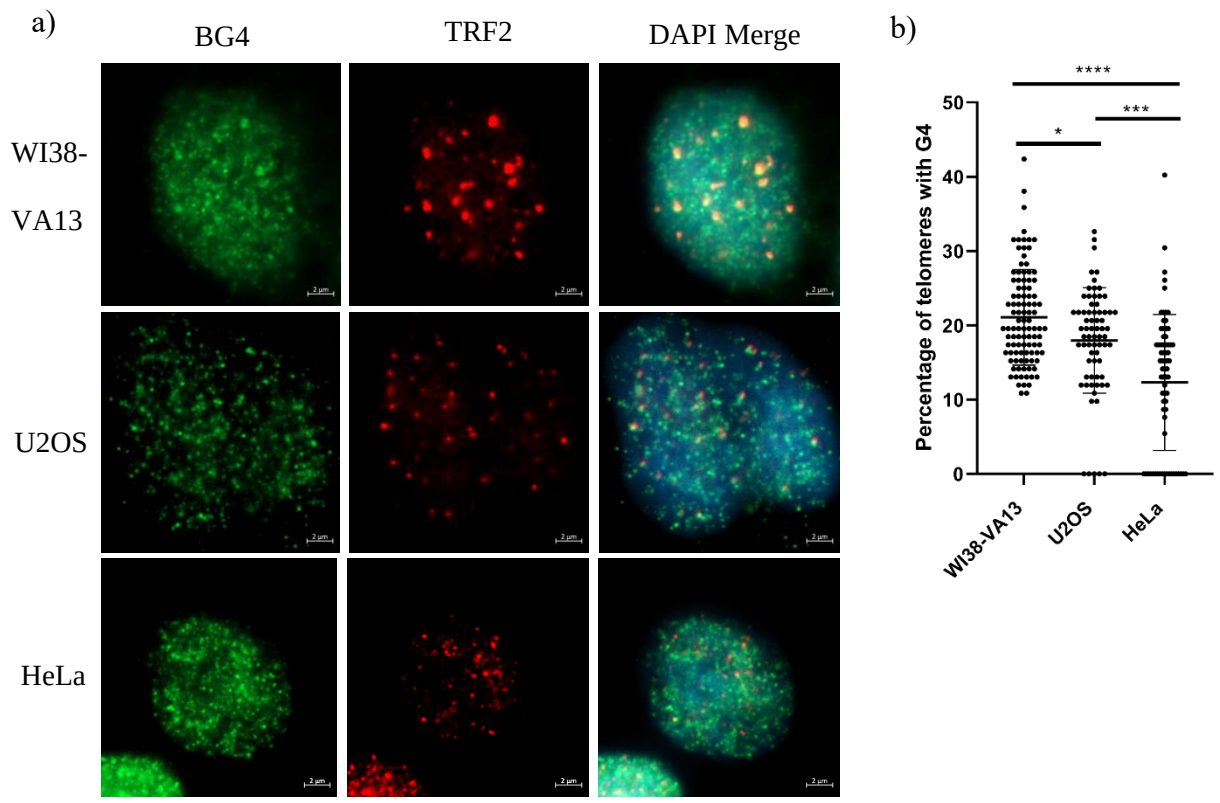

<u>Figure 15: G4 are found to localise at the telomeres, known G4 hotspots.</u> a) Representative immunofluorescence images at 100x magnification for WI38-VA13, U2OS and HeLa cells with TRF2 (red) and G4 (green) staining showing clear co-localisation. **b)** Quantification of the number of telomeres with G4 staining represented as a percentage of total telomeres per cell. Statistical analysis by One-Way ANOVA with Brown-Forstythe correction and Welches multiple comparison test P = <0.05*, 0.001***, 0.0001**** (n=2; >30 cells per repeat).

a)

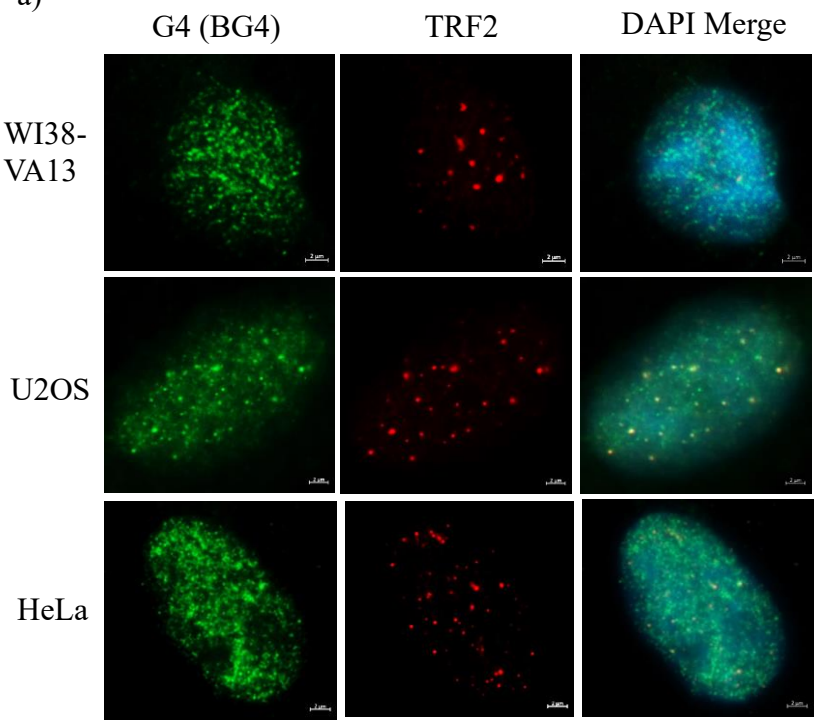
G4 (BG4)
TRF2
DAPI Merge
WI38-VA13
U2OS
HeLa

b)

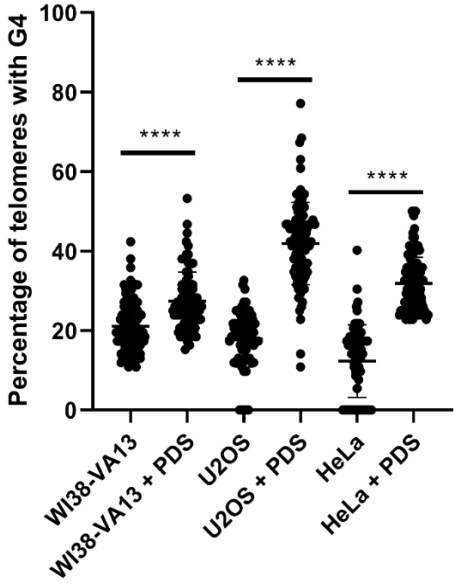
Percentage of telomeres with G4
100
80
60
40
20
0
****
****
****
WI38-VA13
WI38-VA13 + PDS
U2OS
U2OS + PDS
HeLa
HeLa + PDS

Figure 16: Telomeric G4 following treatment with Pyridostatin. **a)** Representative immunofluorescence images at 100x magnification for WI38-VA13, U2OS and HeLa cells stained for TRF2 (red) and G4 (green) showing clear co-localisation following treatment with 1mM Pyridostatin. **b)** Quantification of telomeres with G4 staining represented as a percentage of total telomeres per cell. Statistical analysis by One-Way ANOVA with Brown-Forstythe correction and Welches multiple comparison test. P = <0.05*, 0.0001**** (n=2; >30 cells per repeat).

Upon analysis of the IF results, it became clear that there are significant disadvantages to using this method for global G4 analysis, highlighting a key gap in the field. This confirmed the need for more standardized and quantifiable techniques. Below, I describe the development and optimization of a novel method for G4 detection using an ELISA-based assay, enabling rapid quantification of G4 in genomic DNA.

G4 ELISA design and optimization

The design for the G4 ELISA was a modification of existing DNA ELISA protocols (Figure 17) (149)(150). For DNA to adhere to a 96-well culture plate, the plate must be coated in a cationic solution to allow the negatively charged DNA to bind and adhere to it. For this, protamine sulfate (protamine) was chosen due to its basic nature, arising from its high concentration of Arginine (151). Various concentrations of protamine were tested for optimal DNA binding in a 96-well plate. Based on recommended DNA concentrations for ELISAs, genomic DNA was tested at both 1 and 2.5µg per well and assessed for binding via Ethidium Bromide staining under an Ultra-Violet light (Figure 18a). It was determined that 800µg/ml of protamine for coating and 1µg DNA per well produced the best result and was therefore used for all future experiments. Of note, performing the DNA adherence step in a humid environment did not generate sufficient binding to the protamine-coated plate. However, when DNA was left to adhere onto the plate in a non-humid, 37°C incubator, the amount of DNA bound to the plate was much higher. This method of preparation is already recommended for some DNA ELISAs, supporting its validity in this context (152).

Table 3: Summary of control oligonucleotide sequences for the G4 standard (Telo 34mer) and negative controls (Telo 18mer and AT-rich 34mer) with sequence, predicted G4 formation score according to the QGRS mapper and the percentage GC content for each sequence.

Name	Sequence	Predicted G4-score	Guanine %
Example sequence	GGGNNNGGGNNNGGGNNNGGG	n/a	57%
Telo 34mer	TTAGGGTTAGGGTTAGGGTTAGGGTTAGGGTTAG	40%	47%
Telo 18mer	TTAGGGTTAGGGTTAGGG	0%	50%
AT-rich 34mer	ATATCTCAGCTTAATCGCAATTGTTCGATATCAA	0%	11%

Development of oligonucleotide standards for G4 analysis

It has been well established that the telomeric sequence, TTAGGG, is highly prone to G4 formation, thereby providing an excellent template for the generation of G4 DNA *in vitro* (140)(153)(154). However, the length of sequence will impact G4 formation depending on the desired orientation and assembly of the G4 structure. According to the canonical G4 motif sequence, we established that 3 telomeric repeats $(TTAGGG)_3$ will be insufficient for intra-strand G4 formation, thereby providing a suitable negative control (12) (Table 3). This is due to the assembly of G-tetrads requiring 4 guanine runs broken up by looping regions in order to form a stable structure. Therefore, GGG + $(TTAGGG)_3$ would be the minimum length for G4 to form within the telomeric sequence. Additionally, it has been reported that the telomeric 34mer sequence, $(TTAGGG)_5$ + TTAG, forms stable intra-strand G4 *in vitro* (142), providing a suitable positive control for G4 detection (Table 3). Initial optimizations were used to determine if annealing was required for G4 detection in the telomeric 34mer (Telo-34mer) and 18mer (Telo-18mer) oligonucleotides. Results showed that allowing the oligos to anneal produced a lower G4 signal compared to the non-annealed sequences (Figure 18b). This suggests that annealing is not required for G4 formation to occur in the control sequences.

Next, different antibody dilutions were tested with the control sequences in the presence of standard DNA buffer (TE) or G4 stabilization buffers (K+ or PDS). G4 signal in all conditions was consistent at 1:100 antibody dilution, suggesting saturation at this concentration. At 1:500, subtle differences in signal can be seen in Telo-18mer vs Telo-34mer, however at 1:1000, clear difference in G4 signal can be seen between Telo-18mer and Telo-34mer, supporting the use of 1:1000 BG4 dilution for this assay (Figure 18c).

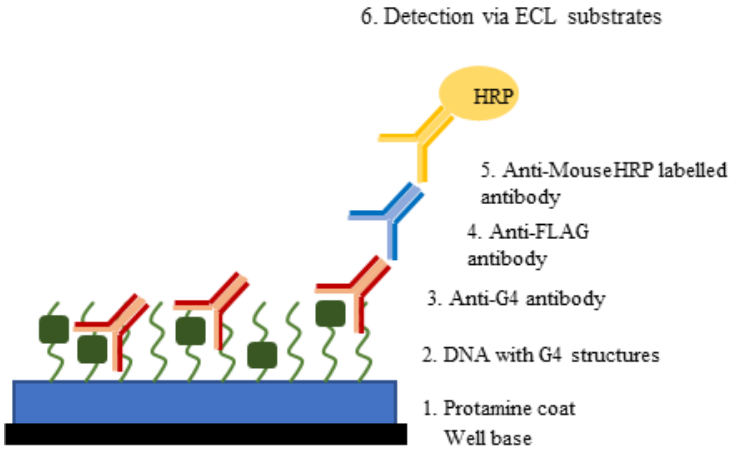

Figure 17: Principle of the G4 ELISA method. 1) Plates are prepared with a protamine coat followed by 2) coating wells with DNA of interest. 3) anti-G4 antibody is applied followed by 4) anti-FLAG antibody (when using BG4 primary) and 5) HRP-labelled secondary antibody. 6) G4 are detected via addition of ECL substrate which is processed by bound HRP. Signal is measured for each well and used to develop a standard curve for absolute quantification of G4 in gDNA samples.

To further confirm the efficacy of the positive and negative controls in the DNA ELISA, serial dilutions of the Telo-18mer and Telo-34mer were tested for G4 signal. Serial dilutions of Telo-34mer resulted in a dose-dependent increase in G4 signal between 0.3125 and 50nM DNA. Conversely, we found that the telomeric 18mer oligonucleotide showed minimal signal at the highest concentration (50nM) and no detectable signal <50nM of the oligonucleotide (Figure 18d). To ensure that the signal seen in the telomeric 34mer was not length dependent and independent of G-content, an AT-rich 34mer was also tested. This oligonucleotide contains no guanine stretches and therefore should not be able to form a G4 quadruplex (Table 3). When tested, the AT-rich 34mer showed no detectable signal at any concentration between 3.125 and 50nM (Figure 18d). This data confirms that the Telo-34mer is forming a structure detectable by a G4 specific antibody, and that this structure is not detectable in the AT-rich 34mer and the G-rich 18mer at concentrations <50nM. We did observe some signal in the 18mer at concentrations >50nM, likely due to clustering of G-rich sequences in the well, resulting in bi-molecular and/or tetramolecular G4 structures forming, and not the intramolecular G4 structures we are likely seeing in the 34mer at lower concentrations. Therefore, I decided that standard curves starting at the highest concentration of 50nM should be used for the assay to avoid intermolecular G4 forming in the control sequences.

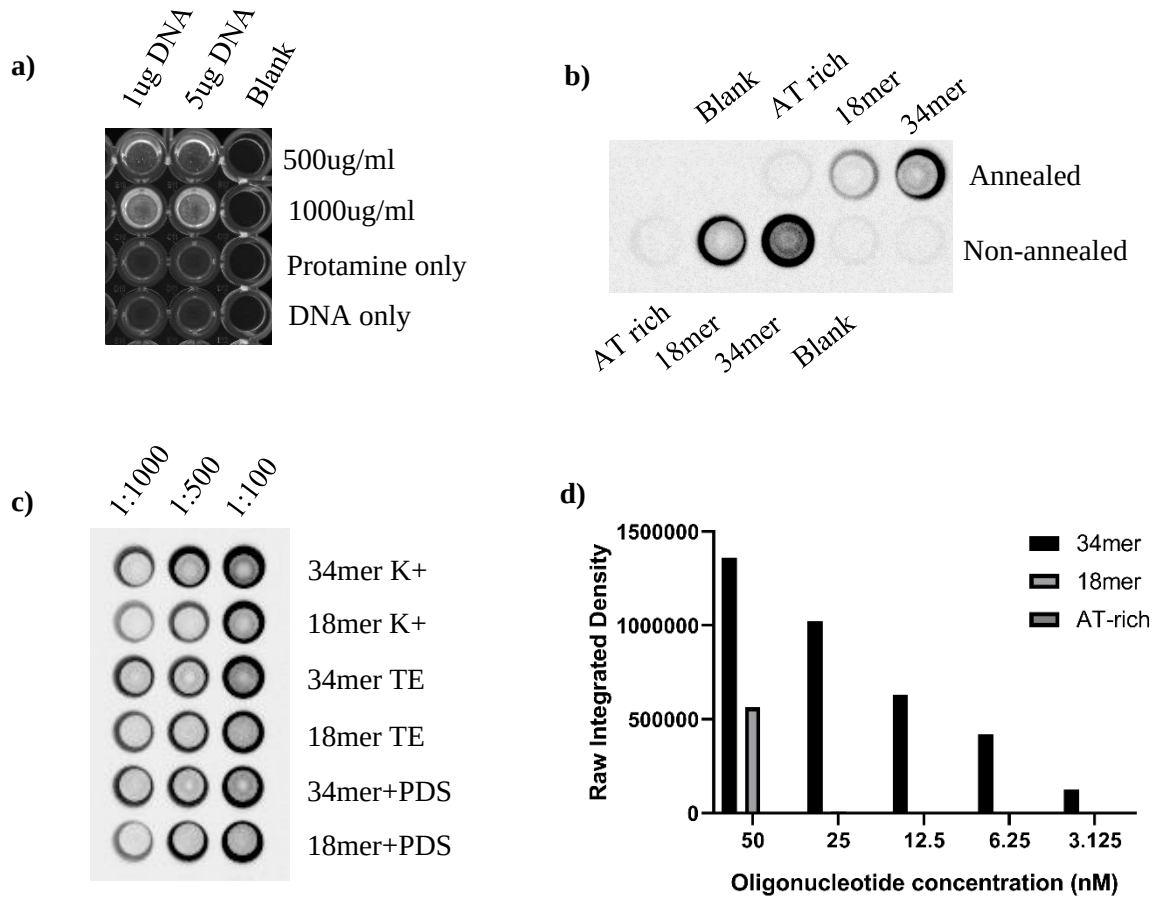

Figure 18: Development of oligonucleotide standards for G4 quantification. **a)** Initial testing for protamine concentration to adhere DNA. Protamine was coated onto a 96-well plate at 500 and 1000 ug/ml. DNA at 1 and 5ug was then added and Ethidium Bromide was used to determine DNA adherence. **b)** Oligonucleotides were tested for G4 signal following either overnight annealing or no annealing. **c)** Different concentrations of BG4 antibody were used to determine the optimal dilution. The antibody was added at 1:100, 1:500 and 1:1000 dilutions to 0.05uM of 34mer or 18mer treated with stabilising buffer containing Pyridostatin (PDS), Potassium (K+) at 150mm or Tris-EDTA (TE). **d)** G4 signal was measured for a 10x dilution series of each standard to confirm signal not due to oligo G-content or length alone.

Quantification of G4 using Telo-34mer standards

To determine a suitable range of detection for this assay, we generated serial dilutions of the Telo-34mer and tested for G4 signal using the G4 ELISA method. The Telo-34mer was tested at 3 different serial dilutions; 2-fold (50-3.125nM), 5-fold (50-0.08nM) and 10-fold (100-0.001nM). Results show all 34mer serial dilutions produced moderate to strong R^2 values (>0.8), with the strongest R^2 being the 2-fold dilution (R^2 = 0.997) (Figure 19a). Based on the previous data suggesting 50nM should be the maximum concentration value for this assay, the 2-fold standard was with a range of 50-0.3125nM was subsequently used for all gDNA quantification (Figure 19b)**.**

Next, G4 content in our gDNA samples was determined using the 2-fold Telo-34mer standard curve to calculate the total G4 in each well. This provided maximum G4 concentration value in the 1µg sample, assuming 100 % of the Telo-34mer had formed stable G4. However, we recognise that this is unlikely due to the complex nature of G4 in this *in vitro* setting. One potential way to counter this error is by using G4 prediction software. These software programs, such as the QGRS mapper, take into account the length of sequence and G-content of putative DNA sequences to provide a G-score (155). This score relates to the probability of the input sequence forming stable G4, when compared to a 'perfect' G4 forming sequence. The Telo-34mer produced a G-score of 40 %, whereas the 18mer and AT-rich oligos both generated scores of 0 % (Table 4). Using this probability, I was able to determine an approximate nanomolar concentration value for G4 formation in our gDNA samples.

Development of a protocol for G4 ELISA image analysis

For the ELISA, images were taken using enhanced chemiluminescence reagents after 1-minute exposure on a BioRad ChemiDoc Imaging system. It was essential that the wells were

clearly visible for analysis; therefore, multiple images were taken of each plate to avoid signal loss at the edges of the wells. All images were subsequently analysed with ImageJ software following conversion to binary using the same threshold for each plate. Integrated density was then measured with reference to the original, non-binary image.

Averages over 3 plates were combined to give a final figure, which was plotted on a graph with standard error. For standard curves, linear regression analysis was performed and R^2 values calculated. Statistical analysis for ELISA results with gDNA were performed using two-way ANOVA and Tukey's post-hoc multiple comparison test ($P<0.05$*). For IF analysis one-way ANOVA with Tukey's multiple comparison test was used, as only one independent variable was measured ($P<0.05$*). All statistics were performed using Graphpad Prism 8.1.2.

Absolute G4 quantification in human gDNA samples using the G4 DNA ELISA

Following optimization of the Telo-34mer standard curve, we wanted to validate and test for G4 content with this method using human gDNA samples. Using 1μg gDNA from U2OS, WI38-VA13, HeLa, HEK293 and BT073M cells, total G4 was determined. G4 in each cell line was calculated using Logarithmic and reverse Logarithmic calculations to provide the total G4 content in nanomoles. The concentration of baseline G4 in each cell line was determined to be between 4 and 13nM based on the standard curve, confirming G4 are detectable in a panel of gDNA samples from different cell lines (Figure 19c). G4 concentration values were also measured in the presence of 1μM PDS to confirm the signal was responding to increases in global G4 stabilization. The G4 ELISA successfully detected an increase in G4 signal following 24 hours of PDS treatment, further confirming the assay's validity (Figure 19c). Conversely, G4 destabilizing agents were also used to confirm the assay's accuracy.

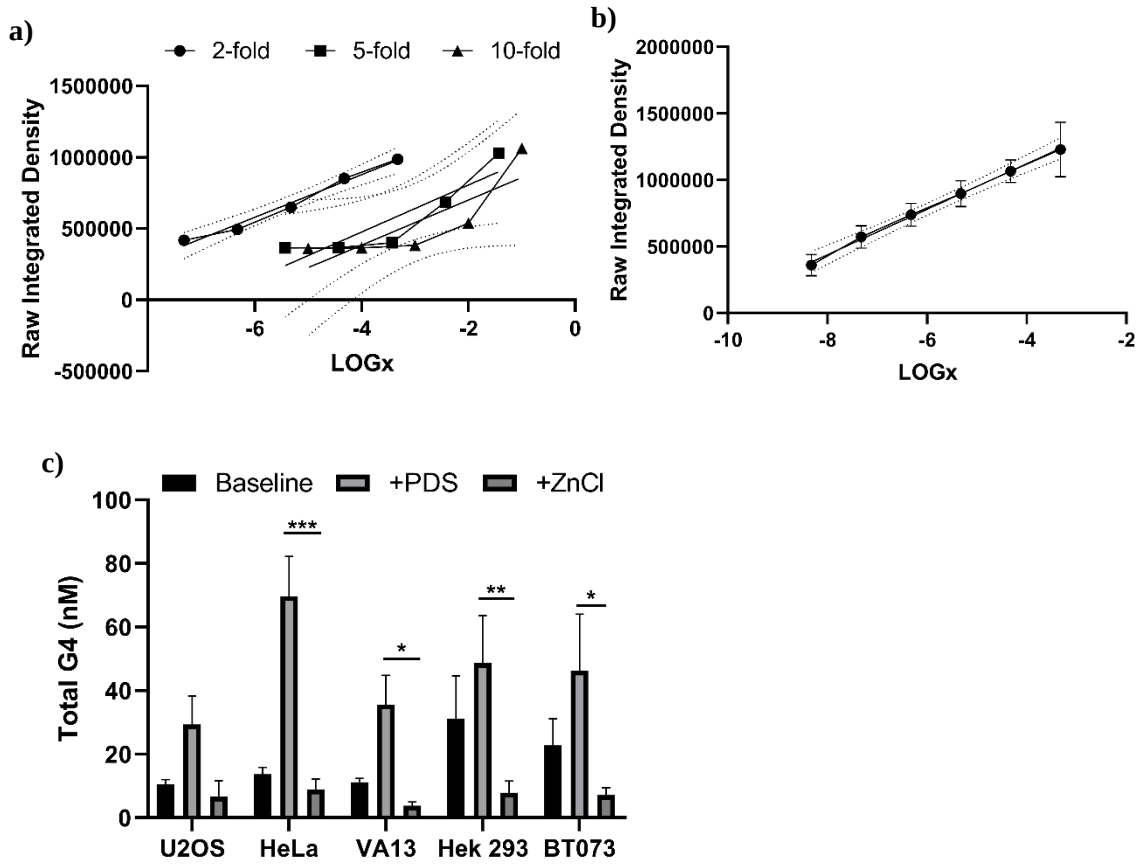

Figure 19: Quantification of G4 in genomic DNA using oligonucleotide standards in a novel DNA ELISA. a) To develop the correct range for the standard curve, the 34mer oligonucleotide was subjected to G4 detection at 2, 5 and 10x dilution series. **b)** The 34mer, 2-fold dilution series was determined to be the best standard for these experiments with an R2 of 0.9977 using a LOG scale. **c)** Specificity of G4 detection was confirmed using divalent cation buffers; lithium chloride (LiCl2) and Zinc Chloride (ZnCl2), to reduce stability and abundance of G4 in U2OS and BT073M cells. Both buffers significantly reduced G4 signal. **d)** 1mM Pyridostatin (PDS) was added to genomic DNA to stabilise G4. Treatment lead to increased G4 signal detection. Statistical analysis by two-way ANOVA with mixed-effect analysis. P<0.05*, 0.01**, 0.001*** (n=5).

Buffers containing certain divalent cations have been shown to disrupt G4 formation and reduce global G4 expression (90). To further assess the efficacy of the G4 ELISA, cells were cultured in 2mM Zinc Chloride ($ZnCl_2$) for 4 hours prior to harvesting to allow intracellular disruption of G4 formation (90). Treatment with $ZnCl_2$ lead to a consistent reduction in G4 signal for all cell lines. supporting the role of zinc ions in disruption of G4 and confirming the detection of G4 in this assay (Figure 19c). This data supports that the G4 ELISA is detecting G4 in gDNA samples and this signal can be altered through addition of both G4 stabilizing and destabilizing agents.

Calculations used to generate G4 values are seen below:

$$Logx^2 = Log(x) \text{standard curve}$$

$$(y\text{-}c) \div m = Logx\ G4$$

$$2^{logx\ G4} = G4 \text{ concentration (nM)}$$

The novel G4 ELISA described in this chapter was designed to determine how ATRX loss might affect global G4 in human DNA samples. However, during development and optimization of this assay, it became clear how important this technique may be in the study of G4. One limitation of the assay is that the BG4 antibody has been shown to bind to RNA G4 as well as DNA G4 (156). However, due to the nature of assay preparation, it is extremely unlikely that any RNA is stable enough to withstand the temperature changes and wash steps used prior to antibody detection.

The importance of measuring G4 globally in genomic DNA samples is becoming increasingly apparent with the use of G4 stabilizers as anti-cancer drugs (157)(158)(159). It has been demonstrated that by stabilizing G4, cancer cells can be sensitised to radiation, leading to

enhanced DNA damage and cell death (100)(160). In order for these drugs to be tested *in vitro*, initial optimization of dose and efficacy should be performed on a broad scale. The G4 ELISA developed in this chapter provides an excellent tool for broad analysis of global G4 following drug treatment in a time and cost-effective manner. The potential for high-throughput screening using this technique is another advantage. As this assay is performed in a 96-well plate format using a standardized protocol, the transition to a larger scale output could be relatively simple, affording a more straightforward screening strategy for new compounds.

Following the successful development and optimisation of the G4 ELISA, this method, amongst others, was used to investigate the effect of ATRX loss on telomerase activity and G4 formation, to determine the role of ATRX in telomere maintenance. In combination with IF, the results demonstrate how ATRX loss affects G4 expression both globally and specifically at the telomere, helping to answer a key question in cancer research; How is ATRX involved in TMM regulation in cancer?

Identifying the role of ATRX in telomerase-mediated telomere maintenance

ATRX is mostly associated with cancer through its roles in telomere maintenance; primarily due to its regulation of ALT activity (161). It is widely accepted that loss of ATRX is a defining feature of ALT, although the reason for this remains largely unclear as knockdown of ATRX does not appear to induce the ALT phenotype (14)(62). Initial studies suggested that ATRX acts to repress the ALT pathway, preventing cells from becoming immortalized using this mechanism(41) (143)(122). However, ***I hypothesize that ATRX has an active role in G4 resolution at the telomere, thereby facilitating telomerase mediated telomere maintenance and indirectly repressing ALT activation.*** This would explain some of the current data regarding how the loss of ATRX affects immortalized cells, making it an avenue of scientific interest.

Many studies have induced the loss of ATRX using RNAi techniques in aim of inducing ALT activation in cells immortalized via telomerase activity. However, under these conditions the prevailing pathway remains to be telomerase and complete induction of ALT has been unsuccessful (162). Following ATRX knockdown, some studies have reported a moderate increase in ALT features, including APBs and C-circles, however telomerase activity remains detectable. This suggests that ATRX loss may indeed relieve repression of the ALT pathway but is insufficient to induce a complete switch in mechanism (122)(163)(164). Interestingly, another chromatin associated complex, Anti-Silencing Factor-1A and -1B (ASF-1A and ASF-1B), was shown to induce a switch in pathway activity following knockdown in telomerase positive cells with long telomeres. The ASF1A/B heterodimer acts as a histone chaperone during nucleosome assembly and disassembly, removing and depositing histones H3 and H4 in both replication dependent and independent manners (52). This function is somewhat similar to that of ATRX, in that ATRX along with its binding partner DAXX deposits H3.3 at repeat regions of DNA in a replication independent manner (165). This data suggests chromatin organisation may be linked with a switch to the ALT phenotype, however no mutations in ASF-1 have been reported in ALT cancers, making it extremely unlikely that this protein is directly involved. This does, however, represent this first incidence of complete ALT induction following gene knockdown, prompting interest in chromatin organisation in TMM regulation.

Although neither ASF-1A nor ASF1B have the helicase activity of ATRX, following ASF1A depletion obstructs histone transfer at the replication fork is obstructed, leading to deregulated histone assembly and disassembly (166). As this obstruction continues to impede fork progression, replication fork stalling can occur, leading to free, partially replicated, single-strand DNA. If this process occurs in certain regions, such as the telomere, single-stranded G-rich DNA

may be able to form intra-strand G4, further inhibiting fork progression and the activity of telomerase (167). Other proteins in addition to ATRX have been shown to possess G4 resolution ability, however none of these have been tied to ALT+ cancers (73)(168). As the telomere is a known hotspot for both G4 formation and fork stalling due to its G-rich and repetitive nature, it seems plausible that both factors combined, provide enough resistance to force the cell into the ALT pathway if unresolved (169)(170). Therefore, the loss of ATRX could, over time, promote the switch from telomerase activity to ALT through lack of G4 resolution at the telomere, leading to telomerase inhibition and telomere-state induced genomic instability (171). Therefore, I wanted to investigate how the loss of ATRX effects global and telomeric G4 and how this in turn effects telomerase activity under G4 neutral and stabilizing conditions.

Telomerase activity is inhibited by Pyridostatin

Pyridostatin is a small G4-binding molecule shown be effective in stabilizing G4 both *in vivo* and *in vitro,* supposedly inhibiting cancer cell growth through telomere and telomerase dysfunction (111). It appears to do this by sitting at the centre of the G4 and 'locking in' to stabilize the structure. Using a Conventional Telomerase Assay (CTA) we tested the ability of telomerase to elongate the telomeric sequence *in vitro* (172). For this, telomerase was produced via the Rabbit Reticulocyte Lysate (RRL) *in vitro* translation system, using a plasmid containing the full hTERT sequence in addition to recombinant hTR RNA. This system utilises rabbit reticulocytes to produce protein from plasmid DNA, which in the presence of recombinant hTR, forms the basic functional unit of the telomerase enzyme (173). To confirm hTERT was indeed being produced successfully using this system, western blots were performed with RRL lysates containing either 250 or 1000ng hTERT plasmid DNA. Results confirmed expression of hTERT with both 250 and 1000ng DNA,

Table 4: Telomeric primer sequences for CTA analysis. Telomeric 12mers and 18mers are unable to form inter-strand G4 due to insufficient length of sequence. Telomeric 24mer is the shortest sequence predicted to be capable of forming G4.

Primer name	Primer sequence	G content
Telo 18mer	TTAGGGTTAGGGTTAGGG	50%
Telo 24mer	TTAGGGTTAGGGTTAGGGTTAGGG	50%

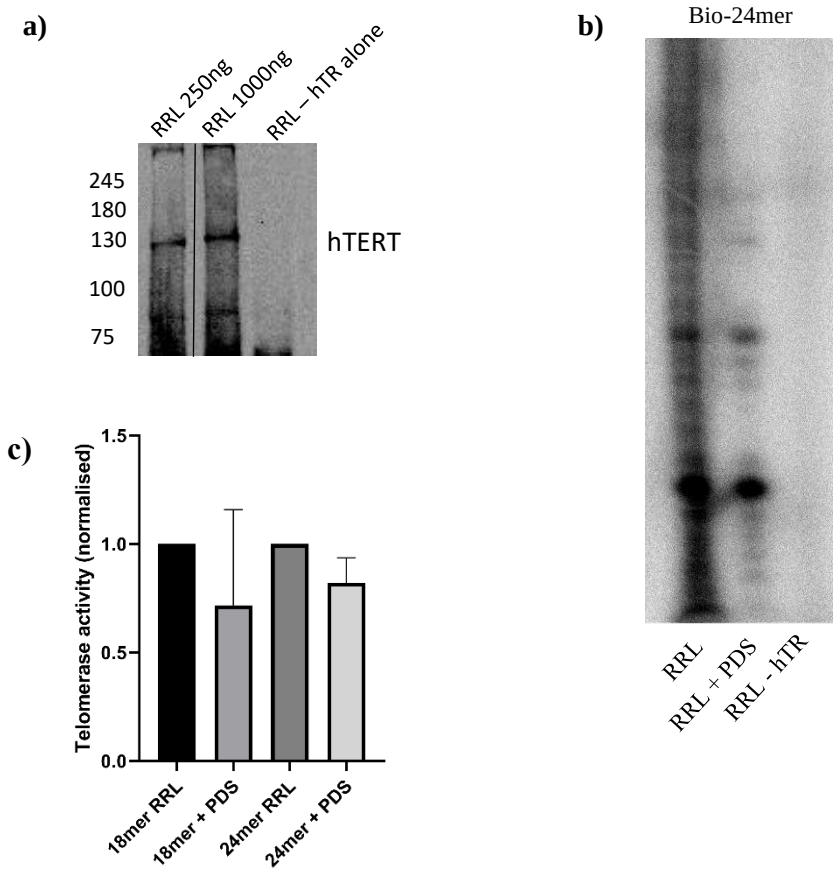

Figure 20: *In-vitro* analysis of Telomerase activity with G4 stabilizing and de-stabilizing compounds. a) Rabbit Reticulocyte Lysate (RRL) reactions with pCI-hTERT plasmid and recombinant hTR protein were tested for efficiency at producing hTERT protein via western blot. **b**) Representative image of Conventional Telomerase Assay (CTA) with Telomeric primers 24 nucleotides in length (Bio-24mer) in the presence or absence of Pyridostatin, a potent G4 stabilizer. Statistical analysis performed by One-way ANOVA with Tukeys multiple comparison test (n=3).

demonstrating that hTERT protein was being successfully produced in this system (Figure 20a). Following generation of telomerase *in vitro,* the ability of telomerase to elongate telomeric sequences was assessed with either a telomeric 18mer or 24mer in the presence or absence of PDS. The telomeric 18mer, similar to that in the G4 ELISA assay, is too short to form stable intra-strand G4, thereby acting as a suitable negative control (99). The telomeric 24mer, however, contains a sequence capable of intra-strand G4 formation which should be stabilised by PDS, therefore inhibiting telomerase activity (Table 4). CTA analysis showed that telomerase activity was similar for both 18 and 24mer primers at baseline, but with addition of PDS, telomerase activity was markedly reduced (Figure 20b and 20c). This confirms that PDS inhibits telomerase activity and suggests that telomerase is unable to effectively resolve stable G4 structures in the telomeric sequence.

To further analyse the role of telomerase in G4 DNA resolution, we utilised the Telomere Repeat Amplification Protocol (TRAP) assay to detect telomerase activity in human protein lysate samples from cells in the presence or absence of PDS. This assay differs from the CTA as it involves a PCR amplification step and utilises endogenous telomerase protein extracted from human cells. The CTA has one key advantage over the TRAP as it doesn't require PCR amplification. For the purpose of this study, it was essential to demonstrate the effect of G4 stability on telomerase in a PCR-free setting as it could be argued that the addition of PDS would interfere with the activity of Taq in the PCR reaction. These effects would likely produce a similar result in a TRAP but are eliminated in the PCR-free CTA. However, for us to test telomerase activity in ATRX knockdown cells, the TRAP is the only suitable assay, since it is difficult to detect endogenous telomerase activity without PCR amplification of the extension products (127).

a)

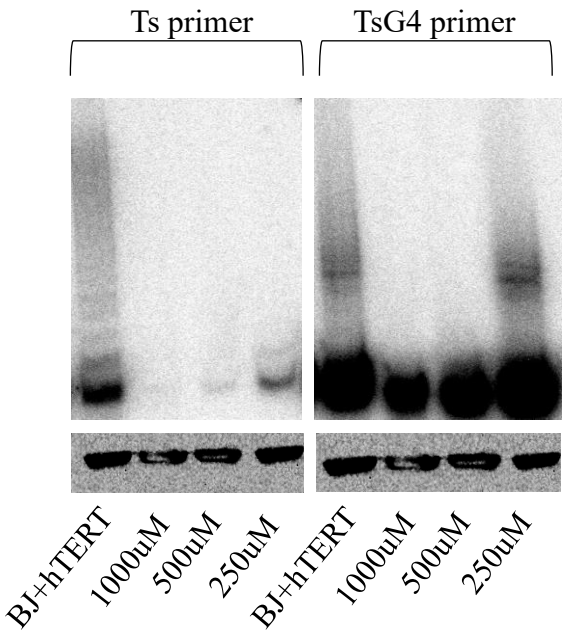

Figure 21: The potent G4-stabilizer, Pyridostatin, inhibits endogenous telomerase activity in a dose dependent manner. a) Protein from BJ+hTERT cells were treated with increasing doses of Pyridostatin (PDS) and tested for telomerase activity via a TRAP assay. Telomerase activity was notably inhibited at even the lowest concentration of PDS (250uM). Normal telomeric substrate (ts) primer was used in addition to a published TsG4 primer designed to form G4 structures.

Using two telomeric substrate primers, Ts and TsG4, telomerase activity was measured at various PDS doses (174). In both primer conditions, telomerase activity was significantly inhibited at 1000 and 500μM PDS, confirming the results seen in the CTA (Figure 21). At the lowest concentration of PDS (250μM), telomerase activity appeared to be restored in presence of TsG4 primer but remains largely inhibited in the presence of Ts primer. This suggests the Ts primer is forming G4 structures more readily than the TsG4 primer. For this reason, the Ts primer was used for all further TRAP assays. These data confirm that G4-forming telomeric sequences can be stabilised in vitro by PDS treatment and that PDS inhibits telomerase activity in a dose-dependent manner.

Generation of ATRX knockout HEK293 and HeLa cells by shRNA

As I have demonstrated PDS successfully inhibits telomerase activity, I wanted to next determine the effects of ATRX loss on G4 expression and telomerase activity. If ATRX does act to resolve G4 at the telomere, knockdown using shRNA should result in increased G4 expression at the telomere as well as globally. Further, I wanted to establish if loss of ATRX was synergistic with PDS treatment, sensitizing cells to lower concentrations of the G4 stabilizing drug. To determine the effect of ATRX loss on G4 and telomerase activity, ATRX knockdown cells were generated using the PiggyBac expression system to transfect shRNA into both HEK293 and HeLa cell lines. These two cell lines were chosen as they both utilise telomerase mediated telomere maintenance and both express ATRX (see figures 4 and 7). This provides the ideal background to test the effect of ATRX loss on endogenous telomerase activity. Additionally, HeLa have proven to consistently produce relatively clean staining for G4 in IF analysis, providing a suitable cell line to analyse G4 expression at the telomere. shRNA targeted to ATRX and scramble shRNA controls were designed based on published sequences which demonstrated successful knockdown of ATRX

in HeLa cells (Table 5) (163). Our sequences were produced by the DNA Laboratory core facility at the University of Calgary and cloned into a PB-CMV-GreenPuro-H1-MCS (Piggybac) vector gifted to our lab by the Senger Lab at the University of Calgary (Figure 22b). All cloning was performed in a collaboration between me, Bo Young-Ahn of the Senger Lab and Beattie lab undergraduate student, Vanessa Huynh. shRNA sequences were designed to contain EcoRI and BamHI cut sites at either end to facilitate ligation into the Piggybac plasmid following linearization of the plasmid using those same enzymes. Following ligation of the shRNA sequences into the plasmid, EcoRI and BamHI were again used to linearize the ligated plasmid to determine if the shRNA had been successfully cloned into the vector. Results from gel electrophoresis of linearized products showed successful ligation of all sequences into the plasmid (Figure 22a). However, to fully confirm successful addition of the shRNA sequences to the vector, Sangar sequencing was performed using primers which covered the entire shRNA sequence region, including flanking regions. These results show successful insertion of the shRNA and scramble sequences (Figure 22c).

Following successful cloning with shATRX sequences into the PiggyBac vector, HeLa and HEK293 cells were transfected using the lipid-based transfection reagent, Lipofectamine 3000. The Piggybac system works using a transposase which, once transfected successfully into a host cell alongside the Piggybac vector, cuts out a section of the vector containing the desired sequence and inserts it randomly into the host genome. This generates stable expression of the shRNA, thereby providing long term knockdown of the target protein (175). In this study, the shRNA sequence was under an H1 promoter with both GFP and puromycin resistance genes under a separate CMV promoter. This allowed visualisation of transfected cells via GFP as well as selection via puromycin to produce a stable cell line populated by only those cells transfected with

Table 5: Design of shRNA sequences to target ATRX. The below sequences were designed to knockdown ATRX following insertion into a piggybac vector and successful transformation in TOP10 E. coli. Following transformation, surviving clones were sequenced to confirm the presence of shRNA before transfection into mammalian cells.

Sequence name	Sequence composition
shATRX #1	CGACAGAAACTAACCCTGTAA
shATRX #2	CCGGTGGTGAACATAAGAAAT
Scramble	GCCAGATCCGTAAACCATAAA

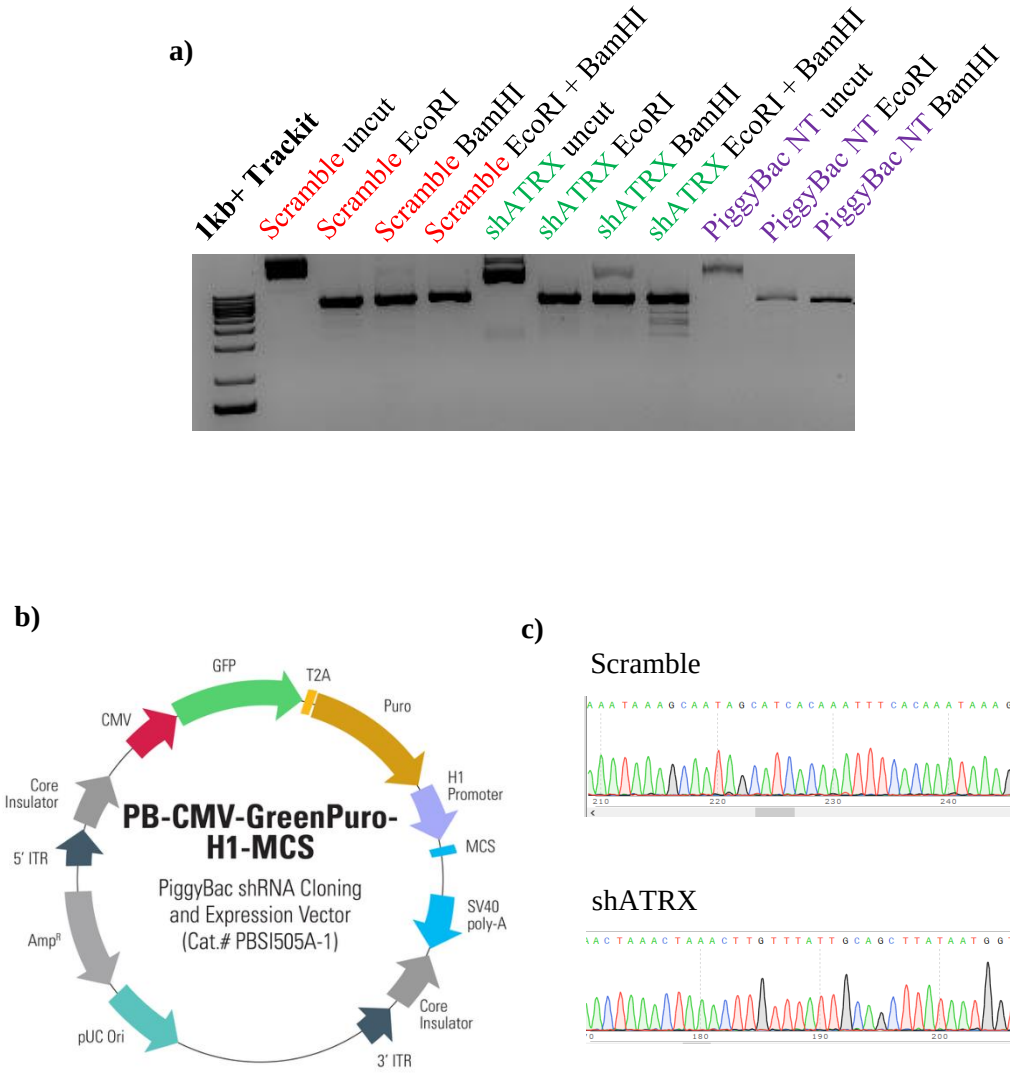

Figure 22: Generation of shATRX and scramble controls vectors for ATRX knockdown. **a)** Plasmid preps were digested in fastdigest buffer with no enzyme (uncut) EcoRI/BamHI alone or in combination for 1 hour at 37 degrees. Linearized plasmids were then run on a DNA gel for imaging. **b)** Plasmid map for PiggyBac PB-CMV-GreenPuro-H1-MCS construct used in shRNA cloning and transfections. **c)** Representative chromatograms following Sanger sequencing confirm the successful incorporation of shRNA sequences into the Piggybac vector.

a)

Scramble

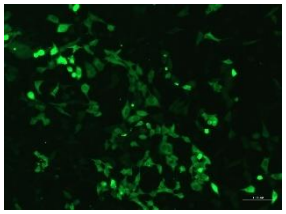

shATRX-1

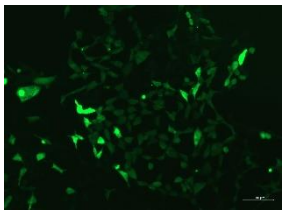

shATRX-2

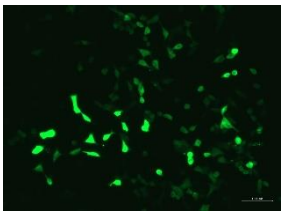

shATRX-1 + 2

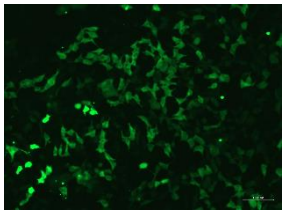

b)

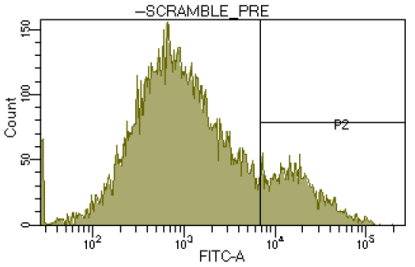

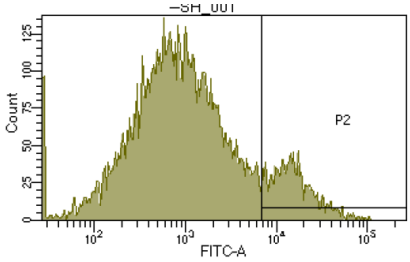

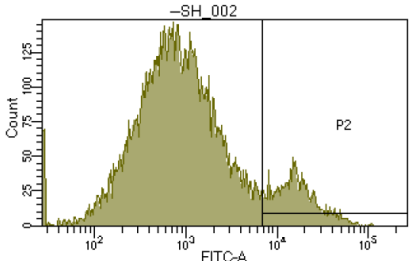

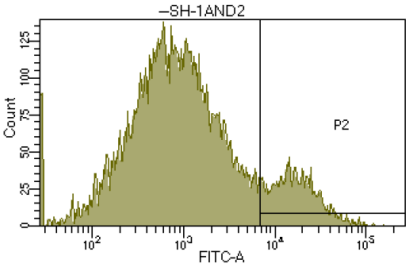

c)

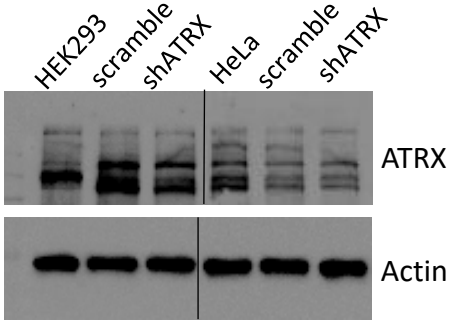

Figure 23: Generation of stable ATRX knockdown in HEK293 and HeLa cells. **a)** Representative images (10x magnification) following transfection of HEK293 cells with PM-CMV-GreenPuro-H1-MCS plasmid containing either shATRX or Scramble sequences. **b)** Representative graphs showing GFP distribution among HEK293 cell populations following transfection with the PB-CMV-GreenPuro-H1-MCS vector containing shATRX or scramble sequences. Cells were FACS sorted based upon GFP signal intensity after 2 weeks in puromycin-supplemented selection media. Populations with the highest GFP signal were isolated and grown up for experiments. **c)** Following transfection, western blots were performed to detect ATRX expression in both HEK293 and HeLa cells (n=5).

the plasmid. Initially, cells were transfected with; shATRX #1, shATRX#2, shATRX #1 and #2 combined or scramble control and imaged for GFP expression (Figure 23a). The aim of using 2 sequences in combination is to reduce the potential off-target effects of each individually whilst maintaining a robust knockdown (176). Transfected HEK293 and HeLa cells were put under puromycin selection for 2 weeks before further sorting by Fluorescence Associated Cell Sorting (FACS) to select the population of cells with highest GFP expression (Figure 23b). Although the GFP and shRNA sequences are under different promoters in these cells, expression of GFP is still somewhat indicative of shRNA expression as they are present in the same genomic region. Therefore, if the shRNA is silenced, GFP is likely to be affected also.

Following selection and FACS sorting, western blot analysis for ATRX expression was performed to detect successful knockdown. Unfortunately, the expression of ATRX in HEK293 remained unchanged following shRNA transfection. In Hela cells, a knockdown was seen but this was not significantly different from the scramble control, suggesting potential effects of the scramble in culture (Figure 23c). Occasionally, scramble sequences can have detrimental effects on cell lines as they accumulate in the cell with no defined role or function. This can cause toxicity and can in some cases, also affect protein expression (177). Unfortunately, for the purposes of this study, repeated attempts at generating stable cell lines with ATRX knockdown proved unsuccessful. Therefore, we decided to attempt transient knockdown in HeLa due to the partial response seen in the long-term cultures. Using the same Piggybac vector without the transposase, HeLa cells were transfected using Lipofectamine 3000. At 48 hours post-transfection, cells were imaged for GFP expression and any transfection with an estimated efficiency over 50% was harvested for western blot analysis (Figure 24a). At 48 hours, knockdown of ATRX using shRNA #1 was seen (Figure 24b). This knockdown was reproducible and maintained a consistent reduction

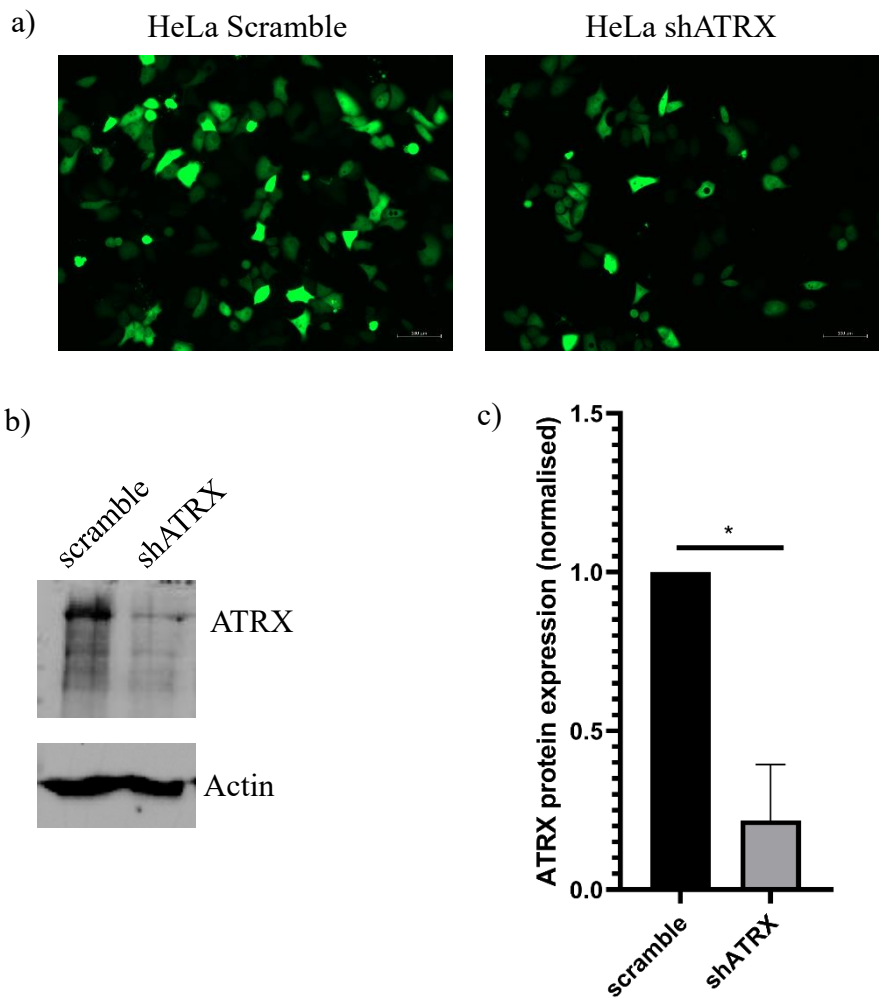

Figure 24: Generation of transient ATRX knockdown in HeLa cells. **a)** Representative images (10x magnification) of HeLa cells 48 hours post-transfection with PB-CMV-GreenPuro-H1-MCS plasmid containing either shATRX or Scramble sequences. **c)** Cells were harvested at 60 hours post-transfection and western blots were performed to detect ATRX expression. **d)** Quantification of western blot results. Statistical analysis by students T-test. $P<0.05$* (n=3).

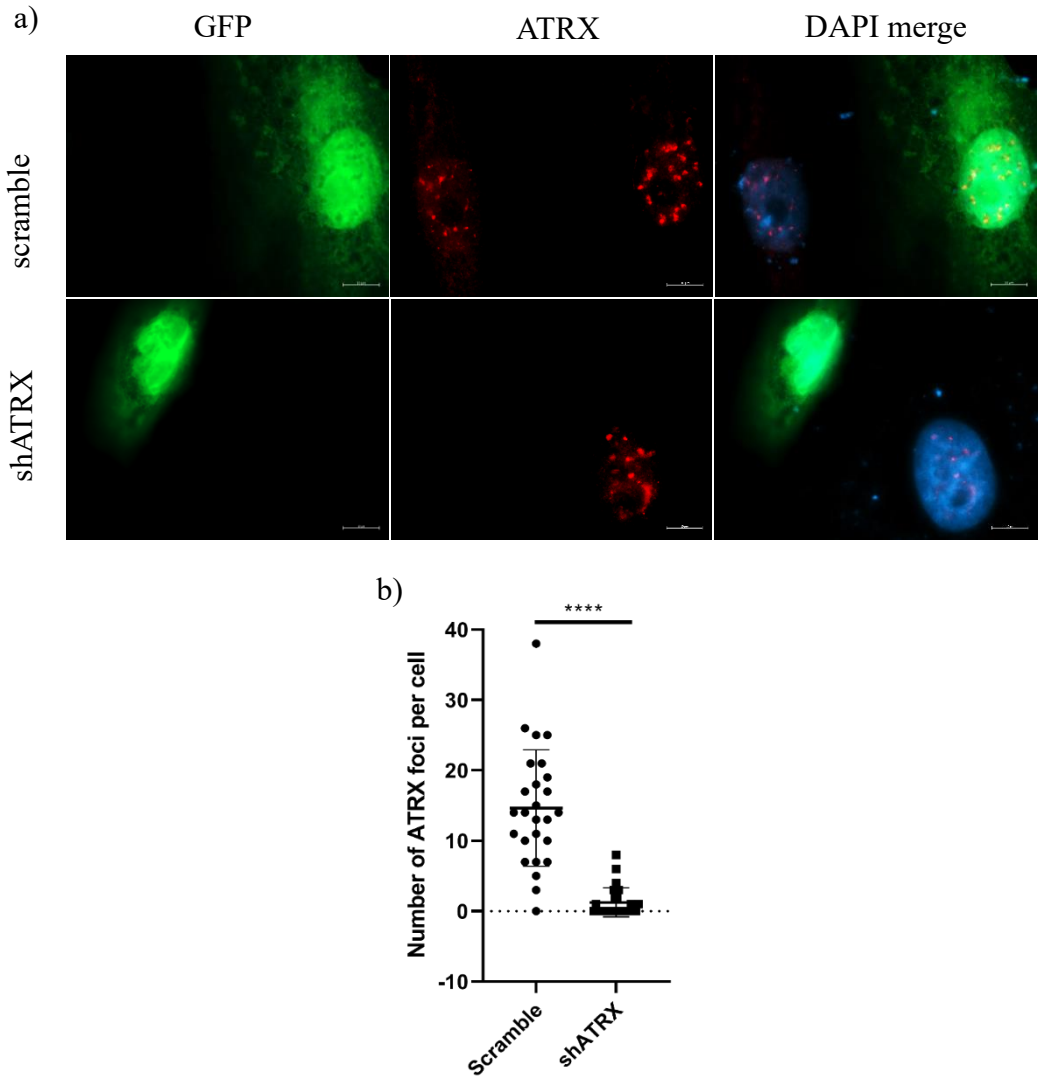

Figure 25: Immunofluorescence analysis confirms lack of ATRX protein expression following shRNA knockdown. **a)** Representative images showing immunofluorescence staining for ATRX in HeLa cells following transfection with PB-CMV-GreenPuro-H1-MCS at 100x magnification. **b)** Foci count analysis shows a clear and significant reduction in ATRX protein in shATRX cells vs scramble controls. Only GFP+ cells were included in the analysis. Statistical analysis by students T-test. P<0.0001**** (n=3; >30 cells per repeat).

in ATRX expression by ~75-80% in multiple transient transfections (Figure 24b and 24c). This method provided us with the ATRX deficient cells needed to test the effect of ATRX loss on G4 and telomerase activity.

ATRX loss leads to increased G4 at the telomere in HeLa cells

Following successful knockdown of ATRX in HeLa cells, IF for ATRX was performed. This experiment was designed to act as an additional control to ensure the GFP+ cell population has reduced ATRX expression. This allows us to perform single cell analysis of G4 at the telomere, without the need for complex staining methodology required for multiple primary antibodies of the same species. HeLa cells transfected with either shATRX #1 or scramble control sequences were stained and imaged at 488nm and 568nm. Data collected from triplicate experiments shows a significantly reduced number ATRX foci in shATRX cells compared with scramble controls (Figure 25a and 25b). As only GFP+ cells were included in analysis, this data confirms a significant reduction in ATRX in this population. Following this, only GFP+ cells were used for G4 and TRF2 staining. As knockdown in this population, I could be confident I was targeting cells with successful ATRX knockdown or scramble transfection.

IF analysis of G4 and TRF2 was performed to determine if G4 expression at the telomere was affected by ATRX loss specifically. As the shelterin protein, TRF2 clusters at the telomere, distinct TRF2 foci can be used to identify the location of telomeres in the cell (78)(10). As our Peptide Nucleic Acid (PNA) probe, which binds directly to telomeric DNA, is labelled with AlexaFluor-488 it cannot be used for GFP+ cells. However, as TRF2 acts as an excellent marker for the telomere and our primary TRF2 antibody is not fluorescently labelled, we can use any fluorescent marker to probe for it. Therefore, TRF2 foci were used as telomeric markers in this assay and co-localisation with G4 foci was deemed to represent telomeric G4.

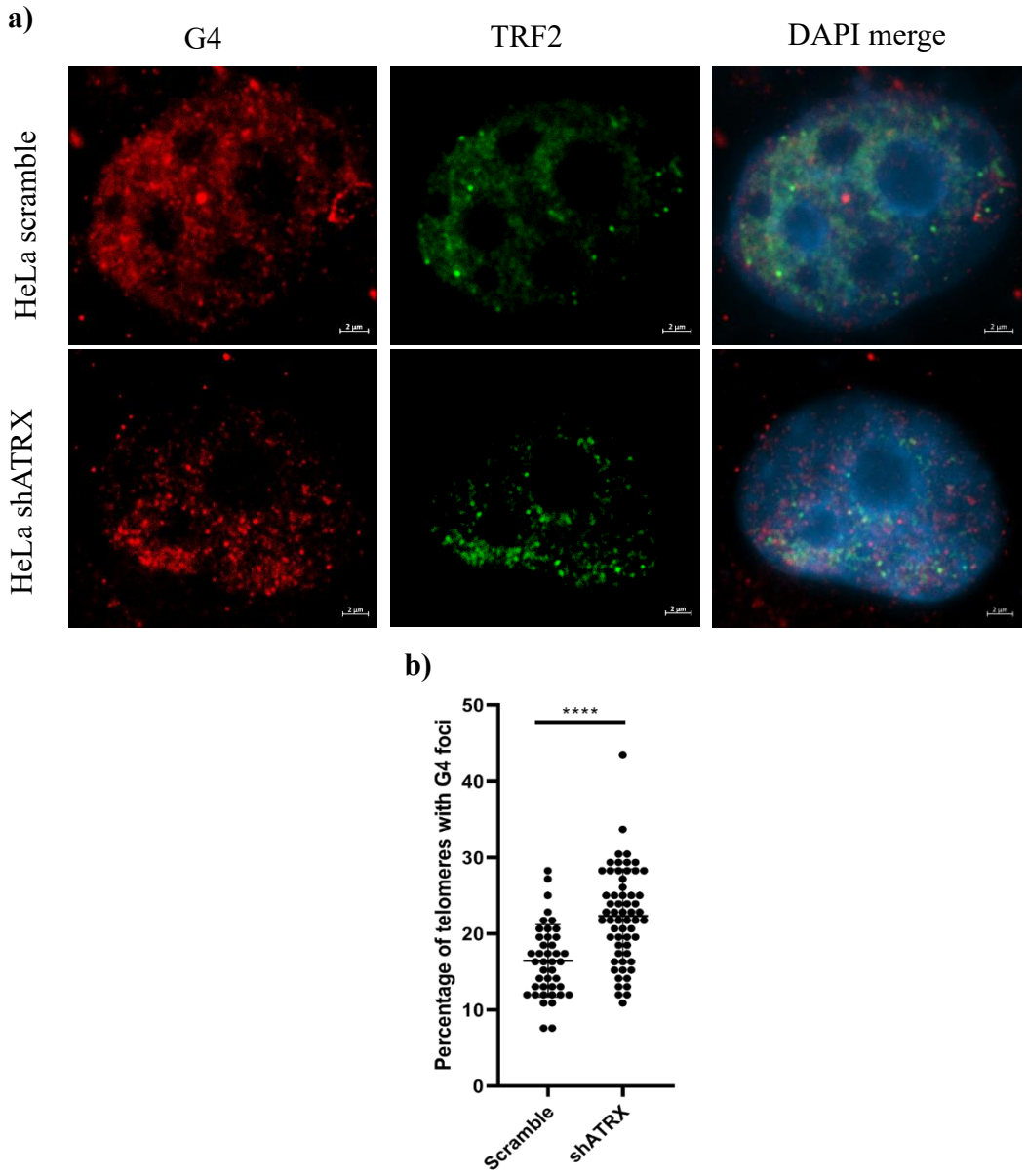

Figure 26: G4 at the telomere is not significantly affected by ATRX knockdown. **a)** Representative immunofluorescence images at 100x magnification show staining for TRF2 and G4 in HeLa$_{scramble}$ and HeLa$_{shATRX}$ cells. **b)** Quantification of the percentage of telomeres (TRF2 foci) colocalised with G4 foci. Quantification was performed on <30 cells per condition. Statistical analysis was performed by Welchs T-test (n=3; <30 cells per repeat).

Results of TRF2 and G4 co-localisation show a significant increase in telomeric G4 following ATRX knockdown, suggesting the loss of ATRX effects G4 expression at the telomere directly (Figure 26a and 26b). This loss of ATRX expression in telomerase positive cells may therefore be directly influencing telomeric G4 and telomerase activity. The next step was to analyse global G4 expression following ATRX knockdown using the G4 ELISA.

Hela cells transfected with either shATRX #1 or scramble control sequences were harvested at 48 hours and DNA isolated for the G4 ELISA. Data from triplicate repeats shows a marked increase in global G4 levels following ATRX knockdown, however this is not deemed statistically significant according to one-way ANOVA (Figure 27a). This data does follow the same trend as telomeric G4, however remains only a trend. The reason for lack of significance may be due to some compensatory mechanisms which are more effective globally than specifically at the telomere. As it has been previously shown that ATRX localises to telomeric DNA and can resolve telomeric G4, it follows that ATRX may act more specifically at the telomere, thereby producing a more significant effect in this region compared to globally. Activity of other helicases shown to breakdown G4, such as BLM or WRN, could counter ATRX loss enough to limit G4 accumulation in the global setting (178)(73). Despite the statistical significance for the G4 ELISA lacking, it is of interest to note the expression of global G4 following ATRX knockdown increases from ~0.008nM to ~0.0015nM, almost doubling from baseline. Scientifically speaking, changes like this warrant further investigation as something as minor as inter-plate variations could skew data to appear insignificant due to high standard deviations. Further investigation into this aspect of ATRX expression represents a definite area of interest for the future of this project.

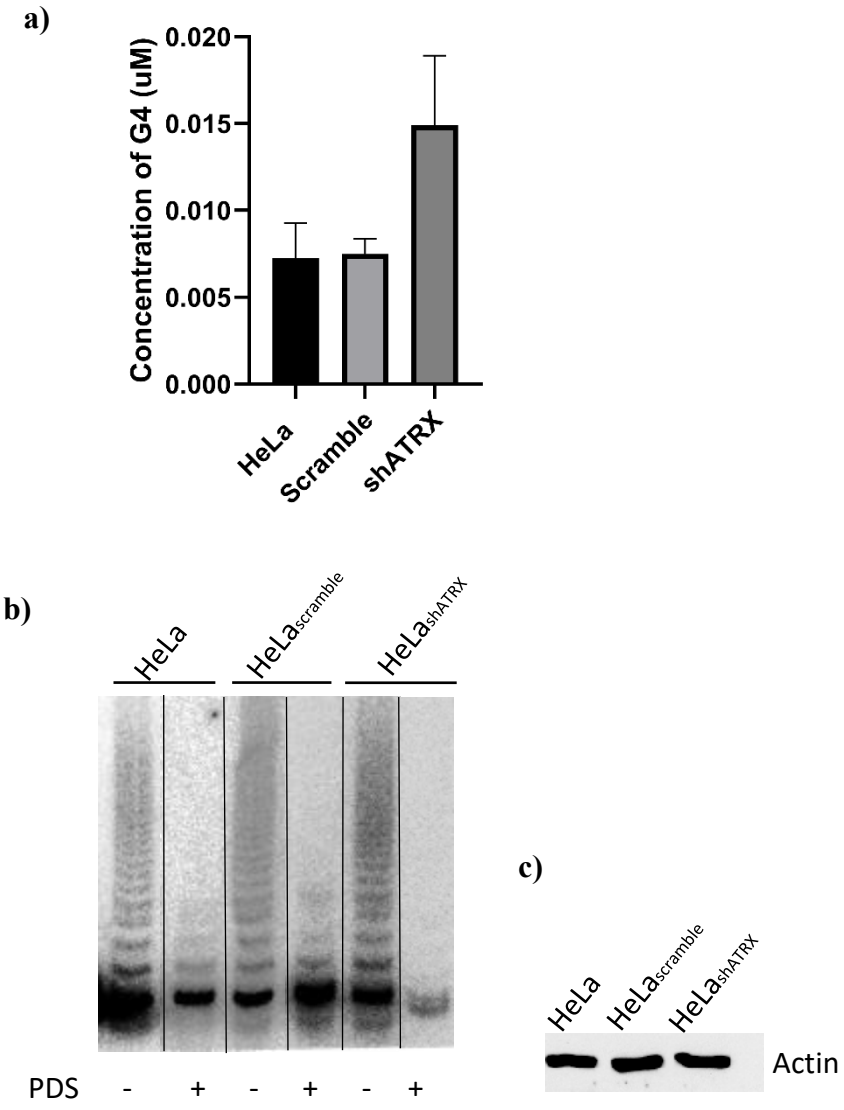

Figure 27: Impact of ATRX expression on telomerase activity. **a)** G4 ELISA results show that ATRX knockdown leads to an increase in global G4 signal (n=3; mean±SEM). **b)** TRAP analysis shows telomerase activity is inhibited by G4 stabilisation following Pyridostatin treatment and that this inhibition is enhanced upon ATRX knockdown (n=3). **c)** Actin immunoblot was used for internal control for protein loading (n=3)

Telomerase activity is impaired by ATRX loss in HeLa cells

Finally, to determine how expression of ATRX effects telomerase activity, TRAP assays were performed using protein lysate samples from HeLa cells, 48 hours after transfections with shATRX #1 or scramble control. All lysates were also treated with 250μM PDS to stabilize G4 in the Ts primer sequence. Results from TRAP analysis show inhibition of telomerase activity following PDS treatment, reducing total activity to ~25% of the untreated sample. However, in HeLa cells with ATRX knockdown, this inhibition is markedly amplified, with telomerase activity almost undetectable following PDS treatment (Figure 27b and 27c). This effect was consistent and repeatable across triplicate biological and technical samples, suggesting that ATRX loss in the presence of stable G4 significantly impairs the ability of telomerase to elongate the telomeric sequence. This novel observation provides the first evidence for ATRX as a direct regulator of telomerase activity in cancer. It highlights a previously unestablished role for ATRX in telomeric G4 resolution, thereby enabling telomerase access to telomeres and facilitating telomerase activity. This function could be direct or indirect, meaning that ATRX may be directly responsible for the G4 resolution, or responsible for recruitment of G4 resolving helicases to the telomere. In either case, it appears an essential factor in the regulation of telomeric G4.

The data described in this chapter help establish how the loss of ATRX in telomerase positive cancer cells may contribute to increased global and telomeric G4 expression which in turn, can compromise telomerase-mediated telomere maintenance. It also highlights ATRX as a potential target for anti-cancer drugs as cells can be sensitized to G4 stabilizers. The treatment of cancer with G4 stabilizers has already been shown to induce DNA damage in the absence of ATRX, and now, the evidence shown in this thesis provides an explanation as to why this is happening (100). The novelty of identifying a direct association between ATRX and telomerase

activity is clear and helps to fill a significant gap in understanding in cancer cell immortality. Taken together, the data in this thesis identifies a clear role of ATRX in G4 resolution and confirms the ability of G4 to inhibit telomerase activity in telomerase positive cancer cells, providing excellent support for both ATRX and G4 as targets for cancer therapy.

Chapter 4: Discussion, limitations and future directions

Discussion

Understanding cellular immortality continues to be of great importance in developing agents to target cancer cells, in addition to the study of premature ageing disorders. Much has been done to expand our knowledge of the role of telomerase in telomere maintenance, a property that remains the dominant mechanism of immortality for many cancers (21). However, some aspects of ALT activity in addition to the key players in pathway choice, remain unclear. This thesis identifies a novel role for ATRX, a key regulator of chromatin state at repeat regions of DNA, in telomerase-mediated telomere maintenance, providing evidence for ATRX as a key regulator of telomeric G4. This data sheds light on the role of ATRX in telomere maintenance and helps resolve the longstanding question, why is ATRX lost in ALT?

Many studies have focused on the impact of ATRX loss on ALT activity, by way of inducing features of the ALT phenotype and reduction in telomerase activity (71)(164)(121). However, I took an alternate approach in this thesis, working to understand the role of ATRX in telomerase positive cancers and how its loss may result in telomere dysfunction. It has been reported that loss of ATRX alone is insufficient to induce complete ALT activation, however it does appear to induce a decrease in telomerase activity and increase global levels of G4 (122)(179). Using this evidence, I postulated that ATRX acts to resolve telomeric G4 in telomerase positive cells, thereby facilitating cellular immortality by telomerase-mediated telomere elongation.

In the first phase of this study I established a suitable panel of cell lines to test my hypothesis by characterising TMM and ATRX expression profiles. Despite selecting a panel of human BTICs with genetic mutations in ATRX, none of the chosen cell lines tested ALT+. Much to my surprise, neither ATRX mutations nor lack of expression of full-length ATRX appeared to correlate with ALT activity, contradicting the literature (180). This is not the first report

demonstrating a discrepancy in the ATRX loss/ALT activity dynamic. In 2019, Chami et al published an article describing the high incidence of ATRX mutations being missed using clinical IHC analysis (181). This report mirrors my own results using murine models, where BTICs with ATRX mutations stained positive for ATRX using IHC and clinical antibodies. This could have a significant impact on patient diagnosis as ATRX mutant glioma has a significantly better survival rate compared with its telomerase+ counterpart (depicted in figure 1). ATRX loss has been consistently linked to the ALT phenotype in Glioma, with lack of ATRX expression being indicative of ALT activity (106)(125). However, the data generated in this study contradict that notion, suggesting that the inability to detect full-length ATRX is insufficient evidence to conclude ALT activity in adult glioma. It is possible that the mutant ATRX genes are being transcribed and translated only to produce a dysfunctional protein and the functional analysis of ATRX in this study is not robust enough to establish this. However, I would expect that if ATRX is so heavily involved in telomere maintenance, a severe loss of function would produce an observable phenotype, likely with persistent G4, reduced telomerase activity and telomere dysfunction as seen in the literature. However, it seemed possible that alternative isoforms of ATRX may be compensating in some way for the lack of full-length expression in some of the BTIC panel. Analysis of the ATRX isoform ATRXt, determined this variant of the protein was expressed in all telomerase positive cell lines, BTICs included (133). This suggested that ATRXt, a known and semi-functional isoform of ATRX, could be acting in place of the full-length protein. However, the exact functions maintained by ATRXt are unknown (133). Of interest, when I combined the expression of ATRXt with the expression of full-length ATRX using densitometry, the correlation between ATRX expression and ALT becomes much clearer. In this instance, total ATRX expression (ATRX full-length and ATRXt) was significantly higher in all telomerase+ BTICs

compared with ALT+ controls, which expressed little to no ATRX of any isoform. This highlights the importance of alternative ATRX isoforms when considering telomere maintenance as it may be that expression of a handful of alternative ATRX isoforms, yet to be fully characterized, is sufficient to repress ALT. Therefore, using ATRX IHC or mutational analysis alone will likely miss a portion of telomerase+ cancers, mis-labeling them as ALT+. A positive correlation was also found between total ATRX expression and telomerase activity (using densitometry), suggesting that as the levels of ATRX increase, telomerase activity increases. This again supports a role for ATRX in facilitating telomerase activity, albeit in a non-causal manner.

Further, overexpression of ATRXt in an ATRX null background showed that ATRXt maintained partial affinity for PML in U2OS cells. The association between ATRX and PML is thought to be essential in repressing the ALT pathway, as PML bodies localize to the telomeres of ALT cells and are considered the 'hub' of ALT activity (121)(74). Thus, by maintaining ~40% of the co-localization with PML, ATRXt may be able to compensate for lack of full-length ATRX and uphold ALT repression by preventing the movement of PML to the telomere. Taken together this data provides evidence for ATRXt as a functionally relevant isoform of ATRX, which may compensate in part for lack of the full-length protein expression, repressing the ALT phenotype and promoting telomerase activity.

Due to the reported link between ATRX and telomerase activity as well as the known association between ATRX and G4, I wanted to determine if changes in ATRX expression altered either global or telomeric G4 in the selected cells and how this would, in turn, effect telomerase activity. The G-quadruplex has been established as a cellular mechanism for gene regulation and expression, and is becoming increasingly important in many areas of research (95)(145). Currently, despite the great deal of interest in the role of G4 in the cell, the availability of assays to reliably

detect and measure G4 DNA remains a major barrier to research. Other than the widely used IF assays, there are limited quantitative detection methods to measure global changes in DNA G4 (87). Based on my experience using IF for global G4 quantification, it became clear how variable and inconsistent the results can be and how time-consuming analysis methods are. The novel DNA G4 ELISA detection assay described in this thesis provides an accurate and reproducible method of global G4 detection within genomic DNA. It also permits quantitation of total G4 within a sample of synthetic or genomic DNA, allowing accurate comparison between samples using a standard curve. The R^2 values for the telomeric standard curve also demonstrate the consistency of the method and intra-plate error rates in gDNA samples were consistently low. Additionally, the moderate inter-plate variations are specific to gDNA samples and not seen in the standard curves, suggesting a biological cause unrelated to assay design. It should also be noted that the error rate in IF analysis was consistently over 10% higher than in the ELISA when comparing integrated density analysis, further demonstrating the superiority of this assay for total G4 analysis.

The ability to quantify and measure G4 DNA is significant in many fields as the role of G4 becomes clearer. It has been established that G4 DNA can result in replication fork stalling and eventual collapse if unresolved (111)(182). This can pose many issues for the cell as it prolongs replication, causes DNA damage around the site of collapse and can trigger cell cycle arrest (100)(183). In addition to this, unresolved G4 can also block the progression of transcription machinery, thereby affecting gene expression and again triggering DNA damage responses (95)(98). Certain enzymes with helicase activity are able to resolve G4 and allow the smooth progression of replication and transcription machinery through patches of G-rich DNA (178)(73). However, in larger G-rich regions such as the telomere, the repetitive nature of the G-rich DNA makes it a hotspot for G4 formation and genomic instability (184). Therefore, stabilizing G4

through treatment with small molecules has potential as an anti-cancer therapy. It has been shown that telomerase, although capable of partial G4 resolution, is unable to elongate telomeric DNA containing stable G4 (142)(185). This is of particular importance in cancer and ageing, as manipulating G4 stability at the telomere could impact the cellular lifespan. By exogenously stabilising G4 in the telomeres of cancer cells, telomerase would be unable to successfully maintain telomere length, possibly leading to accelerated cell death as the cells age. It has been recently reported that G4 stabilisation promotes cellular DNA damage making cells susceptible to other DNA damaging agents (179). It could be that some of this damage occurs at the telomere, possibly triggering cell cycle checkpoints and subsequent arrest (100). Currently, there are no targeted G4 ligands that could be used specifically at the telomere, however as these agents continue to be developed, it may be possible to generate a ligand which binds telomeric G4 with a higher affinity than other DNA G4, using the specific orientation and sequence of the telomeric G4 for a more direct approach.

The importance of DNA G4 will continue to be established in many areas of research as we build tools to study these structures. The development of the G4 ELISA addresses the need for an accurate and reproducible method of G4 detection, which is vital when studying subtle differences in global genomic G4. Further, although the ELISA has been designed specifically to detect DNA G4, it could easily be adapted for quantification of RNA G4 or to study specific sequences for the presence of G4. Additionally, many ELISA assays have been modified for high-throughput screening. By modifying this assay for high-throughput analysis, multiple compounds could be screened with high efficiency, providing a modifiable tool for DNA structure analysis in an accurate, reliable and time-effective manner.

Utilising the G4 ELISA in combination with IF, I was able to determine how ATRX expression impacted the prevalence of both global and telomeric G4 in telomerase positive cancer cells. ATRX knockdown using shRNA constructs led to a mild increase in global G4 and significant increase in telomeric G4 expression. This supports a role for ATRX specifically in telomeric G4 resolution. It may be that ATRX has additional roles in G4 resolution at other regions of the cell enriched for repetitive DNA, such as pericentromeres, which is masked by the activity of other helicases compensating for a loss of ATRX (178). Certain helicases such as BLM, WRN and RTEL1 have been reported to possess moderate to high G4 resolving abilities, suggesting ATRX may be one of many acting to maintain genomic stability via this process (73).

Following treatment with the G4 stabilizer PDS, a dose-dependent reduction in telomerase activity was observed, a response even more pronounced upon loss of ATRX. This suggests ATRX actively functions to facilitate telomeric G4 breakdown and to support telomerase activity in cancer cells. This novel finding supports the role of ATRX in G4 resolution despite its poor performances in resolving G4 *in vitro* (107). I postulate that ATRX acts as a recruitment protein, detecting unresolved G4 and promoting the localisation of other helicases wit more robust G4 resolving abilities. The most logical candidate for this role would be RTEL1 as it is known to localise to the telomere and possess strong G4 resolving functions (168). This could explain, in part, why the expression of ATRXt is sufficient to repress ALT and promote telomerase-mediated telomere elongation in cells lacking full-length ATRX. As ATRXt is truncated 183bp into intron 11, it does not possess the c-terminal helicase domains of the full-length protein (133). Perhaps this isoform, amongst others, acts to guide other telomeric helicases to G4 sites to resolve G4, thereby allowing telomerase to access the telomere and maintain cellular immortality. This appears to be a fairly straightforward hypothesis to test with regard to telomerase activity in the presence of ATRXt

versus full-length ATRX, however significant issues with exogenously expressing ATRX create a barrier to experimentally confirming this theory. I attempted to express both ATRX and ATRXt in a number of immortalized cell lines in an effort to determine whether ATRX and ATRXt had a direct role in resolving G4, however, at best I could achieve 30% transfection efficiency using lipid-based reagents. Following advice from experts in the field, I deemed lipofection to be best most likely to work as electroporation results in extremely high levels of cell death with little to no successfully transfected cells. It may be possible to us CRISPR to insert the ATRX or ATRX genes however, due to their size (the ATRX gene is 281339bp), this may also prove difficult and due to time limitations, fell outside the realm of possibility for this project.

The data presented in this thesis help to fill a significant gap in knowledge with regard to the role of G4 and ATRX in cellular immortality. The data show that expression of ATRX is essential to regulate G4 at the telomere, acting to facilitate the resolution of G4, thereby providing telomerase access to telomeres, promoting telomerase-mediated telomere elongation. This concept fits with recent evidence showing ATRX loss induces sensitivity of cancer cells to G4 stabilizing agents, leading to increased DDR and cell death (179)(160). Additionally, the data highlight a key point for the diagnosis and treatment of glioma patients, providing evidence to suggest ATRX expression and/or mutations are insufficient to determine ALT activity. This alone provides novel evidence supporting the revision of existing clinical procedures in glioma patient diagnosis and treatment. The data provided here also support the role of telomeric G4 in regulating telomerase activity, confirming these structures as a suitable target for anti-cancer therapy. Interestingly, the data also suggest ATRX may be a novel anti-cancer target as loss of this protein appears to sensitize cells to G4 treatment, which was reported by the Huse lab to confer synthetic lethality (179).

Further, through my assessment of G4 in this study, I was able to develop and test a novel G4 detection method that is capable to measuring small changes in global G4 expression in human gDNA. This assay is easily standardizable and could prove to be a beneficial tool for quantifying G4 in a variety of ways. The assay in this instance was developed for detection of global G4 but is highly adaptable to other nucleic acid sequences and as anti-G4 antibodies become more specific, the method itself will become more accurate. Additionally, an assay of this kind lends itself to high-throughput screening and would be an excellent tool to test efficacy of G4 ligands on a large scale against multiple G4 sequences.

Together, the results presented in this thesis provide novel data for the role of ATRX in G4 resolution at the telomere and in the promotion of telomerase activity. It also provides evidence suggesting the alternative ATRX isoform, ATRXt, retains some WT activity and may be capable of repressing ALT in the absence of the full-length protein. Additionally, expression of full-length ATRX alone is not correlational with ALT activity and suggests care should be taken when utilising ATRX as an ALT marker both at the bench and more clinically. As many uncharacterised isoforms of the protein may exist, we do not yet know how expression of these might affect TMM, and focusing on the full-length protein alone could be misleading. Finally, this thesis provides a tried and tested method of G4 detection in human gDNA samples which allows for quantification of global G4 in a time- and cost-effective manner. These findings represent a significant contribution to the fields of cancer research, cellular immortality and ageing and help to fill a substantial gap in knowledge, providing evidence which has both biological and clinical relevance for many cancer types.

Limitations and future directions

This study has provided a wealth of information regarding the role of G4 and ATRX in cellular immortality, but avenues of interest remain and should be looked into in the future. First, I think analysis of a larger panel of cell lines for ATRX expression and ALT activity would be extremely helpful. For this, IHC analysis in combination with ATRX western blots and qPCR would help reinforce the data shown in this study regarding the correlation between ATRX and ALT. Generation of an ATRXt specific antibody would also be a significant step forward in identifying the relevance of this isoform in cancer. By furthering this analysis, we could obtain a better understanding of the how ATRX and ATRXt expression is distributed in cancer and whether loss or one, both or either is specifically associated with ALT activity. This information would also help to inform clinical diagnosis and prognosis of patients with glioma.

Another future direction for this research would be to generate stable ATRX and ATRXt overexpressing cells. This would provide a vital resource for analysing the role of ATRXt as well as other ATRX functions in G4 resolution, providing evidence to either support or reject ATRXt as a functionally relevant isoform in TMM. Due to technical issues in this study, I was unable to generate stable ATRX and ATRXt overexpressing lines. As the full-length ATRX sequence is over 7000 nucleotides and the plasmids each being between 5-7000 nucleotides, getting the cells to take-up and retain the plasmid proved difficult. Multiple reagents and time points were used to increase efficiency; however, 30% was the maximum transfection efficiency I could reach. This was acceptable for certain IF experiments as I could screen for ATRX/ATRXt positive cells, but analysis of a whole cell populations was not possible with such a mixed population.

Similarly, IF analysis for G4 was more complex than expected as G4 foci are highly abundant and very small, meaning analysis took much optimisation. Using image J, I was able to

set specific thresholds which helped to measure G4, but due to the proximity of G4 foci to each other, total foci count was impossible at this resolution. Therefore, integrated density was used as this accounts for the total area of G4 signal as well as the intensity of each foci, producing a total value for each nucleus. This protocol was followed throughout my study but is not standardized in the field, meaning comparison with results from other published articles could be inaccurate.

With the development of the G4 ELISA in this thesis, quantification of global G4 was simplified in wake of difficulties with the IF procedure. However, one limitation of this method is that despite its utility in DNA G4 detection both in specific synthetic sequences and, more globally, in genomic DNA, it cannot be used to detect specific G4 sequences in genomic DNA samples. For instance, we cannot use this assay to compare telomeric G4 formation between cell lines, only global G4. However, if sequences are suspected of forming G4 and need to be tested in a fast and cost-effective manner, the G4 ELISA assay is ideal. Using the G4 ELISA in this context, future studies could assess the impact of ATRX and ATRXt expression on global G4 in the presence of G4 ligands. These experiments would provide evidence for the role of ATRXt in global G4 resolution and determine if certain G4 ligands are more or less effective against certain genetic backgrounds. For instance, does pyridostatin trigger a significant increase in G4 in the absence of ATRXt and not in the absence of full-length ATRX? Questions such as these could be answered using the method described here. Again, due to issues with transfection efficiency, I was unable to obtain a population of cells with ATRX expression to perform this study, but if stable ATRX/ATRXt overexpressing cells were generated, this would be overcome.

Finally, and perhaps most critically, future studies could use stable ATRX and ATRXt over and under-expressing cell lines to screen for sensitivities to certain therapeutic combinations. As has been published, ATRX deficient glioma cells are more sensitive to DNA damage following

G4 ligand treatment. To further this, U2OS cells expressing ATRX or ATRXt could be subjected to G4 ligand treatment followed by irradiation and/or other DNA damaging agents to determine if the expression of these proteins has any impact on the efficacy of these treatments. Based on published data and the results from this thesis, I would expect ATRX and ATRXt to provide some level of resistance to G4 ligand treatment in the presence and absence of DNA damaging agents as they can resolve telomeric G4, reducing baseline and ligand induced DDR in this region. This data would further define the suitability of ATRX as a therapeutic target and perhaps help identify the best approach to cause synthetic lethality.

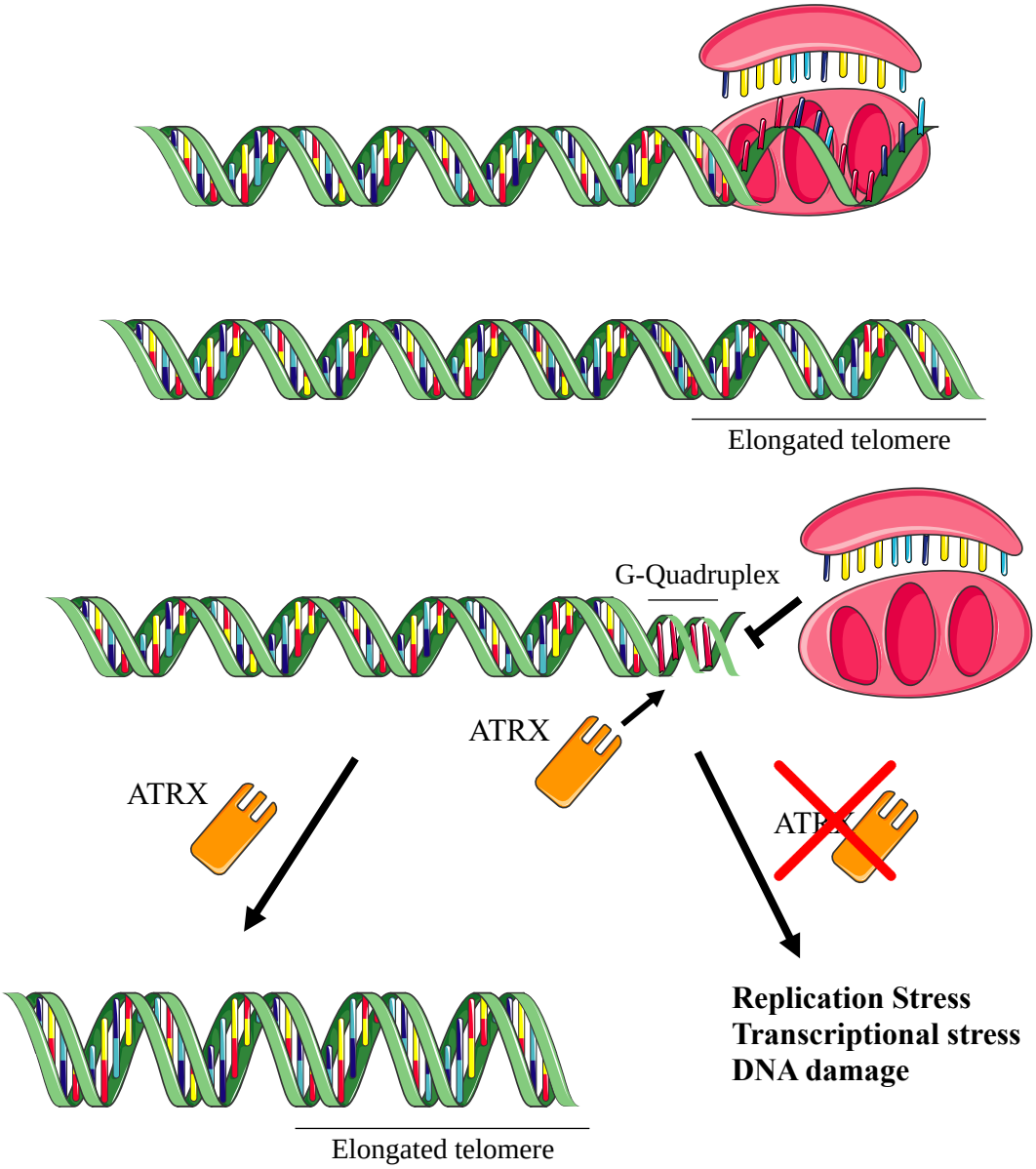

Figure 28: Model figure for proposed role of ATRX in telomerase-mediated telomere elongation. Under normal circumstances, telomerase activity at the telomere is blocked by G4. ATRX acts to resolve these structures either directly or indirectly, allowing telomerase to bind to telomere ends and elongate the DNA sequences. Upon ATRX loss, telomeric G4 persist, inhibiting telomerase activity and preventing telomere elongation. In cancer cells, this can lead to replicative and transcriptional stress and DNA damage.

Bibliography

1. Hanahan D, Weinberg RA. The Hallmarks of Cancer. Cell [Internet]. 2000 Jan [cited 2014 Jul 9];100(1):57–70. Available from: http://www.sciencedirect.com/science/article/pii/S0092867400816839
2. Hanahan D, Weinberg RA. Hallmarks of cancer: the next generation. Cell [Internet]. 2011 Mar 4 [cited 2014 Jul 9];144(5):646–74. Available from: http://www.ncbi.nlm.nih.gov/pubmed/21376230
3. Hoeijmakers JH. Genome maintenance mechanisms for preventing cancer. Nature [Internet]. 2001 May 17 [cited 2015 Jan 9];411(6835):366–74. Available from: http://dx.doi.org/10.1038/35077232
4. Levy MZ, Allsopp RC, Futcher AB, Greider CW, Harley CB. Telomere end-replication problem and cell aging. J Mol Biol [Internet]. 1992 Jun [cited 2015 Nov 15];225(4):951–60. Available from: http://www.sciencedirect.com/science/article/pii/0022283692900963
5. Frick DN, Richardson CC. DNA Primases. Annu Rev Biochem. 2001 Jun;70(1):39–80.
6. (No Title). 1997.
7. De Lange T. How telomeres solve the end-protection problem. Vol. 326, Science. 2009. p. 948–52.
8. Karlseder J, Smogorzewska A, de Lange T. Senescence induced by altered telomere state, not telomere loss. Science [Internet]. 2002 Mar 29 [cited 2016 Apr 5];295(5564):2446–9. Available from: http://science.sciencemag.org/content/295/5564/2446.abstract
9. Proctor CJ, Kirkwood TBL. Modelling cellular senescence as a result of telomere state. Aging Cell. 2003;2(3):151–7.
10. de Lange T. Shelterin: the protein complex that shapes and safeguards human telomeres.

Genes Dev [Internet]. 2005 Sep 15 [cited 2015 Dec 29];19(18):2100–10. Available from: http://genesdev.cshlp.org/content/19/18/2100.full

11. Ben-Porath I, Weinberg RA. The signals and pathways activating cellular senescence. Int J Biochem Cell Biol [Internet]. 2005 May [cited 2016 Mar 15];37(5):961–76. Available from: http://www.sciencedirect.com/science/article/pii/S1357272504003875

12. Wu P, Takai H, de Lange T. Telomeric 3' overhangs derive from resection by Exo1 and Apollo and fill-in by POT1b-associated CST. Cell [Internet]. 2012 Jul 6 [cited 2019 Oct 31];150(1):39–52. Available from: http://www.ncbi.nlm.nih.gov/pubmed/22748632

13. Griffith JD, Comeau L, Rosenfield S, Stansel RM, Bianchi A, Moss H, et al. Mammalian Telomeres End in a Large Duplex Loop. Cell [Internet]. 1999 May [cited 2015 Oct 16];97(4):503–14. Available from: http://www.sciencedirect.com/science/article/pii/S0092867400807606

14. De Vitis M, Berardinelli F, Sgura A. Telomere length maintenance in cancer: At the crossroad between telomerase and alternative lengthening of telomeres (ALT). Vol. 19, International Journal of Molecular Sciences. MDPI AG; 2018.

15. Shay JW, Pereira-Smith OM, Wright WE. A role for both RB and p53 in the regulation of human cellular senescence. Exp Cell Res [Internet]. 1991 Sep [cited 2019 Oct 31];196(1):33–9. Available from: http://www.ncbi.nlm.nih.gov/pubmed/1652450

16. Xu H-J, Zhou Y, Ji W, Perng G-S, Kruzelock R, Kong C-T, et al. Reexpression of the retinoblastoma protein in tumor cells induces senescence and telomerase inhibition. 1997.

17. Wang Y, Wang X, Flores ER, Yu J, Chang S. Dysfunctional telomeres induce p53-dependent and independent apoptosis to compromise cellular proliferation and inhibit tumor formation. Aging Cell [Internet]. 2016 [cited 2019 Oct 31];15(4):646–60. Available

from: http://www.ncbi.nlm.nih.gov/pubmed/27113195

18. Deng Y, Chang S. Role of telomeres and telomerase in genomic instability, senescence and cancer. [cited 2019 Oct 31]; Available from: www.laboratoryinvestigation.org

19. Blasco MA. Telomere length, stem cells and aging. Nat Chem Biol [Internet]. 2007 Oct [cited 2016 Mar 17];3(10):640–9. Available from: http://dx.doi.org/10.1038/nchembio.2007.38

20. Calado RT, Dumitriu B. Telomere dynamics in mice and humans. Semin Hematol [Internet]. 2013 Apr [cited 2016 Mar 17];50(2):165–74. Available from: http://www.pubmedcentral.nih.gov/articlerender.fcgi?artid=3742037&tool=pmcentrez&rendertype=abstract

21. Shay JW, Wright WE. Role of telomeres and telomerase in cancer. Semin Cancer Biol [Internet]. 2011 Dec [cited 2015 May 18];21(6):349–53. Available from: http://www.pubmedcentral.nih.gov/articlerender.fcgi?artid=3370415&tool=pmcentrez&rendertype=abstract

22. Muntoni A, Reddel RR. The first molecular details of ALT in human tumor cells. Hum Mol Genet [Internet]. 2005 Oct 15 [cited 2018 Jun 20];14(suppl_2):R191–6. Available from: http://academic.oup.com/hmg/article/14/suppl_2/R191/663270/The-first-molecular-details-of-ALT-in-human-tumor

23. Greider CW, Blackburn EH. Identification of a specific telomere terminal transferase activity in tetrahymena extracts. Cell. 1985;43(2 PART 1):405–13.

24. Huang FW, Hodis E, Xu MJ, Kryukov G V, Chin L, Garraway LA. Highly recurrent TERT promoter mutations in human melanoma. Science [Internet]. 2013 Feb 22 [cited 2015 Jun 8];339(6122):957–9. Available from:

http://www.pubmedcentral.nih.gov/articlerender.fcgi?artid=4423787&tool=pmcentrez&rendertype=abstract

25. Kim N, Piatyszek M, Prowse K, Harley C, West M, Ho P, et al. Specific association of human telomerase activity with immortal cells and cancer. Science (80-) [Internet]. 1994 Dec 23 [cited 2016 Apr 18];266(5193):2011–5. Available from: http://science.sciencemag.org/content/266/5193/2011.abstract

26. Holt SE, Wright WE, Shay JW. Regulation of telomerase activity in immortal cell lines. Mol Cell Biol [Internet]. 1996 Jun 1 [cited 2016 Apr 18];16(6):2932–9. Available from: http://mcb.asm.org/content/16/6/2932.short

27. Greider CW, Blackburn EH. A telomeric sequence in the RNA of Tetrahymena telomerase required for telomere repeat synthesis. Nature [Internet]. 1989 Jan 26 [cited 2019 Oct 31];337(6205):331–7. Available from: http://www.ncbi.nlm.nih.gov/pubmed/2463488

28. Wyatt HDM, West SC, Beattie TL. InTERTpreting telomerase structure and function. Nucleic Acids Res [Internet]. 2010 Sep 1 [cited 2016 Apr 18];38(17):5609–22. Available from: http://nar.oxfordjournals.org/content/38/17/5609.full

29. Yuan X, Larsson C, Xu D. Mechanisms underlying the activation of TERT transcription and telomerase activity in human cancer: old actors and new players. Oncogene [Internet]. [cited 2019 Oct 31]; Available from: https://doi.org/10.1038/s41388-019-0872-9

30. Cheng D, Wang S, Jia W, Zhao Y, Zhang F, Kang J, et al. Regulation of human and mouse telomerase genes by genomic contexts and transcription factors during embryonic stem cell differentiation. Sci Rep. 2017 Dec 1;7(1).

31. Heidenreich B, Rachakonda PS, Hemminki K, Kumar R. TERT promoter mutations in

cancer development. Vol. 24, Current Opinion in Genetics and Development. 2014. p. 30–7.

32. Wei W, Sedivy JM. Differentiation between senescence (M1) and crisis (M2) in human fibroblast cultures. Exp Cell Res [Internet]. 1999 Dec 15 [cited 2016 Apr 19];253(2):519–22. Available from: http://www.ncbi.nlm.nih.gov/pubmed/10585275

33. Ouellette MM. Subsenescent Telomere Lengths in Fibroblasts Immortalized by Limiting Amounts of Telomerase. J Biol Chem [Internet]. 2000 Mar 31 [cited 2016 Apr 18];275(14):10072–6. Available from: http://www.jbc.org/content/275/14/10072.full

34. Neumann AA, Reddel RR. Telomere maintenance and cancer -- look, no telomerase. Nat Rev Cancer [Internet]. 2002 Nov [cited 2016 Apr 18];2(11):879–84. Available from: http://dx.doi.org/10.1038/nrc929

35. Vinagre J, Almeida A, Pópulo H, Batista R, Lyra J, Pinto V, et al. Frequency of TERT promoter mutations in human cancers. Nat Commun [Internet]. 2013 Jan 26 [cited 2015 Nov 15];4:2185. Available from: http://www.nature.com/ncomms/2013/130726/ncomms3185/full/ncomms3185.html?message-global=remove

36. Huang DS, Wang Z, He XJ, Diplas BH, Yang R, Killela PJ, et al. Recurrent TERT promoter mutations identified in a large-scale study of multiple tumour types are associated with increased TERT expression and telomerase activation. Eur J Cancer. 2015 May 1;51(8):969–76.

37. Heaphy CM, Subhawong AP, Hong S-M, Goggins MG, Montgomery EA, Gabrielson E, et al. Prevalence of the alternative lengthening of telomeres telomere maintenance mechanism in human cancer subtypes. Am J Pathol [Internet]. 2011 Oct [cited 2016 Apr

12];179(4):1608–15. Available from: http://www.sciencedirect.com/science/article/pii/S0002944011006353

38. Phillips HS, Kharbanda S, Chen R, Forrest WF, Soriano RH, Wu TD, et al. Molecular subclasses of high-grade glioma predict prognosis, delineate a pattern of disease progression, and resemble stages in neurogenesis. Cancer Cell. 2006 Mar;9(3):157–73.

39. Behnan J, Finocchiaro G, Hanna G. The landscape of the mesenchymal signature in brain tumours. Vol. 142, Brain. Oxford University Press; 2019. p. 847–66.

40. Wesseling P, Capper D. WHO 2016 Classification of gliomas. Neuropathol Appl Neurobiol [Internet]. 2018 [cited 2019 Nov 1];44(2):139–50. Available from: http://www.ncbi.nlm.nih.gov/pubmed/28815663

41. Jiao Y, Killela PJ, Reitman ZJ, Rasheed AB, Heaphy CM, de Wilde RF, et al. Frequent ATRX, CIC, FUBP1 and IDH1 mutations refine the classification of malignant gliomas. Oncotarget [Internet]. 2012 Jul [cited 2016 Apr 18];3(7):709–22. Available from: http://www.pubmedcentral.nih.gov/articlerender.fcgi?artid=3443254&tool=pmcentrez&rendertype=abstract

42. Cho NW, Dilley RL, Lampson MA, Greenberg RA. Interchromosomal homology searches drive directional ALT telomere movement and synapsis. Cell [Internet]. 2014 Sep 25 [cited 2016 Apr 19];159(1):108–21. Available from: http://www.sciencedirect.com/science/article/pii/S0092867414011003

43. Cesare AJ, Reddel RR. Alternative lengthening of telomeres: models, mechanisms and implications. Nat Rev Genet [Internet]. 2010 May [cited 2016 Apr 18];11(5):319–30. Available from: http://dx.doi.org/10.1038/nrg2763

44. Lovejoy CA, Li W, Reisenweber S, Thongthip S, Bruno J, de Lange T, et al. Loss of

ATRX, genome instability, and an altered DNA damage response are hallmarks of the alternative lengthening of telomeres pathway. PLoS Genet [Internet]. 2012 Jan 19 [cited 2016 Jan 13];8(7):e1002772. Available from: http://journals.plos.org/plosgenetics/article?id=10.1371/journal.pgen.1002772

45. Chang S, Khoo CM, Naylor ML, Maser RS, DePinho RA. Telomere-based crisis: functional differences between telomerase activation and ALT in tumor progression. Genes Dev [Internet]. 2003 Jan 1 [cited 2016 Apr 19];17(1):88–100. Available from: http://genesdev.cshlp.org/content/17/1/88.abstract

46. Henson JD, Cao Y, Huschtscha LI, Chang AC, Au AYM, Pickett HA, et al. DNA C-circles are specific and quantifiable markers of alternative-lengthening-of-telomeres activity. Nat Biotechnol [Internet]. 2009 Dec [cited 2016 Apr 19];27(12):1181–5. Available from: http://dx.doi.org/10.1038/nbt.1587

47. Zhang T, Zhang Z, Shengzhao G, Li X, Liu H, Zhao Y. Strand break-induced replication fork collapse leads to C-circles, C-overhangs and telomeric recombination. Zhou J-Q, editor. PLOS Genet [Internet]. 2019 Feb 4 [cited 2019 Nov 24];15(2):e1007925. Available from: http://dx.plos.org/10.1371/journal.pgen.1007925

48. Liu H, Xie Y, Zhang Z, Mao P, Liu J, Ma W, et al. Telomeric Recombination Induced by DNA Damage Results in Telomere Extension and Length Heterogeneity. Neoplasia (United States). 2018 Sep 1;20(9):905–16.

49. Yeager TR, Neumann AA, Englezou A, Huschtscha LI, Noble JR, Reddel RR. Telomerase-negative Immortalized Human Cells Contain a Novel Type of Promyelocytic Leukemia (PML) Body. Cancer Res [Internet]. 1999 Sep 1 [cited 2016 Apr 19];59(17):4175–9. Available from:

http://cancerres.aacrjournals.org/content/59/17/4175.short

50. Chung I, Osterwald S, Deeg KI, Rippe K. PML body meets telomere: The beginning of an ALTernate ending? Vol. 3, Nucleus (United States). Landes Bioscience; 2012.

51. Venturini L, Erdas R, Costa A, Gronchi A, Pilotti S, Zaffaroni N, et al. ALT-associated promyelocytic leukaemia body (APB) detection as a reproducible tool to assess alternative lengthening of telomere stability in liposarcomas. J Pathol [Internet]. 2008 Mar [cited 2016 Apr 19];214(4):410–4. Available from: http://www.ncbi.nlm.nih.gov/pubmed/18085522

52. O'Sullivan RJ, Arnoult N, Lackner DH, Oganesian L, Haggblom C, Corpet A, et al. Rapid induction of alternative lengthening of telomeres by depletion of the histone chaperone ASF1. Nat Struct Mol Biol [Internet]. 2014 Mar [cited 2016 Jan 30];21(2):167–74. Available from: http://www.pubmedcentral.nih.gov/articlerender.fcgi?artid=3946341&tool=pmcentrez&rendertype=abstract

53. Napier CE, Huschtscha LI, Harvey A, Bower K, Noble JR, Hendrickson EA, et al. ATRX represses alternative lengthening of telomeres. Oncotarget [Internet]. 2015 Jun 30 [cited 2016 Apr 19];6(18):16543–58. Available from: http://www.pubmedcentral.nih.gov/articlerender.fcgi?artid=4599288&tool=pmcentrez&rendertype=abstract

54. Clynes D, Jelinska C, Xella B, Ayyub H, Scott C, Mitson M, et al. Suppression of the alternative lengthening of telomere pathway by the chromatin remodelling factor ATRX. Nat Commun [Internet]. 2015 Jul 6 [cited 2016 Oct 13];6:7538. Available from: http://www.nature.com/doifinder/10.1038/ncomms8538

55. Stevenson RE. Alpha-Thalassemia X-Linked Intellectual Disability Syndrome [Internet]. GeneReviews®. 1993 [cited 2019 Nov 7]. Available from: http://www.ncbi.nlm.nih.gov/pubmed/20301622

56. Badens C, Lacoste C, Philip N, Martini N, Courrier S, Giuliano F, et al. Mutations in PHD-like domain of the ATRX gene correlate with severe psychomotor impairment and severe urogenital abnormalities in patients with ATRX syndrome. Clin Genet [Internet]. 2006 Jun 23 [cited 2018 Jun 20];70(1):57–62. Available from: http://doi.wiley.com/10.1111/j.1399-0004.2006.00641.x

57. Iwase S, Xiang B, Ghosh S, Ren T, Lewis PW, Cochrane JC, et al. ATRX ADD domain links an atypical histone methylation recognition mechanism to human mental-retardation syndrome. Nat Struct Mol Biol. 2011 Jul;18(7):769–76.

58. Higgs DR, Weatherall DJ. The Alpha Thalassaemias. Vol. 66, Cellular and Molecular Life Sciences. 2009. p. 1154–62.

59. Gibbons RJ, Wada T, Fisher CA, Malik N, Mitson MJ, Steensma DP, et al. Mutations in the chromatin-associated protein ATRX. Hum Mutat [Internet]. 2008 Jun [cited 2019 Nov 7];29(6):796–802. Available from: http://doi.wiley.com/10.1002/humu.20734

60. Gibbons RJ, Picketts DJ, Villard L, Higgs DR. Mutations in a putative global transcriptional regulator cause X-linked mental retardation with α-thalassemia (ATR-X syndrome). Cell. 1995 Mar 24;80(6):837–45.

61. Farashi S, Harteveld CL. Blood Cells , Molecules and Diseases Molecular basis of α - thalassemia. Blood Cells, Mol Dis [Internet]. 2018 [cited 2019 Nov 7];70(10):43–53. Available from: https://doi.org/10.1016/j.bcmd.2017.09.004

62. Heaphy CM, de Wilde RF, Jiao Y, Klein AP, Edil BH, Shi C, et al. Altered Telomeres in

Tumors with ATRX and DAXX Mutations. Science (80-) [Internet]. 2011 Jul 22 [cited 2016 Nov 1];333(6041):425–425. Available from: http://www.sciencemag.org/cgi/doi/10.1126/science.1207313

63. ATRX - My Cancer Genome [Internet]. [cited 2019 Nov 7]. Available from: https://www.mycancergenome.org/content/gene/atrx/

64. Schwartzentruber J, Korshunov A, Liu X-Y, Jones DTW, Pfaff E, Jacob K, et al. Driver mutations in histone H3.3 and chromatin remodelling genes in paediatric glioblastoma. Nature [Internet]. 2012 Feb 9 [cited 2016 Apr 5];482(7384):226–31. Available from: http://dx.doi.org/10.1038/nature10833

65. Sturm D, Witt H, Hovestadt V, Khuong-Quang D-A, Jones DTW, Konermann C, et al. Hotspot mutations in H3F3A and IDH1 define distinct epigenetic and biological subgroups of glioblastoma. Cancer Cell [Internet]. 2012 Oct 16 [cited 2016 Oct 7];22(4):425–37. Available from: http://www.ncbi.nlm.nih.gov/pubmed/23079654

66. Lewis PW, Elsaesser SJ, Noh K-M, Stadler SC, Allis CD. Daxx is an H3.3-specific histone chaperone and cooperates with ATRX in replication-independent chromatin assembly at telomeres. Proc Natl Acad Sci U S A [Internet]. 2010 Aug 10 [cited 2016 Apr 19];107(32):14075–80. Available from: http://www.pubmedcentral.nih.gov/articlerender.fcgi?artid=2922592&tool=pmcentrez&rendertype=abstract

67. Ratnakumar K, Duarte LF, LeRoy G, Hasson D, Smeets D, Vardabasso C, et al. ATRX-mediated chromatin association of histone variant macroH2A1 regulates α-globin expression. Genes Dev [Internet]. 2012 Mar 1 [cited 2016 Nov 2];26(5):433–8. Available from: http://www.ncbi.nlm.nih.gov/pubmed/22391447

68. Bacolla A, Ye Z, Ahmed Z, Tainer JA. Cancer mutational burden is shaped by G4 DNA, replication stress and mitochondrial dysfunction. Prog Biophys Mol Biol. 2019 Mar;

69. Hänsel-Hertsch R, Beraldi D, Lensing S V., Marsico G, Zyner K, Parry A, et al. G-quadruplex structures mark human regulatory chromatin. Nat Genet. 2016 Oct 1;48(10):1267–72.

70. Li Y, Syed J, Suzuki Y, Asamitsu S, Shioda N, Wada T, et al. Effect of ATRX and G-Quadruplex Formation by the VNTR Sequence on α-Globin Gene Expression. ChemBioChem [Internet]. 2016 May 17 [cited 2019 Nov 7];17(10):928–35. Available from: http://doi.wiley.com/10.1002/cbic.201500655

71. Levy MA, Kernohan KD, Jiang Y, Bérubé NG. ATRX promotes gene expression by facilitating transcriptional elongation through guanine-rich coding regions. Hum Mol Genet [Internet]. 2015 Apr 1 [cited 2016 Mar 21];24(7):1824–35. Available from: http://hmg.oxfordjournals.org/content/24/7/1824.long

72. Law MJ, Lower KM, Voon HPJ, Hughes JR, Garrick D, Viprakasit V, et al. ATR-X syndrome protein targets tandem repeats and influences allele-specific expression in a size-dependent manner. Cell [Internet]. 2010 Oct 29 [cited 2016 Apr 19];143(3):367–78. Available from: http://www.sciencedirect.com/science/article/pii/S0092867410010718

73. Wu W, Rokutanda N, Takeuchi J, Lai Y, Maruyama R, Togashi Y, et al. HERC2 Facilitates BLM and WRN Helicase Complex Interaction with RPA to Suppress G-Quadruplex DNA. Cancer Res [Internet]. 2018 Oct 2 [cited 2019 May 28];78(22):6371–85. Available from: http://www.ncbi.nlm.nih.gov/pubmed/30279242

74. Chang FTM, McGhie JD, Chan FL, Tang MC, Anderson MA, Mann JR, et al. PML bodies provide an important platform for the maintenance of telomeric chromatin integrity

in embryonic stem cells. Nucleic Acids Res [Internet]. 2013 Apr 26 [cited 2016 Apr 19];41(8):4447–58. Available from: http://nar.oxfordjournals.org/content/early/2013/03/11/nar.gkt114.full

75. Luciani JJ, Depetris D, Usson Y, Metzler-Guillemain C, Mignon-Ravix C, Mitchell MJ, et al. PML nuclear bodies are highly organised DNA-protein structures with a function in heterochromatin remodelling at the G2 phase. J Cell Sci. 2006 Jun 15;119(12):2518–31.

76. Clynes D, Jelinska C, Xella B, Ayyub H, Taylor S, Mitson M, et al. ATRX dysfunction induces replication defects in primary mouse cells. PLoS One [Internet]. 2014 [cited 2016 Oct 13];9(3):e92915. Available from: http://www.ncbi.nlm.nih.gov/pubmed/24651726

77. Bérubé NG, Healy J, Medina CF, Wu S, Hodgson T, Jagla M, et al. Patient mutations alter ATRX targeting to PML nuclear bodies. Eur J Hum Genet [Internet]. 2008 Feb 24 [cited 2016 Apr 19];16(2):192–201. Available from: http://dx.doi.org/10.1038/sj.ejhg.5201943

78. Benetti R, Schoeftner S, Muñoz P, Blasco MA. Role of TRF2 in the assembly of telomeric chromatin. Cell Cycle [Internet]. 2014 Nov 5 [cited 2016 Apr 19];7(21):3461–8. Available from: http://www.tandfonline.com/doi/abs/10.4161/cc.7.21.7013

79. Bártová E, Krejcí J, Harnicarová A, Galiová G, Kozubek S. Histone modifications and nuclear architecture: a review. J Histochem Cytochem [Internet]. 2008 Aug [cited 2016 Nov 1];56(8):711–21. Available from: http://www.ncbi.nlm.nih.gov/pubmed/18474937

80. Kouzarides T. Chromatin modifications and their function. Cell [Internet]. 2007 Feb 23 [cited 2014 Jul 9];128(4):693–705. Available from: http://www.sciencedirect.com/science/article/pii/S0092867407001845

81. Jazayeri A, Falck J, Lukas C, Bartek J, Smith GCM, Lukas J, et al. ATM- and cell cycle-dependent regulation of ATR in response to DNA double-strand breaks. Nat Cell Biol

[Internet]. 2006 Jan [cited 2016 Feb 21];8(1):37–45. Available from: http://dx.doi.org/10.1038/ncb1337

82. Gutiérrez JL, Chandy M, Carrozza MJ, Workman JL. Activation domains drive nucleosome eviction by SWI/SNF. EMBO J [Internet]. 2007 Feb 7 [cited 2016 Apr 19];26(3):730–40. Available from: http://emboj.embopress.org/content/26/3/730.abstract

83. Episkopou H, Draskovic I, Van Beneden A, Tilman G, Mattiussi M, Gobin M, et al. Alternative Lengthening of Telomeres is characterized by reduced compaction of telomeric chromatin. Nucleic Acids Res [Internet]. 2014 Apr [cited 2016 Apr 19];42(7):4391–405. Available from: http://www.pubmedcentral.nih.gov/articlerender.fcgi?artid=3985679&tool=pmcentrez&rendertype=abstract

84. GELLERT M, LIPSETT MN, DAVIES DR. Helix formation by guanylic acid. Proc Natl Acad Sci U S A. 1962 Dec 15;48:2013–8.

85. Sen D, Gilbert W. Formation of parallel four-stranded complexes by guanine-rich motifs in DNA and its implications for meiosis. Nature. 1988;334(6180):364–6.

86. Sundquist WI, Klug A. Telomeric DNA dimerizes by formation of guanine tetrads between hairpin loops. Nature. 1989;342(6251):825–9.

87. Biffi G, Tannahill D, McCafferty J, Balasubramanian S. Quantitative visualization of DNA G-quadruplex structures in human cells. Nat Chem [Internet]. 2013 Mar 20 [cited 2018 Jun 20];5(3):182–6. Available from: http://www.nature.com/articles/nchem.1548

88. Hoffmann RF, Moshkin YM, Mouton S, Grzeschik NA, Kalicharan RD, Kuipers J, et al. Guanine quadruplex structures localize to heterochromatin. Nucleic Acids Res [Internet]. 2016 Jan 8 [cited 2019 May 27];44(1):152–63. Available from:

http://www.ncbi.nlm.nih.gov/pubmed/26384414

89. Jamroskovic J, Obi I, Movahedi A, Chand K, Chorell E, Sabouri N. Identification of putative G-quadruplex DNA structures in S. pombe genome by quantitative PCR stop assay. DNA Repair (Amst). 2019 Oct;82:102678.

90. Bhattacharyya D, Mirihana Arachchilage G, Basu S. Metal Cations in G-Quadruplex Folding and Stability. Front Chem [Internet]. 2016 [cited 2019 Feb 12];4:38. Available from: http://www.ncbi.nlm.nih.gov/pubmed/27668212

91. Bochman ML, Paeschke K, Zakian VA. DNA secondary structures: stability and function of G-quadruplex structures. Nat Rev Genet [Internet]. 2012 Nov 3 [cited 2019 May 27];13(11):770–80. Available from: http://www.nature.com/articles/nrg3296

92. Bhattacharyya D, Mirihana Arachchilage G, Basu S. Metal Cations in G-Quadruplex Folding and Stability. Front Chem [Internet]. 2016 Sep 9 [cited 2019 May 27];4:38. Available from: http://journal.frontiersin.org/Article/10.3389/fchem.2016.00038/abstract

93. Lipps HJ, Rhodes D. G-quadruplex structures: in vivo evidence and function. Trends Cell Biol [Internet]. 2009 Aug [cited 2016 Apr 19];19(8):414–22. Available from: http://www.sciencedirect.com/science/article/pii/S0962892409001238

94. Ruggiero E, Richter SN. G-quadruplexes and G-quadruplex ligands: targets and tools in antiviral therapy. Nucleic Acids Res [Internet]. 2018 Apr 20 [cited 2019 May 27];46(7):3270–83. Available from: https://academic.oup.com/nar/article/46/7/3270/4937544

95. Mao S-Q, Ghanbarian AT, Spiegel J, Martínez Cuesta S, Beraldi D, Di Antonio M, et al. DNA G-quadruplex structures mold the DNA methylome. Nat Struct Mol Biol [Internet]. 2018 Oct 1 [cited 2019 May 28];25(10):951–7. Available from:

http://www.ncbi.nlm.nih.gov/pubmed/30275516

96. Burge S, Parkinson GN, Hazel P, Todd AK, Neidle S. Quadruplex DNA: sequence, topology and structure. Nucleic Acids Res [Internet]. 2006 Nov [cited 2019 Nov 21];34(19):5402–15. Available from: https://academic.oup.com/nar/article-lookup/doi/10.1093/nar/gkl655

97. Smaldino PJ, Routh ED, Kim JH, Giri B, Creacy SD, Hantgan RR, et al. Mutational Dissection of Telomeric DNA Binding Requirements of G4 Resolvase 1 Shows that G4-Structure and Certain 3'-Tail Sequences Are Sufficient for Tight and Complete Binding. Deb S, editor. PLoS One [Internet]. 2015 Jul 14 [cited 2019 Nov 21];10(7):e0132668. Available from: https://dx.plos.org/10.1371/journal.pone.0132668

98. Hänsel-Hertsch R, Beraldi D, Lensing S V, Marsico G, Zyner K, Parry A, et al. G-quadruplex structures mark human regulatory chromatin. Nat Genet [Internet]. 2016 Oct 12 [cited 2019 May 28];48(10):1267–72. Available from: http://www.nature.com/articles/ng.3662

99. Fogolari F, Haridas H, Corazza A, Viglino P, Corà D, Caselle M, et al. Molecular models for intrastrand DNA G-quadruplexes. BMC Struct Biol. 2009;9:64.

100. Wang Y, Yang J, Wild AT, Wu WH, Shah R, Danussi C, et al. G-quadruplex DNA drives genomic instability and represents a targetable molecular abnormality in ATRX-deficient malignant glioma. Nat Commun [Internet]. 2019 Dec 26 [cited 2019 May 28];10(1):943. Available from: http://www.nature.com/articles/s41467-019-08905-8

101. Wong LH, McGhie JD, Sim M, Anderson MA, Ahn S, Hannan RD, et al. ATRX interacts with H3.3 in maintaining telomere structural integrity in pluripotent embryonic stem cells. Genome Res. 2010 Mar;20(3):351–60.

102. Wright WE, Tesmer VM, Liao ML, Shay JW. Normal human telomeres are not late replicating. Exp Cell Res. 1999 Sep 15;251(2):492–9.

103. Daekyu Sun †, Brian Thompson ‡, Brian E. Cathers ‡, Miguel Salazar ‡, Sean M. Kerwin ‡, John O. Trent §, et al. Inhibition of Human Telomerase by a G-Quadruplex-Interactive Compound. 1997 [cited 2018 Jun 20]; Available from: https://pubs.acs.org/doi/full/10.1021/jm970199z

104. Clynes D, Jelinska C, Xella B, Ayyub H, Scott C, Mitson M, et al. Suppression of the alternative lengthening of telomere pathway by the chromatin remodelling factor ATRX. Nat Commun. 2015 Jul 6;6.

105. Salvati E, Leonetti C, Rizzo A, Scarsella M, Mottolese M, Galati R, et al. Telomere damage induced by the G-quadruplex ligand RHPS4 has an antitumor effect. J Clin Invest. 2007 Nov 1;117(11):3236–47.

106. Haase S, Garcia-Fabiani MB, Carney S, Altshuler D, Núñez FJ, Méndez FM, et al. Mutant ATRX: uncovering a new therapeutic target for glioma. Vol. 22, Expert Opinion on Therapeutic Targets. Taylor and Francis Ltd; 2018. p. 599–613.

107. Clynes D, Jelinska C, Xella B, Ayyub H, Taylor S, Mitson M, et al. ATRX dysfunction induces replication defects in primary mouse cells. PLoS One. 2014 Mar 20;9(3).

108. Zhang QS, Manche L, Xu RM, Krainer AR. hnRNP A1 associates with telomere ends and stimulates telomerase activity. RNA. 2006 Jun;12(6):1116–28.

109. Marsico G, Chambers VS, Sahakyan AB, McCauley P, Boutell JM, Antonio M Di, et al. Whole genome experimental maps of DNA G-quadruplexes in multiple species. Nucleic Acids Res. 2019;47(8):3862–74.

110. Yoshida W, Saikyo H, Nakabayashi K, Yoshioka H, Bay DH, Iida K, et al. Identification

of G-quadruplex clusters by high-throughput sequencing of whole-genome amplified products with a G-quadruplex ligand. Sci Rep. 2018 Dec 1;8(1).

111. Moruno-Manchon JF, Koellhoffer EC, Gopakumar J, Hambarde S, Kim N, McCullough LD, et al. The G-quadruplex DNA stabilizing drug pyridostatin promotes DNA damage and downregulates transcription of Brca1 in neurons. Aging (Albany NY) [Internet]. 2017 Sep 12 [cited 2019 Feb 12];9(9):1957–70. Available from: http://www.ncbi.nlm.nih.gov/pubmed/28904242

112. Kim MY, Vankayalapati H, Shin-Ya K, Wierzba K, Hurley LH. Telomestatin, a potent telomerase inhibitor that interacts quite specifically with the human telomeric intramolecular G-quadruplex. J Am Chem Soc. 2002 Mar 13;124(10):2098–9.

113. Asamitsu S, Obata S, Yu Z, Bando T, Sugiyama H. Recent progress of targeted G-quadruplex-preferred ligands toward cancer therapy. Vol. 24, Molecules. MDPI AG; 2019.

114. Dose-escalation Study of Quarfloxin in Patients With Advanced Solid Tumors or Lymphomas - Full Text View - ClinicalTrials.gov [Internet]. [cited 2019 Nov 24]. Available from: https://clinicaltrials.gov/ct2/show/NCT00955292

115. Quarfloxin in Patients With Low to Intermediate Grade Neuroendocrine Carcinoma - Full Text View - ClinicalTrials.gov [Internet]. [cited 2019 Nov 21]. Available from: https://clinicaltrials.gov/ct2/show/NCT00780663

116. Richards DA, Kindler HL, Oettle H, Ramanathan RK, Van Laethem J-L, Peeters M, et al. A randomized phase III study comparing gemcitabine + pemetrexed versus gemcitabine in patients with locally advanced and metastatic pancreas cancer. J Clin Oncol. 2004 Jul 15;22(14_suppl):4007–4007.

117. Chiappori AA, Kolevska T, Spigel DR, Hager S, Rarick M, Gadgeel S, et al. A randomized phase II study of the telomerase inhibitor imetelstat as maintenance therapy for advanced non-small-cell lung cancer. Ann Oncol. 2015 Feb 1;26(2):354–62.

118. Nemunaitis J, Tong AW, Nemunaitis M, Senzer N, Phadke AP, Bedell C, et al. A phase i study of telomerase-specific replication competent oncolytic adenovirus (telomelysin) for various solid tumors. Mol Ther. 2010 Feb;18(2):429–34.

119. Henson JD, Neumann AA, Yeager TR, Reddel RR. Alternative lengthening of telomeres in mammalian cells. Oncogene [Internet]. 2002 Jan 11 [cited 2018 Jun 20];21(4):598–610. Available from: http://www.nature.com/articles/1205058

120. Nabetani A, Ishikawa F. Alternative lengthening of telomeres pathway: Recombination-mediated telomere maintenance mechanism in human cells. Vol. 149, Journal of Biochemistry. 2011. p. 5–14.

121. Napier CE, Huschtscha LI, Harvey A, Bower K, Noble JR, Hendrickson EA, et al. ATRX represses alternative lengthening of telomeres. Oncotarget [Internet]. 2015 Jun 30 [cited 2016 Nov 1];6(18):16543–58. Available from: http://www.ncbi.nlm.nih.gov/pubmed/26001292

122. Brosnan-Cashman JA, Yuan M, Graham MK, Rizzo AJ, Myers KM, Davis C, et al. ATRX loss induces multiple hallmarks of the alternative lengthening of telomeres (ALT) phenotype in human glioma cell lines in a cell line-specific manner. PLoS One [Internet]. 2018 [cited 2019 Oct 16];13(9):e0204159. Available from: http://www.ncbi.nlm.nih.gov/pubmed/30226859

123. Silvestre DC, Pineda JR, Hoffschir F, Studler J-M, Mouthon M-A, Pflumio F, et al. Alternative lengthening of telomeres in human glioma stem cells. Stem Cells [Internet].

2011 Mar [cited 2016 Apr 18];29(3):440–51. Available from: http://www.ncbi.nlm.nih.gov/pubmed/21425407

124. Ohgaki H, Kleihues P. The definition of primary and secondary glioblastoma. Clin Cancer Res [Internet]. 2013 Feb 15 [cited 2015 Dec 12];19(4):764–72. Available from: http://clincancerres.aacrjournals.org/content/19/4/764.long

125. Wiestler B, Capper D, Holland-Letz T, Korshunov A, von Deimling A, Pfister SM, et al. ATRX loss refines the classification of anaplastic gliomas and identifies a subgroup of IDH mutant astrocytic tumors with better prognosis. Acta Neuropathol [Internet]. 2013 Sep 1 [cited 2016 Nov 1];126(3):443–51. Available from: http://link.springer.com/10.1007/s00401-013-1156-z

126. Draskovic I, Arnoult N, Steiner V, Bacchetti S, Lomonte P, Londoño-Vallejo A. Probing PML body function in ALT cells reveals spatiotemporal requirements for telomere recombination. Proc Natl Acad Sci U S A. 2009 Sep 15;106(37):15726–31.

127. Mender I, Shay J. Telomerase Repeated Amplification Protocol (TRAP). BIO-PROTOCOL. 2015;5(22).

128. Lin J, Smith DL, Esteves K, Drury S. Telomere length measurement by qPCR – Summary of critical factors and recommendations for assay design. Vol. 99, Psychoneuroendocrinology. Elsevier Ltd; 2019. p. 271–8.

129. Dagnall CL, Hicks B, Teshome K, Hutchinson AA, Gadalla SM, Khincha PP, et al. Effect of pre-analytic variables on the reproducibility of qPCR relative telomere length measurement. PLoS One. 2017 Sep 1;12(9).

130. Nettle D, Seeker L, Nussey D, Froy H, Bateson M. Consequences of measurement error in qPCR telomere data: A simulation study. bioRxiv. 2018 Dec 10;491944.

131. Mender I, Shay JW. Telomere Restriction Fragment (TRF) Analysis. Bio-protocol [Internet]. 2015 Nov 20 [cited 2019 Oct 18];5(22). Available from: http://www.ncbi.nlm.nih.gov/pubmed/27500189

132. Mitson M, Kelley LA, Sternberg MJE, Higgs DR, Gibbons RJ. Functional significance of mutations in the Snf2 domain of ATRX. Hum Mol Genet. 2011 Jul;20(13):2603–10.

133. Garrick D, Samara V, McDowell TL, Smith AJH, Dobbie L, Higgs DR, et al. A conserved truncated isoform of the ATR-X syndrome protein lacking the SWI/SNF-homology domain. Gene [Internet]. 2004 Feb 4 [cited 2018 Feb 11];326:23–34. Available from: https://www.sciencedirect.com/science/article/pii/S0378111903010473

134. Heaphy CM, de Wilde RF, Jiao Y, Klein AP, Edil BH, Shi C, et al. Altered Telomeres in Tumors with ATRX and DAXX Mutations. Science (80-) [Internet]. 2011 [cited 2017 Aug 14];333(6041). Available from: http://science.sciencemag.org/content/333/6041/425

135. Yost KE, Clatterbuck Soper SF, Walker RL, Pineda MA, Zhu YJ, Ester CD, et al. Rapid and reversible suppression of ALT by DAXX in osteosarcoma cells. Sci Rep. 2019 Dec 1;9(1):1–11.

136. Cai J, Zhu P, Zhang C, Li Q, Wang Z, Li G, et al. Detection of ATRX and IDH1-R132H immunohistochemistry in the progression of 211 paired gliomas. Oncotarget. 2016 Mar 29;7(13):16384–95.

137. Ikemura M, Shibahara J, Mukasa A, Takayanagi S, Aihara K, Saito N, et al. Utility of ATRX immunohistochemistry in diagnosis of adult diffuse gliomas. Histopathology. 2016 Aug 1;69(2):260–7.

138. Delbarre E, Ivanauskiene K, Spirkoski J, Shah A, Vekterud K, Moskaug JØ, et al. PML protein organizes heterochromatin domains where it regulates histone H3.3 deposition by

ATRX/DAXX. 2017 [cited 2019 Oct 18]; Available from: http://www.genome.org/cgi/doi/10.1101/gr.215830.116.

139. Reece-Hoyes JS, Walhout AJM. Gateway recombinational cloning. Vol. 2018, Cold Spring Harbor Protocols. Cold Spring Harbor Laboratory Press; 2018. p. 1–6.

140. Lin C, Yang D. Human Telomeric G-Quadruplex Structures and G-Quadruplex-Interactive Compounds. Methods Mol Biol [Internet]. 2017 [cited 2019 May 27];1587:171–96. Available from: http://www.ncbi.nlm.nih.gov/pubmed/28324509

141. Moye AL, Porter KC, Cohen SB, Phan T, Zyner KG, Sasaki N, et al. Telomeric G-quadruplexes are a substrate and site of localization for human telomerase. Nat Commun [Internet]. 2015 Nov 9 [cited 2019 May 27];6(1):7643. Available from: http://www.nature.com/articles/ncomms8643

142. Daekyu Sun †, Brian Thompson ‡, Brian E. Cathers ‡, Miguel Salazar ‡, Sean M. Kerwin ‡, John O. Trent §, et al. Inhibition of Human Telomerase by a G-Quadruplex-Interactive Compound. 1997 [cited 2019 Feb 12]; Available from: https://pubs.acs.org/doi/abs/10.1021/jm970199z?journalCode=jmcmar

143. Napier CE, Huschtscha LI, Harvey A, Bower K, Noble JR, Hendrickson EA, et al. ATRX represses alternative lengthening of telomeres. Oncotarget. 2015;6(18):16543–58.

144. Bayer, B Fabian, W Hübl PM. Immunofluorescence assays (IFA) and enzyme-linked immunosorbent assays (ELISA) in autoimmune disease diagnostics - technique, benefits, limitations and applications. Scand J Clin Lab Invest. 2002;

145. Hänsel-Hertsch R, Spiegel J, Marsico G, Tannahill D, Balasubramanian S. Genome-wide mapping of endogenous G-quadruplex DNA structures by chromatin immunoprecipitation and high-throughput sequencing. Nat Protoc. 2018;13(3):551–64.

146. Marsico G, Chambers VS, Sahakyan AB, McCauley P, Boutell JM, Antonio M Di, et al. Whole genome experimental maps of DNA G-quadruplexes in multiple species. Nucleic Acids Res [Internet]. 2019 May 7 [cited 2019 May 27];47(8):3862–74. Available from: https://academic.oup.com/nar/article/47/8/3862/5403498

147. Mestre-Fos S, Penev PI, Suttapitugsakul S, Ito C, Petrov AS, Wartell RM, et al. G-quadruplex formation on specific surface-exposed regions of the human ribosomal RNA. bioRxiv [Internet]. 2018 Nov 16 [cited 2019 Jun 4];435594. Available from: https://www.biorxiv.org/content/10.1101/435594v2.full

148. Ma D-L, Wang M, Lin S, Han Q-B, Leung C-H. Recent Development of G-Quadruplex Probes for Cellular Imaging.

149. Stokes RP, Cordwell A, Thompson RA. A simple, rapid ELISA method for the detection of DNA antibodies. J Clin Pathol. 1982;35(5):566–73.

150. Sutjita M, Hohmann A, Boey ML, Bradley J. Microplate ELISA for detection of antibodies to DNA in patients with systemic lupus erythematosus: specificity and correlation with Farr radioimmunoassay. J Clin Lab Anal [Internet]. 1989 [cited 2019 Sep 22];3(1):34–40. Available from: http://www.ncbi.nlm.nih.gov/pubmed/2715873

151. Balhorn R. The protamine family of sperm nuclear proteins. Vol. 8, Genome Biology. 2007.

152. Co CB. Protamine Sulfate Coated ELISA Plate. [cited 2019 Sep 22]; Available from: https://search.cosmobio.co.jp/cosmo_search_p/search_gate2/docs/CSR_/NMMAP003.20150601.pdf

153. Ambrus A, Chen D, Dai J, Bialis T, Jones RA, Yang D. Human telomeric sequence forms a hybrid-type intramolecular G-quadruplex structure with mixed parallel/antiparallel

strands in potassium solution. Nucleic Acids Res [Internet]. 2006 May 19 [cited 2018 Jun 20];34(9):2723–35. Available from: https://academic.oup.com/nar/article-lookup/doi/10.1093/nar/gkl348

154. Henderson E, Hardin CC, Walk SK, Tinoco I, Blackburn EH. Telomeric DNA oligonucleotides form novel intramolecular structures containing guanine-guanine base pairs. Cell [Internet]. 1987 Dec 24 [cited 2019 May 27];51(6):899–908. Available from: http://www.ncbi.nlm.nih.gov/pubmed/3690664

155. QGRS Mapper | G-quadruplex analysis tool [Internet]. [cited 2019 May 27]. Available from: http://bioinformatics.ramapo.edu/QGRS/index.php

156. Biffi G, Di Antonio M, Tannahill D, Balasubramanian S. Visualization and selective chemical targeting of RNA G-quadruplex structures in the cytoplasm of human cells. Nat Chem. 2014 Jan;6(1):75–80.

157. Tsai Y-C, Qi H, Lin C-P, Lin R-K, Kerrigan JE, Rzuczek SG, et al. A G-quadruplex Stabilizer Induces M-phase Cell Cycle Arrest. J Biol Chem [Internet]. 2009 Aug 21 [cited 2019 May 28];284(34):22535. Available from: http://www.ncbi.nlm.nih.gov/pubmed/19531483

158. Kim M-Y, Vankayalapati H, Shin-Ya K, Wierzba K, Hurley LH. Telomestatin, a potent telomerase inhibitor that interacts quite specifically with the human telomeric intramolecular g-quadruplex. J Am Chem Soc [Internet]. 2002 Mar 13 [cited 2019 Oct 23];124(10):2098–9. Available from: http://www.ncbi.nlm.nih.gov/pubmed/11878947

159. Local A, Zhang H, Benbatoul KD, Folger P, Sheng X, Tsai C-Y, et al. APTO-253 stabilizes G-quadruplex DNA, inhibits MYC expression and induces DNA damage in acute myeloid leukemia cells. 2019 [cited 2019 Oct 23]; Available from:

http://www.lls.org/beat-aml

160. De Magis A, Manzo SG, Russo M, Marinello J, Morigi R, Sordet O, et al. DNA damage and genome instability by G-quadruplex ligands are mediated by R loops in human cancer cells. Proc Natl Acad Sci U S A. 2019 Jan 15;116(3):816–25.

161. Jiao Y, Killela PJ, Reitman ZJ, Rasheed AB, Heaphy CM, de Wilde RF, et al. Frequent ATRX, CIC, FUBP1 and IDH1 mutations refine the classification of malignant gliomas. Oncotarget [Internet]. 2012 Jul [cited 2017 Aug 14];3(7):709–22. Available from: http://www.ncbi.nlm.nih.gov/pubmed/22869205

162. Mukherjee J, Johannessen TC, Ohba S, Chow TT, Jones L, Pandita A, et al. Mutant IDH1 cooperates with ATRX loss to drive the alternative lengthening of telomere phenotype in glioma. Cancer Res. 2018 Jun 1;78(11):2966–77.

163. Lovejoy CA, Li W, Reisenweber S, Thongthip S, Bruno J, de Lange T, et al. Loss of ATRX, Genome Instability, and an Altered DNA Damage Response Are Hallmarks of the Alternative Lengthening of Telomeres Pathway. Scott HS, editor. PLoS Genet [Internet]. 2012 Jul 19 [cited 2018 Jun 20];8(7):e1002772. Available from: http://dx.plos.org/10.1371/journal.pgen.1002772

164. Brosnan-Cashman JA, Yuan M, Graham MK, Rizzo AJ, Myers KM, Davis C, et al. ATRX loss induces multiple hallmarks of the alternative lengthening of telomeres (ALT) phenotype in human glioma cell lines in a cell line-specific manner. PLoS One [Internet]. 2018 [cited 2019 Oct 25];13(9):e0204159. Available from: http://www.ncbi.nlm.nih.gov/pubmed/30226859

165. Lewis PW, Elsaesser SJ, Noh K-M, Stadler SC, Allis CD. Daxx is an H3.3-specific histone chaperone and cooperates with ATRX in replication-independent chromatin

assembly at telomeres. Proc Natl Acad Sci U S A [Internet]. 2010 Aug 10 [cited 2017 Aug 14];107(32):14075–80. Available from: http://www.ncbi.nlm.nih.gov/pubmed/20651253

166. O'Sullivan RJ, Arnoult N, Lackner DH, Oganesian L, Haggblom C, Corpet A, et al. Rapid induction of alternative lengthening of telomeres by depletion of the histone chaperone ASF1. Nat Struct Mol Biol. 2014 Feb;21(2):167–74.

167. O'Sullivan RJ, Almouzni G. Assembly of telomeric chromatin to create ALTernative endings. Vol. 24, Trends in Cell Biology. Elsevier Ltd; 2014. p. 675–85.

168. Mendoza O, Bourdoncle A, Boulé JB, Brosh RM, Mergny JL. G-quadruplexes and helicases. Vol. 44, Nucleic Acids Research. Oxford University Press; 2016. p. 1989–2006.

169. Martínez P, Blasco MA. Replicating through telomeres: a means to an end. Trends Biochem Sci [Internet]. 2015 Sep [cited 2019 Oct 25];40(9):504–15. Available from: http://www.ncbi.nlm.nih.gov/pubmed/26188776

170. Zhang T, Zhang Z, Li F, Hu Q, Liu H, Tang M, et al. Looping-out mechanism for resolution of replicative stress at telomeres. EMBO Rep. 2017 Aug;18(8):1412–28.

171. Graham MK, Kim J, Da J, Brosnan-Cashman JA, Rizzo A, Baena Del Valle JA, et al. Functional loss of ATRX and TERC activates Alternative Lengthening of Telomeres (ALT) in LAPC4 prostate cancer cells. Mol Cancer Res [Internet]. 2019 Oct 14 [cited 2019 Oct 25]; Available from: http://www.ncbi.nlm.nih.gov/pubmed/31611308

172. Wyatt HDM, Tsang AR, Lobb DA, Beattie TL. Human telomerase reverse transcriptase (hTERT) Q169 is essential for telomerase function in vitro and in vivo. PLoS One. 2009 Sep 24;4(9).

173. Bachand F, Kukolj G, Autexier C. Expression of hTERT and hTR in cis reconstitutes and active human telomerase ribonucleoprotein. RNA [Internet]. 2000 May [cited 2019 Oct

29];6(5):778–84. Available from: http://www.ncbi.nlm.nih.gov/pubmed/10836798

174. Gomez D, Mergny JL, Riou JF. Detection of telomerase inhibitors based on G-quadruplex ligands by a modified telomeric repeat amplification protocol assay. Cancer Res. 2002 Jun 15;62(12):3365–8.

175. Zhao S, Jiang E, Chen S, Gu Y, Shangguan AJ, Lv T, et al. PiggyBac transposon vectors: The tools of the human gene encoding. Vol. 5, Translational Lung Cancer Research. AME Publishing Company; 2016. p. 120–5.

176. Boettcher M, Hoheisel JD. Pooled RNAi Screens - Technical and Biological Aspects. Curr Genomics. 2010 Apr 14;11(3):162–7.

177. Fellmann C, Lowe SW. Stable RNA interference rules for silencing. Vol. 16, Nature Cell Biology. 2014. p. 10–8.

178. Popuri V, Bachrati CZ, Muzzolini L, Mosedale G, Costantini S, Giacomini E, et al. The Human RecQ Helicases, BLM and RECQ1, Display Distinct DNA Substrate Specificities. J Biol Chem [Internet]. 2008 Jun 27 [cited 2019 May 28];283(26):17766–76. Available from: http://www.ncbi.nlm.nih.gov/pubmed/18448429

179. Wang Y, Yang J, Wu W, Shah R, Danussi C, Kannan K, et al. G-quadruplex DNA drives genomic instability and represents a targetable 1 molecular abnormality in ATRX-deficient malignant glioma 2 3. [cited 2019 Nov 13]; Available from: http://dx.doi.org/10.1101/347542

180. Jiao Y, Killela PJ, Reitman ZJ, Rasheed AB, Heaphy CM, de Wilde RF, et al. Frequent ATRX, CIC, FUBP1 and IDH1 mutations refine the classification of malignant gliomas. Oncotarget [Internet]. 2012 Jul [cited 2018 Jun 20];3(7):709–22. Available from: http://www.ncbi.nlm.nih.gov/pubmed/22869205

181. Chami R, Marrano P, Teerapakpinyo C, Arnoldo A, Shago M, Shuangshoti S, et al. Immunohistochemistry for ATRX Can Miss ATRX Mutations: Lessons from Neuroblastoma. Am J Surg Pathol. 2019 Sep 1;43(9):1203–11.

182. Sarkies P, Reams C, Simpson LJ, Sale JE. Article Epigenetic Instability due to Defective Replication of Structured DNA. Mol Cell [Internet]. 2010 [cited 2019 May 28];40:703–13. Available from: https://www.cell.com/molecular-cell/pdf/S1097-2765(10)00847-6.pdf

183. Hasegawa D, Okabe S, Okamoto K, Nakano I, Shin-ya K, Seimiya H. G-quadruplex ligand-induced DNA damage response coupled with telomere dysfunction and replication stress in glioma stem cells. Biochem Biophys Res Commun [Internet]. 2016 Feb 26 [cited 2019 May 28];471(1):75–81. Available from: http://www.ncbi.nlm.nih.gov/pubmed/26845351

184. Shammas MA. Telomeres, lifestyle, cancer, and aging. Curr Opin Clin Nutr Metab Care [Internet]. 2011 Jan [cited 2015 Dec 11];14(1):28–34. Available from: http://www.pubmedcentral.nih.gov/articlerender.fcgi?artid=3370421&tool=pmcentrez&rendertype=abstract

185. Wang Q, Liu J, Chen Z, Zheng K, Chen C, Hao Y-H, et al. G-quadruplex formation at the 3’ end of telomere DNA inhibits its extension by telomerase, polymerase and unwinding by helicase. Nucleic Acids Res [Internet]. 2011 Aug [cited 2019 May 28];39(14):6229–37. Available from: http://www.ncbi.nlm.nih.gov/pubmed/21441540